WEAK LINK BEHAVIOR OF $(Cu_{0.5}Tl_{0.5})Ba_2Ca_2(Cu_2Sn)O_{10-\delta}$ SUPERCONDUCTORS

BY

SANA NAWAZ

Department of Physics
Quaid-i-Azam University
Islamabad, Pakistan.
2008-09

WEAK LINK BEHAVIOR OF $(Cu_{0.5}Tl_{0.5})Ba_2Ca_2(Cu_2Sn)O_{10-\delta}$ SUPERCONDUCTORS

A dissertation submitted to the department of physics, Quaid-i-Azam University Islamabad, in the partial fulfillment of the requirement for the degree of

Master of Philosophy

in

Physics

by

SANA NAWAZ

Department of Physics
Quaid-i-Azam University
Islamabad, Pakistan.

In the Name of Allah, Most Benevolent, Ever Merciful

Certificate

This is to certify that Miss Sana Nawaz has carried out the experimental work in this dissertation under my supervision in Materials Science Laboratory and is accepted in its present form by the Department of Physics, Quaid-i-Azam University Islamabad as satisfying the dissertation requirement for the degree of Master of Philosophy in Physics

Supervisor

Dr. Nawazish Ali Khan
Department of Physics
Quaid-I-Azam University
Islamabad, Pakistan.

Submitted through

Chairman
Prof. Dr. Pervez Hoodbhoy
Department of Physics
Quaid-I -Azam University
Islamabad, Pakistan

DEDICATION

Idedicate this research work to my parents, my family and my friends who have offered lot of prayers and rendered their complete possible support throughout all phases of its completion. It will be absolutely unfair to exclude my supervisor and my teachers of QAU that have afforded me opportunity to benefit from the rich experience and available facilities; I dedicate it to them all, as well.

Acknowledgement

It gives me great pleasure to express my most profound gratitude to **Allah Almighty,** the most beneficent and the most merciful. It is **His** boundless and infinite mercy that I have been able to complete my research work successfully. I offer my humble and sincere words of thanks to The **Holy Prophet Muhammad (P.B.U.H)** who is forever a source of guidance and knowledge for humanity.

I pay my heartiest gratitude to my Supervisor **Prof. Dr. Nawazish Ali Khan**, who has been very helpful, sympathetic and friendly throughout my M.Phil. His attitude, polite manners and personality always impressed me. He was always available for the fruitful discussion regarding my research problems.

I am thankful to Chairman, Department of Physics, **Prof. Dr. Pervez Hoodbhoy** for the provision of all possible facilities and full cooperation..

I need to also thank all of my Lab fellows. Special thanks to **Najam, Tayyaba, Mumtaz, Irfan, Sajid, Rahim, Adnan, Asad, Sami, Baber , all friends** and ex-Lab fellows. Thanks to **Mr. Najam, Ms. Tayyeba, & Mr.Sajid** specially as they offer their time for guidance and help .Finally, I need to thank to my loving parents, brother, brother in law, sister and cousins, my sincerest gratitude for all they have done. I could not wish for a more supportive, loving family, and for them I am deeply thankful and blessed.

SANA NAWAZ

Abstract

A weak link behavior of$(Cu_{0.5}Tl_{0.5})Ba_2Ca_2(Cu_{3-x}Sn_x)O_{10-\delta}$ (x=0, 0.25, 0.5, 0.75, 1.0, 1.25, 1.5) , superconductors were carried out which were synthesized by solid state reaction method. The crystal structure of these Sn doped samples is tetragonal and the axes lengths are found to increase with enhanced Sn doping concentration. The critical temperature and the magnitude of the diamagnetism are suppressed with enhanced doping of Sn. The samples turn into an insulator with very high room temperature resistivity if the Sn doping concentration is increased beyond y=1.5. The decreased magnitude of diamagnetism with Sn doping is most likely arising from the decreased concentration of mobile carriers in the CuO_2/SnO_2 planes, which may suppress the Fermi-vector and superconducting parameters. The decreased concentration of mobile carriers is most likely arising from the localization of the carriers at the Sn^{+4} sites in the conducting CuO_2/SnO_2 planes. The carrier concentration in the conducting CuO_2/SnO_2 planes has been enhanced by carrying out post-annealing experiments in the air and oxygen atmosphere. These annealing experiments increase oxygen concentration in the $(Cu_{0.5}Tl_{0.5})Ba_2O_{4-\delta}$ charge reservoir layer, which stops the flow of free electrons in the conducting CuO_2/SnO_2 planes. The lower density of free electron in CuO_2/SnO_2 planes at room temperature lowers the electron hole recombination processes at lower temperature. Since holes are majority carriers in the superconducting state, therefore, the density of holes in the conducting CuO_2/SnO_2 planes is enhanced with post-annealing in air and oxygen.

The critical current densities of the samples are calculated by using Bean's critical field model. The J_c values so obtained are fitted to the power law behavior of the type $(1-T/T_c)^n$ of various values of n. Both the as prepared and oxygen post annealed samples gave a best fit for n=1 for the superconductor insulator superconductor junction (SIS). This nature of material is due to oxide formation at the grain boundaries due to oxygen diffusion which possibly provide large surface areas to the shielding currents and enhance the J_c of the final compound.

Contents

List of Figures

1. Introduction and Literature Review:

A superconductor is an element or metallic alloy which, when cooled to near absolute zero, dramatically lose all of its electrical resistance. In principle, superconductors can allow electrical current to flow without any energy loss (although, in practice, an ideal superconductor is very hard to produce).

1.1 History of Superconductivity

James Dewar initiated research into electrical resistance at low-temperatures. Zygmunt Florenty Wroblewski conducted research in the electrical properties at very low temperatures, though his research ended early. Around 1864, Karol Olszewskii and Wroblewski predicted the electrical phenomena in ultra-cold temperatures of dropping resistance levels. Olszewski and Wroblewski documented evidence of this in the 1880s. Dewar and John Ambrose Fleming predicted that at absolute zero, pure metals would become perfect electromagnetic conductors (though, later, Dewar altered his opinion on the disappearance of resistance believing that there would always be some resistance). Walther Hermann Nernst developed the third law of thermodynamics and stated that absolute zero was unattainable [1]. A milestone was achieved on 10 July 1908 when Heike Kamerlingh Onnes at the Leiden University in Leiden for the first time liquified He and was subsequently able to reduce the temperature of liquid helium down to as low as 0.9 K. He had tried to measure the resistivity of metals as a function of temperature at very low temperatures. In 1911, after measuring the resistivity of Mercury, he found that the electrical resistivity of Mercury abruptly dropped to zero, the lowest measurable value, when the sample was cooled below 4.2 K [2]. Initially, Onnes called the phenomenon "*supraconductivity*" and later, adopted the term "*superconductivity*". In 1913, he won a Nobel Prize in Physics for his research in this field. Fig.1 shows disappearance of resistivity of Hg by H. K.Onnes together with his assistant G. Holst.

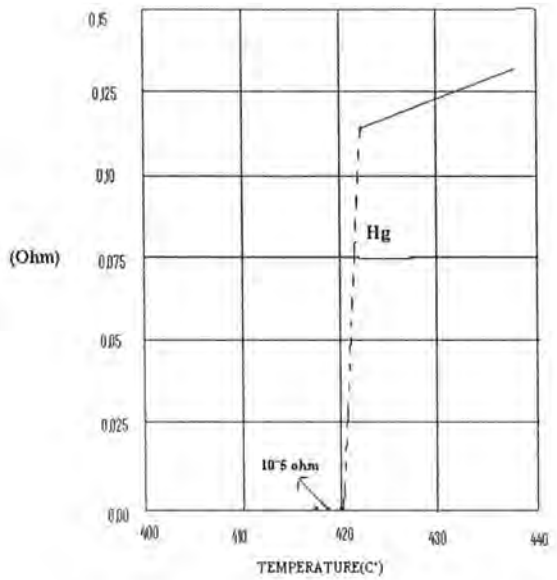

Fig.1: Resistance of Hg at low temperatures showing transition to superconductivity

His further investigation showed that other metals such as tin and lead also enter the superconducting state if they are cooled below 3.8 K and 7.2 K, respectively [4]. The temperature at which the transition from the normal state to the superconducting state occurs was called the *critical temperature* (T_c). Onnes also observed that although it was possible to pass a huge electric current through the superconducting mercury sample, there was a threshold value for the current density above which the sample would return to the normal state [5]. This threshold value, which is extremely important for practical applications, is called the *critical current density* (*Jc*) Moreover, Onnes also discovered that magnetic fields higher than *Hc*, the *critical magnetic field*, can similarly destroy the superconducting state.

A remarkable breakthrough was made in 1986 by Georg Bednorz and Alex Müller, at the IBM Laboratory in Rüschlikon, Switzerland, when they made a ceramic super-conductor from lanthanum, barium, copper, and oxygen with a transition temperature of 35 K [6]. Subsequently, by substitution of yttrium for lanthanum another ceramic superconductor with a transition temperature of 92 K was discovered [7]. This was remarkable because it now became possible to use cheap liquid nitrogen as the refrigerant. Since the transition temperature of the material was considerably higher than

those of the old superconductors, they called these materials the *High Temperature Superconductors* (HTS).

Fig.1.1 showed the history of superconductor development with time [8]. First Hg was discovered in 1911. Up to recent date the highest superconducting temperature (T_c) is still held by the Hg-based superconductor (153K) that was found in 1993. There are a total of 13 Nobel laureates, from H.K. Onnes (1913) to the recent one P. C. Lauterbur and Sir P. Mansfield (2003) on their contributions for theory, experimental results and application of superconductivity.

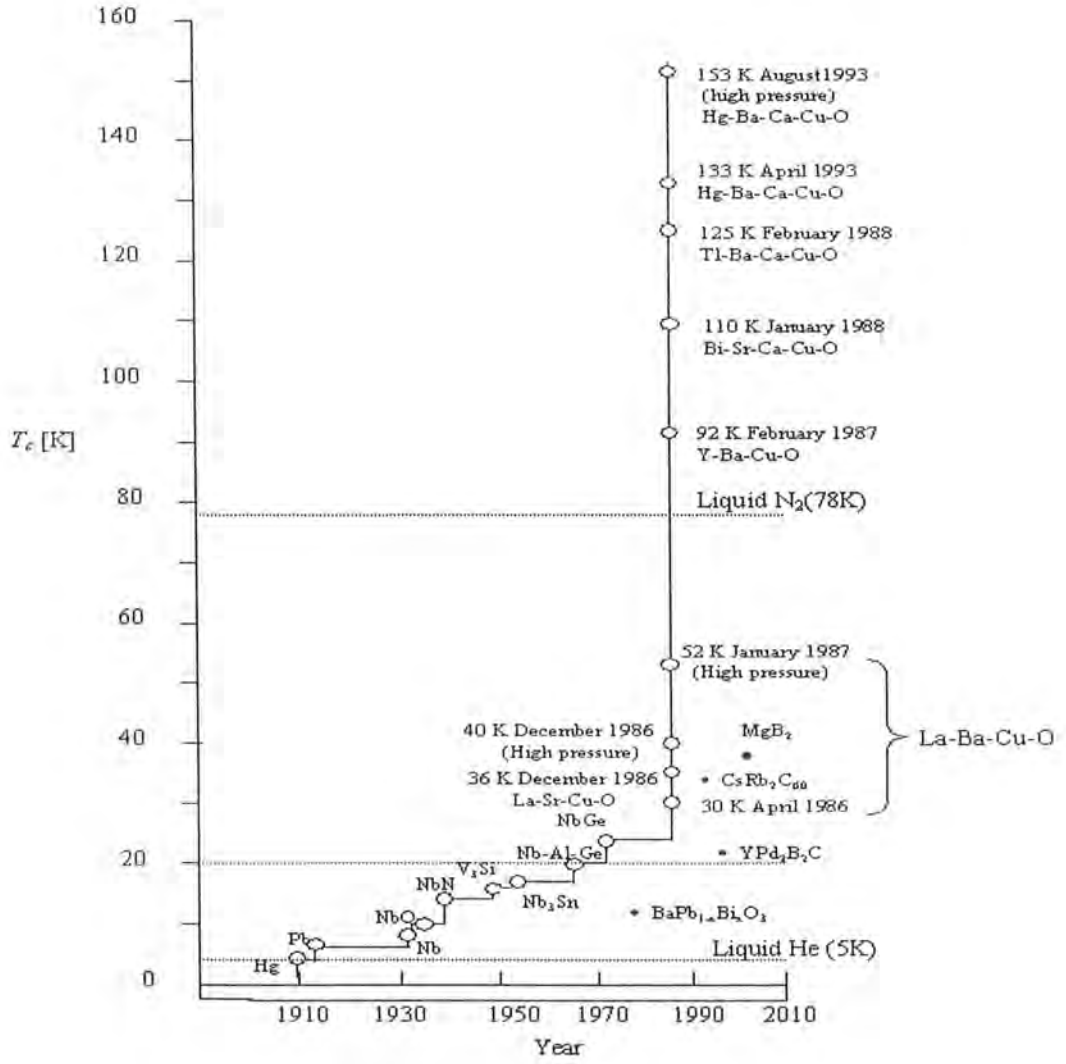

Fig 1.1 Evolution of T_c with time

1.2 Difference between superconductors & Non-superconductor Metals

The Fig.1.2 [3] shows the difference between superconductor and non superconductor behavior by a graph between resistance and temperature. As *critical temperature* (*Tc*) is appeared in superconductors not in non-superconductors.

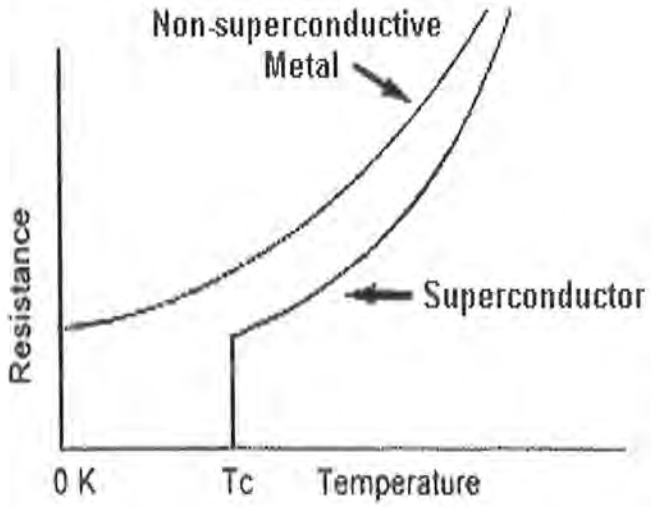

Fig 1.2 Graph between resistivity and temperature

1.3 Basic Parameters & Important Terms in Superconductivity

The important features of superconductor consisting of

1.3.1 Zero resistivity

1.3.2 Meissner effect

1.3.3 BCS Theory

1.3.4 Penetration Depth

1.3.5 Coherence length

1.3.6 Critical Current Density

1.3.7 Critical Magnetic Field

1.3.8 Correlation of Three parameters

1.3.1 Zero Resistivity

When a superconductor is cooled to its critical temperature $T_c(R=0)$, its resistance decreases to zero. Classically, the electrical conductivity σ is defined as

$$\sigma \equiv ne^2\tau/m$$

$$\Theta\ \rho \equiv {}^{1}/_{\sigma}$$

$$\Rightarrow \rho \equiv {}^{m}/_{ne^2\tau}$$

Where m, n, e and τ is mass of electron, number of electrons, charge on electron and mean free time respectively. As the temperature decreases, the lattice vibrations begin to freeze, therefore, the scattering of electrons from lattice vibrations diminishes. This in-turns results of enhancement of τ (the mean free time of the carriers between collisions) and decreases resistivity. For infinite τ at sufficiently low temperature the resistivity vanishes entirely which is observed in superconductors [9].

1.3.2 Meissner Effect

In 1933, Walther Meissner and his student Robert Ochsenfeld discovered an important magnetic property of superconductors. They observed that a magnetic field lower than *Hc* was suddenly expelled by superconductor specimens on cooling below *Tc* [7]. In other words, the material becomes fully diamagnetic in the superconducting state. This is called the *Meissner effect* and was found to be an intrinsic property of superconductors. It has been widely used for the testing of superconducting state. Due to the Meissner effect, if an external magnetic field is applied to a sample which is in the superconducting state, an electric current is produced near the surface of sample, in such a way as to create a magnetic field that exactly cancels the external magnetic field.

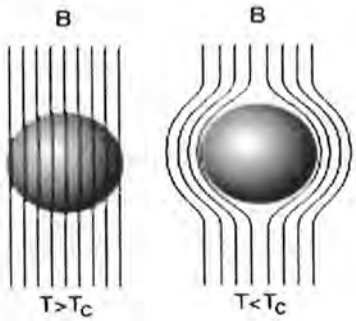

Fig.1.3. Diagram of the Meissner effect. Magnetic field lines, represented as arrows, are excluded from superconductor when it is below its critical temperature.

1.3.3 BCS Theory

In 1957 Bardeen, Cooper and Schreiffer (BCS) published the first truly microscopic theory of superconductivity and they received the Nobel prize in physics in 1972 for this theory.

Consider an electron moving through a lattice shown in figure, it pulls the positive ion cores towards it and changes the charge density in its vicinity. It leaves a somewhat higher positive charge density in its wake than would otherwise be there. This positive charge attracts other electrons. The electrons interact with one another through the intermediary of the lattice. The net result is a slight attraction of the electrons for each other. This theory shows that the electrons system has the lowest possible energy, if the electrons are bound together in pairs called *Cooper Pairs*. When no current exists in a superconductor, the two electrons of a cooper pair have momenta of equal magnitude but exactly opposite directions so that the total momentum and the electric current both vanishes . When a current is generated, both electrons in a pair acquire the same increase in momentum, resulting in a motion of the center of mass of the pair. All cooper pairs acquire the same momentum [11]. This can be seen in fig. 1.4.

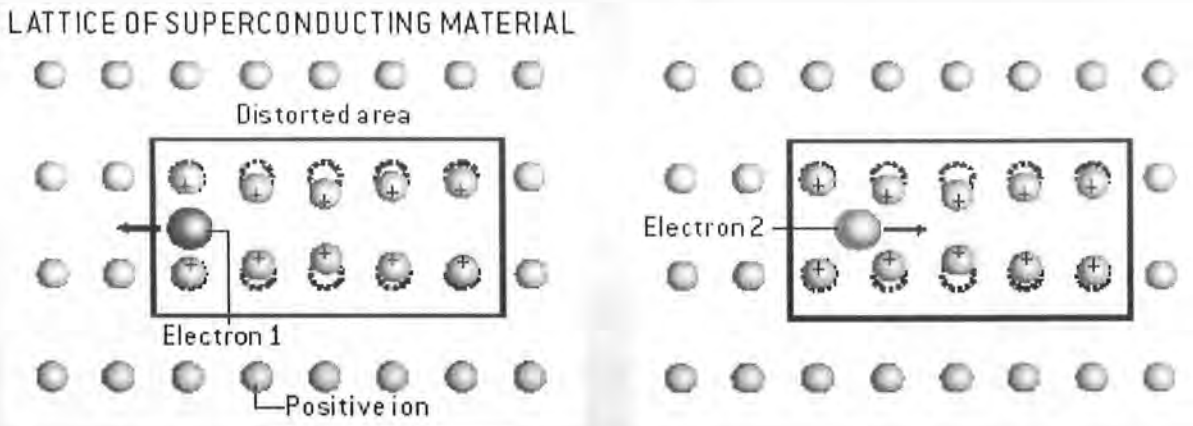

Fig 1.4: Lattice distortion and formation of cooper pairs in superconductors.

The cooper pairs have a binding energy Δ, called pairing energy which is typically in the range of 10^{-4} to 10^{-3} eV. The critical temperature of superconductors is directly related to

the pairing energy. Above T_c the pairs are broken and the material has normal electrical resistance [11].

1.3.4 London penetration depth (λ)

According to London equations[12] the magnetic field falls exponentially with increasing distance inside the surface of a superconducting sample.The characteristic decay length is called the *London penetration depth* (λ).

$$B(x) = B(0)\exp(-\frac{x}{\lambda_l})$$

B(0) is the magnetic field at the surface of the superconductor. The above equation shows magnetic field fall exponentially from the surface of the superconductor towards its interior, where λ_l is called penetration depth and it determines the rate of decay of the magnetic field. The penetration depth for most superconductors is of the order of fractions of microns [13].

1.3.5 Coherence length (ξ)

Seven years later, three physicists at the University of Illinois in Urbana, John Bardeen, Leon Cooper and Robert Schrieffer, presented a theoretical explanation for the superconducting state [14]. This theory was widely accepted and is well known as the *BCS theory*. Based on this theory, despite the Coulomb repulsive forces between the electrons,due to distortion in the crystal structure,slight attraction between pairs of electrons located near the Fermi surface leads to the production of bonded pairs of electrons, called *Cooper pairs* [15]. The size of a Cooper pair in a superconductor is known as the *coherence length* (ξ). The BCS theory explained superconductivity in the low temperature and low magnetic field regime. Soon after that, the BCS theory was extended and become useful for high magnetic fields as well [16].

1.3.6 Critical Current Density

Since there is no loss in electrical energy when superconductors carry electrical current, relatively narrow-wires made of superconducting materials can be used to carry huge currents. However, there is a certain maximum current that these materials can be made to carry, above which they stop being superconductors. If too much current is pushed through a superconductor, it will revert to the normal state even though it may be below its transition temperature. The value of Critical Current Density (J_C) is a function

of temperature; i.e., the colder you keep the superconductor the more current it can carry. Fig.1.5 is a graph of voltage versus current for a superconductive wire.

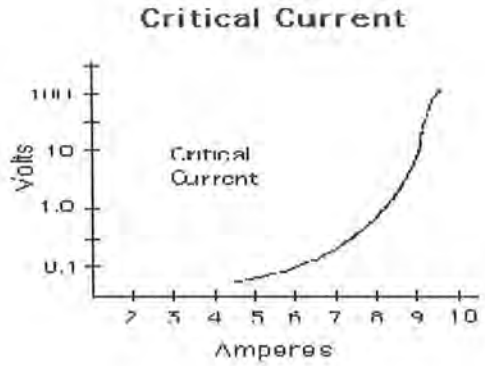

Fig.1.5. Voltage versus current graph for a superconductive- wire.

For practical applications, (J_C) values in excess of 1000 amperes per square millimeter (A/mm^{-2}) are preferred.

1.3.7 Critical Magnetic Field

An electrical current in a wire creates a magnetic field around a wire. The strength of the magnetic field increases as the current in the wire increases. Because superconductors are able to carry large currents without loss of energy, they are well suited for making strong electromagnets. When a superconductor is cooled below its transition temperature (T_C) and a magnetic field is increased around it, the magnetic field turns the superconductor or a portion of it to a normal material. Physicists use the capital letter H as the symbol for Magnetic Field. If the magnetic field is increased to a given point, the superconductor will go to the normal resistive state. The maximum value for the magnetic field at a given temperature is known as the critical magnetic field and is given the symbol (H_C). For all superconductors there exist a region of temperatures and magnetic fields within which the material is superconducting. Outside this region, the material is normal. Fig.1.6 demonstrates the relationship between temperature and magnetic fields.

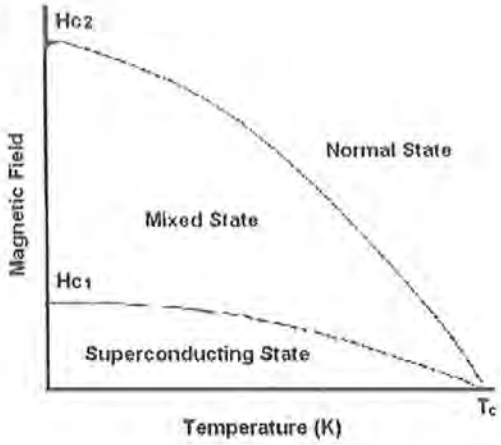

Fig.1.6 Relation between the temperature and magnetic field.

1.3.8 Correlation of three Critical Values:

As we know that superconducting state has three very important factors.

1) Critical Temperature (T_c)

2) Critical Magnetic Field (H_c)

3) Critical Current Density (J_c)

Each of these parameters is very much dependent on the other two properties present. Maintaining the superconducting state requires that the magnetic field and current density as well as the temperature remain below the critical values, all of which depend upon the material. The phase diagram of Fig.1.7 demonstrates the relationship between the three critical properties.

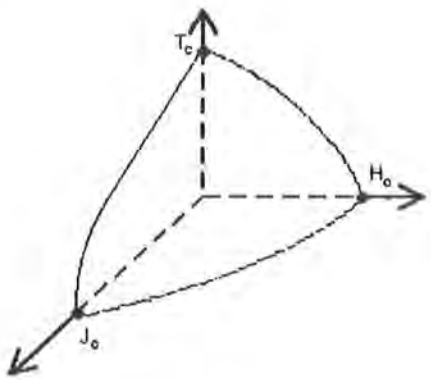

Fig.1.7 A correlation between J_c, T_c, and H_c for a superconductor

The highest values of J_c and H_c occur at 0K, while the highest value of T_c occurs when H and J are zero.

When considering all three parameters, the plot represents a critical surface. From this surface and moving towards the origin, the material is superconducting. In the regions outside of this surface, the material is normal or in a mixed state.

1.4 Types of Superconductors

According to their magnetic properties, superconductors are divided in to two following types

1.4.1 Type I superconductor

1.4.2 Type II superconductors

1.4.1 Type I Superconductors

Type I superconductors or formerly soft superconductors are very pure metals. For example very pure samples of lead, mercury, and tin are examples of Type I superconductors. Complete Meissner effect (i.e. B=0 inside a superconductor) is observed in type I superconductors. Fig.1.8 is a graph of induced magnetic field of a Type I superconductor versus applied field. Fig.1.8 shows that when an external magnetic field (horizontal abscissa) is applied to a Type I superconductor the induced magnetic field (vertical ordinate) exactly cancels that applied field until there is an abrupt change from the superconducting state to the normal state. The values of H_c are always too low for type I superconductors to have any useful technical application in coils for superconducting magnets.

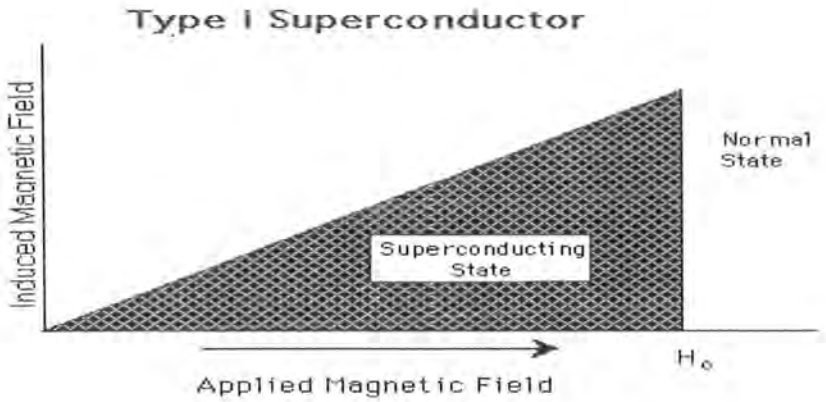

Fig.1.8. Magnetization versus applied mangnetic field for a bulk superconductor exhibiting a complete Meissner effect (perfect diamagnetism). A superconductor with this behavior is called a Type1 superconductor. Above the critical field, H_c the specimen is a normal conductor and the magnetization is too small to be seen on this scale.

1.4.2 Type II Superconductors

High temperature ceramic superconductors such as $YBa_2Cu_3O_7$(YBCO) and $Bi_2CaSr_2Cu_2O_9$ are examples of Type II superconductors. Figure (1.9) is a graph of induced magnetic field of a Type II superconductor versus applied field. Type II superconductor have superconducting electrical properties up to a field denoted by H_{c2}. Between the lower critical field H_{c1} and the upper critical field H_{c2} the flux density $B\neq0$ and the Meissner effect is said to be incomplete. The value of H_{c2} may be 100 times or more higher than the value of the critical field H_c calculated from the thermodynamics of the transition. In the region between H_{c1} and H_{c2} the superconductor is threaded by the flux lines and said to be in vortex state [9]

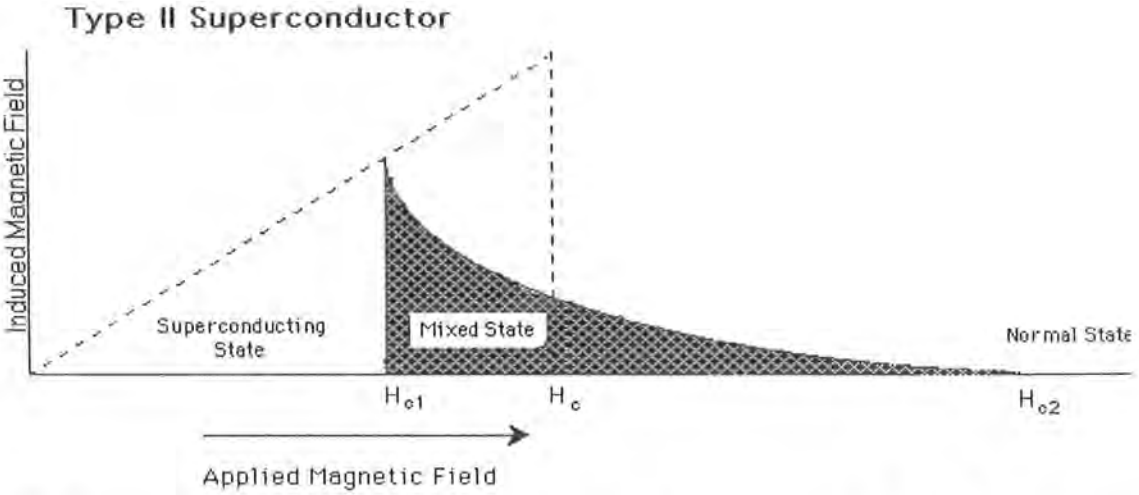

Fig.1.9 Superconducting magnetization curve of a Type II superconductor. The flux starts to penetrate the specimen at a field Hc1 lower than the thermodynamic critical field H_c. The specimen is a vortex state between H_{c1} and H_{c2}, and it has superconducting properties up to Hc2. Above Hc2 the specimen is normal conductor in every respect, except for possible surface effects. For given H_c the area under the magnetization curve is same for Type II superconductor as for a Type I.

A hard superconducter is a Type II superconductor with a large magnetic hysteresis usually induced by mechanical treatment such materials have an important medical application in magnetic resonance imaging (MRI).

1.5 Josephson Effect

In 1962 Brian D. Josephson, a 22 years old British student at Cambridge University, predicted that via a tunneling process, electric current could flow between two superconducting materials separated by a thin (a few nano-meter thick) insulating layer or weak link [13]. Later, his prediction was experimentally confirmed and became known as the *Josephson effect* and the arrangement of two superconductors linked by a non conducting barrier is known as *Josephson junction,* the current that crosses the barrier is the *Josephson current.* This phenomenon is widely used in applications of superconductor.

1.5.1 Types of Weak Links:

Weak link is just a convenient place for letting interference effects become visible. The most famous example is the quantization of magnetic flux in a superconducting ring: which means the corresponding supercurrent will also be quantized and the quantization of super-current (current without a voltage drop) is typically an

interference effect. The current can assume only those values that yield an integral number of wavelengths of the superconducting wave function over the length of the ring. This situation is exactly analogous to the quantization of electron states in Bohr atom [23].

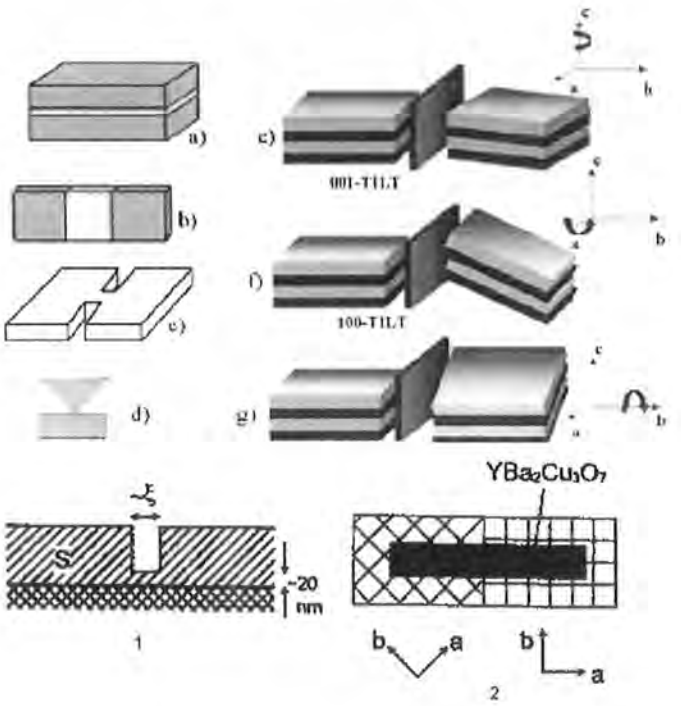

Fig 1.10: Different configurations of weak-links: junction with (a) insulating or (b) normal metal barrier; (c) micro bridge; (d) point contact; (e) 001 tilt, (f) 100 tilt and (g) 100 twist grain boundary Junction, (1) sandwich superconductor between two superconductors, (2) grain boundary weak link.

Different types of weak links are discussed here. First, there are devices without concentration of current such as tunnel junction as shown in fig.1.10(a). The thickness of an insulating layer is typically about 1-2 nm and the critical current density is in the range $10\text{-}10^4 Acm^{-2}$ i.e., much less than critical current density of the bulk superconductors [23].

In superconductor-normal metal-superconductor (SNS) sandwiches, the normal layer can be as thick as 10^{-4}cm as in fig.1.10(b). The wave functions of the superconducting electrons penetrate the normal metal. In the region of their overlap, the wave functions interfere, with the consequence that phase coherence is established

between the bulk superconductors. If the amplitude of the superconducting wave function in the weak link is small, the critical current is also small [23].

The same effect can be achieved if the normal layer between the two superconductors is replaced by another superconductor with a small current density. For example, if a narrow superconducting film is covered with a narrow film of a normal metal as in fig 2(c), the amplitude of the superconducting electron wave function in the film is reduced where the film is in contact with the normal metal. This causes a local decrease of the critical current density, that is, a weak link is established [23].

In devices with concentration of current, the critical current density in the weak link is same as in the bulk, but the absolute value of the critical current is much less. A superconducting film with a short narrow constriction falls into this category provided the size of the constriction is of order of the coherence length ξ as shown in fig. 1.10(d). Another example of a bridge of variable thickness of the bridge itself is only several dozen nm as shown in fig1.10 (1) [23].

Finally, a weak link of high-temperature superconductors is shown in the fig. 1.10(2). It is called a grain boundary (bi-crystal). Due to the extremely short coherence length in high-T_c materials ($\xi \sim 1$nm), defects can be produced between two regions of an epitaxially grown high-T_c film with different crystal orientations. The critical current density of such a weak link can be varied by changing the misorientation angle between two crystalline. Each HTS grain boundary can be considered the composition of the three fundamental operations of: tilt around the *c*-axis (001 tilt): fig. 1.10(e), tilt of the *c*-axis around the *a*- or *b*-axis (100 tilt): fig.1.10 (f) and twist around the *b*-axis (100 twists): fig. 1.10(g). In figs. 1.10(e-g) the orientation of the left electrode has been fixed, but it can also change. Grain boundaries influence the Josephson phenomenology which is still subjected to microstructural barriers imperfections [24].

1.6 Cuprate High-Temperature Superconductors

Cuprate High-Temperature Superconductors (HTS) play an outstanding role in the scientific development and for the present understanding of superconductivity

- A huge number of samples have been produced, in quantities of the order of metrical tons.

- Details of materials science have been diligently elaborated.
- High reproducibility has thus been achieved taking the materials complexity into account.
- The whole tool-set of experimental solid-state physics has been applied. For some techniques such as photoelectron spectroscopy [18, 19], inelastic neutron scattering [20] or scanning tunneling microscopy [21,22] HTS have become a drosophila-like favorite object of investigation which still challenges further methodological development.
- HTS still represent a great challenge to theoretical solid-state physics since not only the superconducting but even more the normal conducting state of HTS is awaiting a satisfactory explanation.

1.6.1 Difference between High-Temperature Superconductors and Low Temperature Superconductors

Cuprate High-Temperature Superconductors (HTS) have number of features in common which make them very unlike typical Low- Temperature Superconductors. They are layer compounds.They are typically tetragonal or orthorhombic and close to tetragonal and contain CuO planes with the formula CuO_2 lying normal to the c direction.These planes contain mobile charge carriers and are thought to be the seat of the superconductivity.The carriers are sharply localized in the planes and this makes contact between the planes relatively weak for this reason the cuprates often have extremely anisotropic properties in both the normal and the superconducting states with poor conduction in c direction.

The carrier density is relatively low comparable with what is found in semi metals such as bismuth. This means that the carriers are less heavily screened than they are in ordinary metals and makes the coulomb repulsion between them more important. It also increases the penetration depth which is typically 0.2 um for current flow in ab plane.

They all have extremely short coherence length typically 2 nm with in CuO_2 planes and as little as 0.3 nm in the c direction. This has many important consequences. It makes thermal fluctuations much larger .It also makes defects such as impurity concentrations, grains boundaries and surface rearrangements much more important.

Finally cuprates are very sensitive to carrier doping and are only superconducting for a particular range of doping level.

1.6.2 Obstacle for supercurrents in High-Temperature Superconductors

Beside many intrinsic obstacles for the transport of supercurrent in single-crystalline HTS materials there are many additional hurdles since HTS materials are not a homogeneous continuum as they are a network of linked grains Fig.1.11. The crystal growth mechanism is such that all material that cannot be fitted into the lattice structure of the growing grains is pushed forward into the growth front with the consequence that in the end all remnants of secondary phases and impurities are concentrated at the boundaries in-between the grains. Such barriers impede the current transport and have to be avoided by careful control of the growth process.

Fig 1.11 Schematics of the HTS microstructure: Differently oriented single crystal grains are separated by regions filled with secondary phases. In addition, oxygen depletion may occur at grain boundaries

Another obstacle for supercurrents in HTS is misalignment of the grains:

1.6.3 Oxygen nonstoichiometry Effects

Oxygen nonstoichiometry is known to play a vital role in the geometric and electronic structure of high Tc superconducting cuprates. The carrier concentration and superconducting properties are essentially controlled by the oxygen content.

1.6.4 Substitutional Studies

The site occupancy in Substitutional studies is controlled by

(1) Ionic radii,

(2) The valence state

(3) The coordination number of the on-site cation.

1. Substitution at Tl site:

The cations which are chosen for substitution at the Tl site as reported in the literature are cadmium, lead, bismuth, antimony, and potassium. Tl^{3+}, Pb^{4+}, Bi^{5+} have identical electronic configuration and somewhat similar chemistry. Their ionic radii for six coordinations are also close to each other and satisfy the criteria for substitution. Pb and Bi also exhibit multi-valency (e.g., thallium)-namely, Pb^{4+}/Pb^{2+} and Bi^{5+}/Bi^{3+}---- and would affect the copper valence on substitution and also the Tl^{3+}/Tl^{+} ratio. Potassium is another important cation which resembles Tl in chemical properties [60].

2. Substitution at Ba/Ca sites:

Ba, Sr, Ca, rare earths and yttrium exhibit high coordination numbers, the ionic radii and are also close to each other and thus satisfy the criteria for substitution. Ba show more closeness in ionic radii to that of lighter lanthanides,whereas, Ca and Y Ionic radii are very close to each other. In view of this, it appears that lanthanides and yttrium can be substituted totally for Ba and Ca in these compounds. The substitutional studies in the Tl based cuprates have been used effectively to stabilize the structure in the single Tl-O layer phases and have helped in the easy synthesis of these phases in bulk.

1.7 Thallium Based High Temperature Cuprates:

In Tl-Ba-Ca-Cu-O system, a number of compounds have been discovered [26]. These compounds differ from one another by the number of superconducting planes and charge reservoir layers. Some Tl-based compounds have double TlO layers in the charge reservoir layer (i.e., $Tl_2Ba_2CuO_{6+y}$, $Tl_2Ba_2CaCu_2O_{8+y}$ and $Tl_2Ba_2Ca_2Cu_3O_{10+y}$ etc.) and are represented by a specific naming scheme Tl-2201, Tl-2212 and Tl-2223 etc. In this naming scheme, the last digit represents the number of CuO_2 planes in the compound. In these materials the transition temperature T_c lies in the range of 80-120K. Another family of Tl-based superconductors, such as $TlBa_2Ca_{n-1}Cu_nO_{2n+3}$ containing only single Thallium atom in the charge reservoir layer has been grown with n CuO_2 planes (n = 1-5) [26-29]. In all these crystal structures, we see that unit cell is composed of one, two, three, four and five CuO_2 planes. So with the increase in the number of CuO_2 planes the T_c also increases up to n = 3 and has been observed to decrease with n > 4. The understanding of crystal chemistry of these Tl-based compounds, leads to the formation

of a compound with n = 4, the composition of this phase is $TlBa_2Ca_3Cu_4O_{11}$ (1234) and its structure is tetragonal with lattice constants a = b = 3.88Å, c = 18.0Å. The $TlBa_2Ca_3Cu_4O_{11}$ (1234) compound is reported to have relatively higher resistances at the room temperatures as compared to the other known structures, possibly due to the presence of completely insulating charge reservoir layer. In order to reduce the effect of high resistance $Cu_{1-x}Tl_xBa_2Ca_3Cu_4O_{12-\delta}$ superconductors have been prepared [30].Unit cell of $Cu_{1-x}Tl_x$-1223 is shown in fig.1.12.

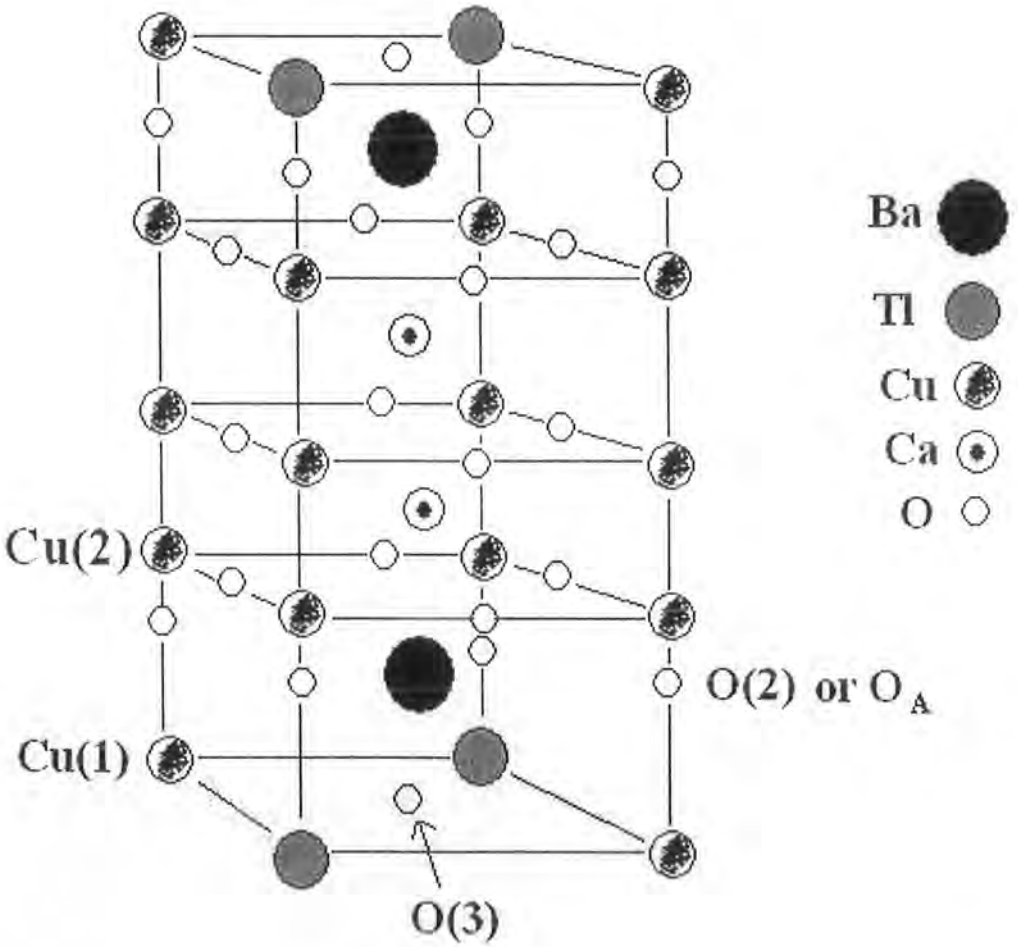

Fig.1.12. Unit cell of CuTl 1223

1.8 Applications

Due to the vast development of superconducting materials, they find a large range and diversity of application in different fields. Following are some of the important applications [32].

Superconducting magnets

Normally, when current flows through a coil, it generates magnetic fields. If the coil is replaced by a superconducting material, it generates a large magnetic field. In the conventional high field electromagnets, the effect of joule heating is a major problem, while in superconducting materials, the current flows without any resistive loss and joule heating. Therefore, high critical magnetic field superconductors are used for the application. The most widely used superconducting materials are type II superconductors such as Nb-Ti and Nb_3Sn compounds. The important applications of superconducting magnets are NMR, medical diagnostics and spectroscopy, magnetic levitation trains.

High field magnets

For the moment the most important practical application of superconductivity is in producing a high magnetic field. There is no doubt that for this purpose a super conducting solenoid is superior to conventional magnets; since these coils withstand vary high critical current density.

Switches and memory elements

The use of superconductors as switches follows from their property of becoming normal in the presence of a magnetic field.

Suspension system and motors

Frictionless suspension systems may be realized by the interaction between a magnetic flux produced externally and the currents flowing in a superconductor. It is quite obvious that the idea of a hundred percent efficient motor can be achieved with superconductor [31].

Magnetic separation

Magnetic separation is a process used for decades in mining and chemical industry. Application of this process may be found in elaboration of iron ores and also in the processing of kaolin clay. This separation processes is based on the different magnetic characteristic of the material to be isolated. If the material to be separated is ferromagnetic, as Fe, Ni and Co then weak magnetic field may be used and there is no need for superconducting magnets. On the contrary, weak magnetic minerals, such as hematite, garnet or limonite, require the use of intense magnetic fields for the separation from a nonmagnetic matrix.

Particle accelerators

Superconductivity technology is applied to particle accelerators into primary areas i.e., to save energy and to produce high magnetic fields, therefore, the superconducting magnet is necessary in the construction of high quality superconducting accelerator cavities; the primary propose in the later case is to achieve high accelerating field gradients and to reduce the radio frequency power requirements.

Microwave antennas

The new ceramic superconductors can be used in antenna applications. HTS films, with very low surface resistance, possess excellent performance in microwave passive devices, compared with the normal conductors. Many superconductive microwave devices need to work in strong dc-magnetic fields.

Besides the scientific interest, the search for applications has always been a driving force for superconductor materials science [33].

Superconductors are materials that lose their resistance to electrical current flow below a certain critical temperature (*Tc*), a certain critical current density (*Jc*) and certain critical field (*Hc*). Superconductors have generated great interest for power applications including loss-free electric transmission cables, motors, generators, transformers, energy storages, levitation trains, ultra-fast computers etc. Besides that, the superconductivity phenomenon also opens the challenges to modern physics of superconductors [34, 35].

1.9 Literature Review

M.M.Abd-Elmeguid et al [36] investigated the effect of Sn doping on the magnetic and superconducting properties of $La_{2-x}Sr_xCu_{1-y}Sn_yO_4$ with $0 < x < 0.15$ and $0 < y < 0.01$.Measurements of the Sn Mossbauer isomer shift reveal that Sn is tetravalent in the whole concentration range $0 < x < 0.15$ .on the other hand ,the electrical resistivity, Neel temperature,and the superconductivity are found to be affected by Sn content.In the anti- ferromagnetic state x=0, 0.008, Neel temperature is Slightly affected by increasing Sn content.In the superconducting state x=0.065, 0.10 and 0.15. *Tc is strongly supressed* with increasing Sn content. It is shown that the variation of Neel temperature upon Sn doping depends on the competition between two mechanism.

(1) Magnetic disorder due to the nonmagnetic impurity which induces an uncompensated local magnetic moment on the CuO_2 lattice and therefore tends to decrease Neel temperature.

(2) Reduction of the free O holes by the excess electrons introduced by Sn which leads to stabilizing the anti ferromagnetic order and increasing Neel temperature.

Candida C. Silva *et al* [37] investigated AC losses in high temperature granular YBCO samples. Individual grains were anisotropic and these polycrystalline samples had randomly oriented c-axes. AC susceptibility was measured as a function of magnetic field, frequency and temperature. Three types of temperature dependent loss peaks were observed. The three peaks types (in χ'') were attributed to intrinsic (London theory), Intergranular Josephson junction, and intragranular pinning loss mechanisms, respectively.

K. C. Hung *et al* [38] investigated the intergranular pinning properties in high-T_c, $YBa_2(Cu_{0.9}Cd_{0.1})_3O_{7-\delta}$ superconductor by ac susceptibility response. Both the intergranular and intragranular peaks were observed. The effective pinning potential was found to be inversely proportional to the power of magnetic field. This indicated the formation of intergrain Josephson tunneling, acted as a weak link network, having a collective pinning behavior. As the dc field increased from 0mT with increment by 0.022mT, the intergranular peak was shifted rapidly to the low temperature side while the intragranular peak showed nearly no shift at all. This was the fact that the Josephson weak link was very sensitive to the external dc field. From the temperature dependence of the intergranular critical current density, the exponent a for the scaling law of $J_c(T) = J_c(O)(1-T/T_c)^a$ was found to be 0.9, where $J_c(0)$ was the critical current density at T = 0K and T_c.

P. Kameli *et al* [39] studied the intergranular properties of $(Bi,Pb)_2Sr_2Ca_2Cu_3O_y$ polycrystalline samples. The XRD results showed that the increasing sintering temperature up to 865°C, the Bi-2212 phase fraction decreased. It was found that the Bi-2212 phase on the grain boundaries was likely to play the role of weak links and consequently reduced the intergranular critical current densities. Ac Susceptibility near the transition temperature was analyzed. The observed variation of intergranular critical current densities (J_c) with temperature indicated that the weak links were changed from

superconductor–normal metal–superconductor (SNS) for well-coupled sample to superconductor–insulator–superconductor (SIS) type of junctions for the sample with high Bi-2212 phase fraction.

M. Tape *et al* [40] investigated weak link profile of $YBa_2Cu_{1-x}Ag_xO_{7-\delta}$ using techniques like (R-T), (χ-T), SEM, and XRD. The improvement in the structural and superconducting properties of the samples were observed with the variation of cationic ratio of Ag up to x = 0.2. The critical current density of the sample C enhanced by the factor of 169% at 77 K and B = 0mT. By the investigation of magnetic field dependence of the critical current density, they observed that the Jc versus B dependence decreased with increased Ag content up to x = 0.2 showed that the Ag doping improved the grain growth and their orientations, and modified the inter-grain weak-links. During processing of YBCO ceramics, liquid Ag filled into the pores of the structure and modified the micro cracks thus strengthened the role of pinning centers. However, when the Ag doping exceeded x = 0.2 the structure and thus the superconducting properties of the samples deteriorated. The excess amount of silver played a role of preventing factor for the growth of YBCO grains. Consequently, grains become smaller and arbitrarily oriented hence showing lower performance for the high current applications.

Francesco Tafuri *et al* [41] made conclusion about weak links that often appear to be independent transport channels, such as for cooper pairs or quasi-particles. These channels would be subject to different selection rules in such an anisotropic and inhomogeneous configurations. These junctions might have some sort of intrinsic quantum protection, despite the poor interface quality and short coherence lengths. Low-energy quasi-particles generated a surprisingly low level of dissipation, allowing the observation of macroscopic quantum effects.

Magnetic susceptibility of bulk thallium based (2223) compound was measured with Au and Ag doping by M.Yang *et al* [42]. Significant enhancement of intergranular critical current density was demonstrated and also methods for convenient determination of the intergranular weak link phase-locking temperature and average lower critical field in the bulk granular superconductors were discussed.

N Balchev et al [43] prepared, investigated and studied a new mercury-based superconductor with nominal composition. $Hg_{1-x}Sn_xBa_2Ca_2Cu_3O_y$ ($0 < x < 0.5$).At that

stage of investigation the material was multiphasic with dominating superconducting phases up to x =0.3. It was established that Sn stimulates the growth of the Hg-1212 phase and enhances the diamagnetic volume fraction together with the weaklink behaviour. The SEM–EDS analysis showed that Sn is incorporated into the superconducting grains. The shift of some of the XRD peaks, as well as the broadening of the magnetic transition and gradual decrease of Tc with the dopant content x, suggested that the substitution really occurs and some of the Sn is incorporated into the structure of the superconducting phases.

Wu Ming Chen et al [44] studied the effects and influence of Sn doping on superconductivity in the Bi-based 2212 phase.The samples were characterized by *R-T* relations, magnetic hysteresis loops, X-ray powder diffraction analysis. For $Bi_{1.75}Pb_{0.25}Sr_2CaCu_{2.3-x}Sn_xO_y$, the experimental results show that by adding the proper amount of Sn, the superconductivity of the samples can be improved. As x = 0.15, the critical temperature *Tc*, the critical current density *Jc*, and the magnetic pinning force density *F* reach a maximum. The experimental results also show that the Sn doping is able to speed up the growth of the 2223 phase. In brief, Sn doping is an effective way of improving the superconductivity in Bi-based superconductors.

A F Dong [45] investigated the structural changes and superconductivity of $La_{1.85-2x}Sr_{2x+0.15}Cu_{1-x}Ru_xO_4$ (I) and $La_{1.85}Sr_{0.15}Cu_{1-x}Ru_xO_4$ (II) systems. It was found that in all $La_{1.85}Sr_{0.15}Cu_{1-x}M_xO_4$ systems investigated (M = Ru, Li, V, Sn, Al, Ga, Co, Fe, Mn, Mg, Ni and Zn), the structure parameter *c/a* ratios decrease with increasing doping content *x*, which is a common characteristic. The mechanisms for *T*c suppression were summarized. Some mechanisms for interpreting *T*c suppression in $La_{1.85}Sr_{0.15}Cu_{1-x}M_xO_4$ systems have been proposed, including the following.

(1) The magnetic pair-breaking effect. *T*c suppression in $La_{1.85}Sr_{0.15}Cu_{1-x}M_xO_4$ (M = Fe, Co, Ni, Zn, Ga and Al) was attributed to the Cooper pair-breaking effect arising from magnetic impurity scattering.

(2) The strong potential scattering effect.

(3) The carrier localization effect. It was asserted that the two-dimensional hole localization induced by doping is the essential origin of the metal–insulator transition. Besides the mentioned above, the structural disorder, oxygen vacancy,

oxidation state of Cu, spin state of the dopant, low energy spin excitation etc were also considered as factors in the *Tc* suppression. These indicate that a universal mechanism for *Tc* suppression has not been found to date.

Halbritter [46] discussed important extrinsic and intrinsic conduction in cuprates, anisotropy and weak links . It was found that defects enhance the intrinsic perpendicular conductivity $\sigma^{\perp} \leq 1/\Omega$-cm whereas large intrinsic parallel conductivity i.e., $\sigma^{//} \geq 10^4/\Omega$-cm degraded by defects. E_f,n_s (density of metallic state), n_L (density of localized state), in various cuprate banks were compared. Different grain boundaries associated with cuprates, evidence for WL was presented by normal and superconducting measurements were discussed. Combined $\rho(T)$, weak link boundary resistance $R_{bn} \approx 10^{-7}$ -10^{-9} Ω-cm^2 were deduced in superconducting state. J_c values were explained by localized states allowing resonant tunneling. Defects enhance $\sigma^{\perp}$ and especially as weak links reduced $\sigma^{//}$ and $J_c^{//}$ in contrast to YBCO for Bi cuprates the intergranular $\sigma^{\perp}$ and $J_c^{\perp}$ stayed large.

Yong Feng [47] investigated a highly textured $YBa_2Cu_{2.95}Sn_{0.015}$, sample prepared by the powder melting process method. They suggested that the surface defects may be responsible for the effective pinning centers in our samples. The J, value and the pinning force were improved by Sn being substituted for Cu. The pinning force density increased as the field increases within the temperature range 60-77 K for the $YBa_2Cu_{0.95}Sn_{0.015}$, specimen. The size of particles can be reduced by Sn addition.

The ac susceptibility of the two compounds $YBa_2Cu_3O_{7-\delta}$ and $YBa_2Cu_{2.985}Ag_{0.015}O_{7-\delta}$ was measured as a function of temperature, ac magnetic field strength and frequency by S. LO. Shinde *et al* [48]. The presence of two loss peaks in the imaginary component of the ac susceptibility was confirmed by comparison of ac and dc magnetic fields on materials with different microstructures. One peak in imaginary part of susceptibility was associated with the matrix transition and other, at lower temperatures, with weak link behavior at grain boundaries.

J Feng [49] studied the relationships between the crystal structure modification, due to the doping element of Sn, and the critical temperature *Tc* of Sn-doped $YBa_2Cu_{3-x}O_7$, with x=0, 0.1, 0.2, 0.3, 0.4, 0.5, 0.6, have been investigated by means of the peak shift and the peak broadening of the powder x-ray diffraction pattern. The substitution of Cu by a Sn atom generates some static thermal vibration effect, which reflects on the

lattice spacing parameters *a*, *b* and *c*. The data of FWMH obtained from XRD patterns confirm that the active mode of the thermal vibration is along the *c*-axis; in accordance with the results obtained from the Raman scattering measurement. The critical temperature, *Tc*, of the superconductors $YBa_2Cu_{3-x}Sn_xO_{7-\delta}$, with $x=0$ to 0.6, is sensitive to its expansions in both of *a*- and *b*-directions. The *c*-axis direction showed no significant expansion due to the Sn-doping effect. In general, the higher the Sn doping level, the greater the expansion along *a* and *b* and the lower the critical temperature. The thermal vibration, however, was found to be dominant along the *c*-direction, and this seems to support the theoretical prediction based on the in-plane sensitive mechanism of high temperature superconductivity.

Weak link behavior of $YBa_2Cu_3O_x$(123) superconductor by L. C. Pathak *et al* [50] sintered in different atmosphere were studied by measuring the variation of critical current densities (J_c) near the superconducting transition temperature (T_c). The weak links were found to change from superconductor-insulator-superconductor to superconductor-insulator-metal-superconductor and superconductor-metal-superconductor type of junctions as the sintering atmosphere was varied from Argon to air and oxygen respectively. The scanning electron microscopy in conjunction with energy dispersive spectroscopic studies indicated that the composition fluctuation at the grain boundaries was supposed to be the reason for such variations.

J.Q. Li et al [51] studied the effects of Sn doping in $Hg_{1-x}Sn_xBa_2Ca_2Cu_3O_8$ samples. Sn doped samples of $Hg_{1-x}Sn_xBa_2Ca_2Cu_3O_8$ with x=0, 0.05, 0.1, 0.2, 0.4, 0.5were synthesized in sealed silica tubes by the solid state reaction method.A small amount of Sn doping in $Hg_{1-x}Sn_xBa_2Ca_2Cu_3O_8$ promotes the formation of superconducting compounds of Hg(Sn)-1223.The effects of Sn doping on the formation and stability, microstructure of grain growth and critical temperature of the $(Hg_{1-x}Sn_x)$-1223 superconductor have been investigated by X-ray diffraction, scanning electron microscopy (SEM) and electron probe microanalysis, resistance measurements and ac susceptibility measurement techniques.

The stability of the product compounds is also enhanced. Sn doping may play a role as a nucleating centre. The Tc for Sn-doped samples $(Hg_{1-x}Sn_x)$-1223 with $x<0.1$ is not noticeably changed as compared with the pure Hg-1223 phase (about 134 K).

However, a further increase of Sn doping into the sample leads to a deterioration on both T~ and the fraction of superconducting phase in the sample. Since there are several residual phases accompanying the addition of Sn in the mercury-based copper oxide superconductors, the clustering particles of these phases seem to contribute some pinning effect on their magnetic behaviour.

A Hassen [52] observed that similar to Nb doping, Ti and Rh dopants reduced the superconductivity but at a different rate due to the difference of their electronic configurations. Despite the fact that the hole concentration is increased, the superconducting transition temperature decreases for all dopants, most likely due to the disorder that prevents charge transfer between the adjacent RuO_2 and CuO_2 layers. Unlike Ti and Rh doping, superconductivity is not suppressed quickly with increasing Sn content. Both normal and superconducting state properties depend strongly on the dopant and substitutional site. It seems that in Ru-1212 a much smaller doping range is accessible as compared to other high-*T*c materials.

The complex ac susceptibility $\chi' + \chi''$ was measured by S. Celebi *et al* [53] as a function of temperature and ac field amplitude on rectangular bar shaped high T_c $Bi_{1.6}Pb_{0.4}Sr_2$ $(Ca_{1-x}Ni_x)_2Cu_3O_\delta$ (x = 0 - 0.10) and found that the increased doping of Ni decreases critical temperature T_c slowly. At x = 0.03 the increase in intergranular critical current J_c and flux pinning of Bi (Pb)-2223 system was observed. It was concluded that Ni doping in the above system changed the effective volume fraction of the grains, the field dependence of the intergranular critical current density, transition temperature and intergranular pinning properties.

The $TlBa_2Ca_2Cu_3O_y$ superconductor is one of the most promising materials for high field applications above the temperature of liquid nitrogen. The introduction of the Mo¨ssbauer nuclei ^{57}Fe, ^{119}Sn and ^{151}Eu into Tl-based 1223 superconductors was investigated by E. Kuzmann [54]. The doped Tl-based superconductors were characterized with respect to critical temperatures, critical currents, microstructure and composition of the superconducting and secondary phases. The samples were then analyzed by Mössbauer spectroscopy. Energy dispersive X-ray EDX analysis showed that both Fe and Eu were incorporated in the superconducting crystallites. Sn was found in secondary phases.

Doping of $Hg_{0.3}Pb_{0.4}Sr_{0.8}Ba_{0.22}Ca_2Cu_3O_y$ superconductors with the Mo¨ssbauer nuclei Fe and Sn was investigated by E. Kuzmann [55] Energy dispersive X-ray EDX analysis showed that Fe entered the superconducting phase. The introduction of Fe into the superconductor led to a decrease in the *Tc*-values from 112 K for the undoped to 105 K for the Fe-doped phase. Sn formed a separate secondary phase, predominately barium stannate with some Sr, Ca, Pb, Cu and low amounts of Fe. Small amounts of Sn were also present in the Sr–Ca–Cu–O secondary phase. The ^{119}Sn Mössbauer spectra mainly reflected the Sn environment in the Sn-rich secondary phase.

A. V. Herzog *et al* [56] reported on a series of magneto resistance measurements of granular Sn wires with widths from 1100–2000Å. The magneto-resistance measured within the superconducting resistive transition of wires with different normal state resistances and the results were compared to two-dimensional granular Sn films. Both the wires and the 2D films exhibit two distinct magnetic-field regimes,a low-field weak positive magneto resistance regime and a high-field strong positive magneto resistance regime. In addition, the wires exhibit strong reproducible magneto-resistance oscillations within the low-field regime near the superconductor-insulator transition were not observed in the 2D films. These magneto resistance oscillations were attributed to the effects of screening currents circulating around phase coherent loops of weakly linked superconducting grains. The observed magneto resistance at different field strengths in the wires and films allowed for clear and coherent interpretation of the mechanisms causing the magneto-resistance behavior, and the magnetic-field tuned superconductor-insulator transition

For the $(La_{1-x}Sr_x)_2Cu_{1-x}Sn_xO_4$ system, through Sn substitution experiments, Yang Li [57] noted that structural parameters change monotonically with Sn-doping, but the Tc remains at 36 K even with increasing Sn-doping. Sn-doping resulted in a significant enhancement of Jc for more highly doped samples. Sn-doping introduced new kinds of pinning centers near the Cu–O layers. These Sn dopants in Cu–O layers are point-like defects on the scale of the superconducting coherence length, so they can effectively pin flux, especially at high temperature.

J Q Li [58] synthesized Tin-doped samples $Hg_{0.9}Sn_{0.1}Ba_2Ca_2Cu_3O_8$ *or* $(Hg_{0.9}Sn_{0.1})$-1223 in sealed silica tubes by a solid-state reaction method. The dominant

phase involved in the sample is a superconducting phase of (Hg(Sn)-1223), which is a solid solution of Sn in the compound. An impurity phase HgCaO2 also exists together with the dominant phase. The results of thermogravity analysis and XRD analysis show that the impurity phase HgCaO2 and superconducting phase Hg(Sn)-1223 have different decomposition temperatures in flowing He gas and in flowing O2 gas atmosphere. The onset decomposition temperatures of these two phases measured in flowing He gas are 560 and 760 C respectively. They increase to 576 and 825 C respectively in flowing O_2 gas. Studies of the effect of annealing temperature on Tc by resistance measurement for this sample show that the superconductivity is reversible in flowing O2 gas below the decomposition temperature of the superconducting phase Hg(Sn)-1223, namely 825 C. The quality of the superconductor, including the critical temperature and the sharpness of the transition, can be improved by removing the impurity phase HgCaO2 from the sample using a high-temperature annealing process under flowing O_2 gas.

YBaCuO thin films were studied By Anton V. Velichko *et al* [59] in which the effect of both dc and RF magnetic fields *H* on the microwave surface impedance, $Zs = Rs + jXs$, of a superconductor containing weak links were discussed. Two types of the weak links were considered; a weak link between two grains, shunted by another grain, and a non-shunted weak link. In both cases, the dependences of *Rs* and *Xs* on applied *H* were found to be anomalous. Under certain conditions, the values of *Zs* (*H*) were found to fall below the zero-field values.

For $La_2Sr_2Cu_{1-x}Sn_xO_4$ 0.075, 0.090 and 0.110.superconductors, the effects of Sn-doping on local microstructure are studied by Yang Li [60]. The results showed that Sn ions in the 4q valence state dominantly occupy Cu sites rather than La_Sr. site. In the view of the effective oxygen content or excess oxygen, the dual role of Sn dopant on the carrier concentration is discussed. Sn directly occupy Cu site on CuO plane, which would deteriorate integrality of 2 CuO plane. Thus, Sn_{4+} doping itself strongly decrease superconducting transition temperature.

L.F. ti [61] studied the tin doped YBCO. A.c. susceptibility measurements from room temperature to liquid nitrogen temperature indicated that the superconducting transition temperature of sintered YB,Cu,O, (about 91 K) was little affected by doping

with tin.. The substitution of Sn for Cu is held responsible for the increasing in pinning fore and thus for the increase in critical current density.

The effect of doping on the superconductivity in $Bi_2Pb_{0.6}Sr_2Ca_{2-x}R_xCu_3O$(6R = Ba, Y, V, Zn and Sn) system has been investigated by S. B. Mohamed [62] characterized by resistivity, ac susceptibility measurements and x-ray diffraction (XRD) analysis. The data curves indicate the presence of a superconducting transition between grains coupled by weak links. The volume percentage of the 2223 phase decreased with the increasing doping concentration. The presence of low T, phase is also visible in the real component *(f),* of the susceptibility data, while the imaginary component *(x"),* show a shift towards lower temperature in the intergranular coupling peak, Tc as the dopant concentration increases. All the doping elements do not enhance the T, zero but decreases.

Takahito Saito [63] studied substitutional effect of YBa2Cu30 7_y by Sn.they report on the Sn doping effect on the superconductivity of YBa2Cu30 7_y to Y ,Ba and Cu sites .Ysites were substituted b Sn up to 4 percent and *Tc* increased by a few degrees.it was found that Sn does not occupy the sites of Ba and Cu.

In the cases of Sn doping to the Y site in the low concentration range ($x< 0.04$), the superconducting transition temperature Tc increased with narrow width and electrical resistivity of the normal state decreased as Sn doping progressed. In highly doped samples toY sites ($0.04<x<0.25$), the resistivity curves shifted to lower temperatures and broadened with higher resistivity in the normal state. The occupation of Sn on a Y site would locally distort the atomic arrangement around it or the doped Sn would deviate from the center position of the Y site and then the lattice distortion would be caused around the site locally. This lattice distortion energy is small, as long as the concentration of Sn that substitutes on the Y site is low. However, as the doping concentration increases, the lattice distortion energy increases and finally impurity phases would appear rather then substitution on Y sites. This would decrease Tc and broaden the transition.

Normal and superconducting transport properties of $Bi_{1.65}Pb_{0.35}Sr_2Ca_2Cu_3O_{10+\delta}$ ceramic samples were observed by E. Govea-Alcaide *et al* [64] in powder form with high pressure of 90 to 600 Mpa. Critical magnetic field ranging from lower to upper (80Oe to 135Oe) was found same for all samples at 77K. The result suggested that the grain orientation and the connectivity between grains were improved with increasing pressures.

$J_c(0)$ was found to increase from 58Acm^{-2} to 418Acm^{-2} in zero applied field. The factor $J_c(B)/J_c(0)$ was showed to be very sensitive to the pressures. It exhibited Josephson like behavior at low compacting pressures which was changed as independent of magnetic field at high pressures. In addition flux trapping curves indicated three superconducting levels i.e., the superconducting grains, the superconducting clusters and weak links. Correlation between normal and superconducting transport properties was also discussed as for as the dissipation was brought in concerned.

J. D. Hettinger *et al* [65] observed current-voltage data in samples $Tl_2Ba_2CaCu_2O_x$ (T1-2212) and $TlBa_2Ca_2Cu_3O_x$ (T1-1223) separately and demonstrated that in some cases *I(V)* data on polycrystals could reveal weak-link contributions to dissipation. To verify this general and potentially useful procedure, they used ion irradiated samples to greatly diminish the flux-creep contribution. As a result of these observations, they suggested that weak-link-free current paths exist in a relatively small fraction of a sample cross-sectional area. For example, they observed the slight decrease of J_c after ion-irradiation in the intermediate-field, plateau region of the $J_c(B)$ data suggested that flux creep was irrelevant. Thus, although the conclusion that the actual area of the current path shrinked as field increased looked reasonable and consistent with available data. This implies that comparing J_c to that of an epitaxial film could only give a lower limit on the area of the actual current-carrying path. Increased in J_c could then result from either increasing the current-carrying area or improving the residual weak-link grain boundaries.

G. V. M. Williams [66] reported the results from a resistance, and magnetization study on $Ru_{12}A_xSr_2RCu_2O_8$ (R = Sn, Nb, La, Eu, Gd). They showed that, there is no significant change in the superconducting transition temperature when Sn is substituted for Ru, implying that there is no significant Sn-induced charge transfer to the CuO2 planes. Furthermore, increasing the Sn concentration has the effect of increasing the temperature where zero resistance and the onset of bulk ac diamagnetic shielding occurs, which we interpret in terms of a decreasing ferromagnetic component leading to an increase in the temperature where the spontaneous vortex phase occurs.

Carrier concentration, superconductivity, and crystal structure in a series of $YBaSrCu_{3-x}Sn_xO$= samples ($0 \lesssim x \lesssim 0.25$) have been investigated by Y. Zhao [67]. The

X-ray diffraction analysis and structural computer simulations reveal that at low doping levels ($x < 0.15$) Sn preferentially occupies the Cu(1) site, but gradually goes into both the Cu(1) and Cu(2) site at higher doping levels. The rate of T c suppression caused by Sn doping is significantly slower for low dopant concentrations than for high dopant concentrations, indicating that different mechanisms operate at the Cu(1) and Cu(2) sites. Another mechanism may be the impurity-scattering effect caused by the Sn doping at CuO_2 planes which is responsible for the dramatic suppression of T~ at high dopant concentrations.

The temperature and ac field amplitude variations susceptibility were measured by P. K. Nayak *et al* [68] on $(La_{1-x}Y_x)_2Ba_2CaCu_5O_z$. They measured temperature and field variations of ac susceptibility on pure and 5wt% of Ag doped $(La_{1-x}Y_x)_2Ba_2CaCu_5O_z$ superconductors for ($x = 0$, 0.25 and 0.5). Critical current density, J_c as function of temperature and effective volume fraction of superconducting grains were estimated for all the samples. $(La_{0.75}Y_{0.25})_2Ba_2CaCu_5O_\delta$ compound with 5wt% Ag was found to exhibit relatively large J_c.They suggested relatively large critical current density due to the improved intergranular coupling. These materials were found to exhibit (SNS) type of junctions.

The influence of SnO dopant on the superconductivity and the phase formation of the Bi(Pb)-Sr-Ca-Cu-O system has been studied by Y. L. CHEN [69] using differential thermal analysis/thermogravimetric analysis, X-ray diffraction, a.c. susceptibility and resistance measurements. It was found that Sn 2+ can be dissolved in the 110 K phase, but reduces the formation of this phase. Resistance measurements show 107 K zero resistance can be obtained for a short-time sintered sample (60 h), but that the T O (0) was found to decrease to 90 and 75 K after the specimens were sintered for 90 and 140 h, respectively.

F. J. Owens [70] seen the effect of dc and ac magnetic fields on the absorption of electromagnetic energy in the superconducting state of $Hg_{0.7}Pb_{0.3}Ba_2Ca_2Cu_3O_{8+x}$ (T_c = 133K) by measuring the magnetic field dependence of the RF penetration depth at 300 KHz - 20 MHz. Absorption depend linearly on the dc magnetic field as $B^{1/2}$ with a change in slope in occurring at a field B^* was associated with the depinning transition. At constant temperature, as observed to decrease with increasing frequency. A comparison

of the field dependence of the RF penetration depth in (Hg, Pb-1223) with that inY-Ba-Cu-0 was done, resulting the flux trapping power of (Hg, Pb-1223) superconductor at 77K. It was shown that low frequency ac magnetic fields also cause an increase in high frequency electromagnetic absorption. This low field ac induced absorption was believed to arise from the same causes as the absorption induced by a small dc magnetic field ,jumped through square micron sized current loops formed by weak links in the material.

K. S. Aleksandrov [71] reported the results of a search for superconductivity in compounds based on tin, which also has an unshared electron pair. This search has resulted in the discovery of superconductivity in certain compounds of the Sn-Ba-Sr-Y-Cu-O system. The alkaline earth elements are used in this system because they play a major role in forming the superconductivity, as stabilizers of the highly oxidized state of the copper cations.

The insulating and metallic behavior of the grain-boundary weak links has been studied recently in thallium rich and the samples by Nawazish .A.Khan *et al* [78] with small amount of thallium in the charge reservoir layer of $Cu_{1-x}Tl_xBa_2Ca_3Cu_4O_{12-\delta}$ superconductor thin films. The influence of the nature of grain boundaries on the inter-granular critical current density (J_c) was also been investigated. From the power law dependence of $H_{ac} \sim (1 - T_p/T_c)^n$, at n = 1, 2 best fitted for the J_c of thallium rich and small amount of thallium respectively. The polycrystalline thin film samples showed the power law dependence of J_c as n = 1 corresponded to (SIS) type while the samples with n = 2 followed (SNS) types of Josephson junctions. The insulating grain boundaries decreased the inter-granular Josephson coupling and hence the transport properties were suppressed.

Thomas W. Krause [73] reported the study of Sn doped $Bi_{0.7}Pb_{0.3}Sr_2Ca_2Cu_3O_y$. Features in the temperature derivative of the resistivity curves were associated with the presence of a superconducting transition between superconducting grains, coupled by weak links with a distribution of critical currents and critical temperatures, and the superconducting transition within grains. The transition between grains was more strongly suppressed in temperature with the application of a magnetic field in samples with weaker coupling between grains.

Substitutions of diamagnetic Cd^{2+} and Sn^{4+} in YBCO and LaSCO structures have been investigated by F. Licci [74]. X-ray diffraction, electrical resistivity measurements

and EDX analysis were used to investigate the doping-induced structural and resistive effects and to identify secondary phases. Our results indicate that Cd and Sn have a limited solubility in LaSCO and they do not substitute in YBCO. Sn substitutes for Cu in Cu-deficient LaSCO up to about 4% (nominal concentration). At such a substitution level it strongly reduces to, with effects comparable to those induced by Zn at the same concentration levels. When doping with Sn for La, only small effects are produced on Tc.

C.V. Tomy [75] investigated the effect of Sb, Sn and In doping on superconductivity in the Cu-rich and Cu-deficient compositions in the Bi-Pb-Sr-Ca-Cu-O system. The compositions rich in copper showed marginal improvement inTc over the copper deficient compositions. Sn and In dopings were also found to result in formation of 2212 phase and lower T c.

Chen Angt [76] investigated that the superconducting properties are directly affected by the substitution for the *Cu* element in YBCO compounds. This substitution will suppress the superconductivity. However, in Sn-doped specimens, T_c did not decrease but has been improved a little. Softening phenomena near T_c were observed in the temperature dependent *f(T)*- factor, and the temperature of phonon softening increased as the amount of Sn substitution increased. This change is in good agreement with the change in superconducting transition temperature T_c of the samples.

Z.H. He [77] one of the obstacles to the applications is its relatively low *J* compared to that of YBCO thin films. One of the c attempts to increase *J* is by doping, especially with c Sn-based compounds. Compared to the other element doping, the addition of Sn or Sn-based compounds has the advantage of not reducing the superconducting transition temperature *Tc*.

The weak link behavior of $Cu_{1-x}Tl_xBa_2Ca_3Cu_4O_{12-y}$ (1234) superconductor thin films was studied by magneto resistance and ac-susceptibility measurements by Nawazish.A.Khan *et al* [72]. From the imaginary part of magnetic susceptibility it was observed that the external magnetic field activates inter-granular decoupling and the carriers can tunnel through these barriers using activation energy around 0.244 eV. T_c was shifted to lower values with the application of an external field and the activation energy of these thermally activated processes was decreased to 0.128eV as a result. The insulating nature of the grain boundaries helps in providing a large surface area to the

shielding currents and promotes high critical current densities in the films. The insulating grain boundaries seem to act as efficient microscopic pinning centers.

1.10 Motivation

It is well known that the properties of a high temperature superconductor are structure sensitive. Undoubtedly, the CuO_2 planes play very important roles in the mechanism of the superconductivity of ceramic cuprates with perovskite structure. When the CuO_2 plane is influenced by external factors, for example, replacement of copper atoms with some foreign atoms of the doped element, what will happen to its superconductivity? This problem has attracted a great deal of interest from scientists around the world. The understanding of these effects may reveal the mechanism of the high temperature superconductivity.

Another approach to investigate the superconducting mechanism is the investigation of the effect of doping on to the CuO_2 site. Particularly interesting is the effect of doping on Tc due to nonmagnetic impurities. The experimental findings suggest that nonmagnetic impurities induce uncompensated magnetic moments on the Cu site which may act as pair breakers. There is an important aspect of Sn doping compared with other dopants, Sn is expected to be substituted for Cu in the Sn^{4+} state because it has an ionic radius (0.71) very close to that of Cu^{2+} (0.69). Such a charge unbalance (Sn^{4+} and Cu^{2+}) will lead to doping the CuO_2 lattice with excess electrons (n-doping).

The Sn^{4+}-ion might be a possible substituent for thallium because of its closed shell d10 electric configuration, and its higher valence state, Sn(IV), could be used for stabilization of the thallium superconductor. Finally, due to the much increased stability and reduced toxicity of its oxides in comparison with those of Tl, this research includes a contribution towards the alleviation of the environmental impact due to the eventual application of this class of materials on a larger scale.

It is thus expected that Sn^{4+}-doping causes not only the magnetic disorder known from doping with nonmagnetic impurities (e.g. Zn^{2+}) but also reduces the number of the free holes in the system. The effect of such n-doping on Tc in TlBaCaCuO should be helpful for a better understanding of the mechanisms involved in the system. Doping with

Sn, therefore, reduces the free-hole concentration in the system. The effect of such excess electrons on the superconducting and of the system will be presented.

Experimental Techniques

This chapter is used to describe the experimental techniques employed to characterize the synthesized materials. To determine the structural, electrical and weak links properties of materials, availability of information is necessary. Particularly, each technique gives different information regarding the type of properties of synthesized materials. Although these systems are based on simple physical laws but the proper arrangement is yet to be explore. The synthesized materials communicated in this thesis are characterized by different studies such as Electrical resistivity, AC Magnetic Susceptibility, In-Field (DC) Magnetic susceptibility measurement, FTIR, X-Ray Diffraction.

2.1 Synthesis of Tl-based High T_c Superconducting Oxides:

Chemical purity is essential for Cuprates. The use of chemicals with a purity of 99.99% is better but still not sufficient. During the preparation procedure, the formation of even a small amount of liquid has to be avoided since this may introduce impurities into the sample. Some of these reaction products have turned out to be well suited as materials for corrosion resistant crucibles for the preparation of cuprate HTS. The inherent tendency towards inhomogeneities and defects, in combination with the very short SC coherence length of the order of the dimensions of the crystallographic unit cell did not allow easy progress in the preparation of these materials [79].

The ability to synthesize powders of high phase purity is essential to many basic studies and practical applications of high T_c superconductors. From the J_c (critical current density) point of view, the presence of impurity phases among superconductive grains impedes the transport of the electrical current, resulting in a low J_c, increasing the flux pinning, the preparation processes in general are employed in single phase superconductive powders as starting material, by following a well defined heating procedure.

One of the problems with the high T_c superconductor cuprates is that they are really hard. Experimentally, these materials are very difficult to work with. They are brittle transition metal oxides, which are highly anisotropic. It is difficult to make electrical contacts to them. It has now become clear that high purity single crystals are

essential in order to obtain reliable and repeatable measurements. Their surfaces are also complicated [79].

Like the other high T_c superconductor oxides, Tl based superconductive oxides have most commonly been prepared by the solid state reaction method. Subsequent methods have been developed to avoid the use of off-stoichiometric starting compositions. Many successful results have been reported in this regard [80-86]. Basically these methods are used to synthesize the desired superconductive phase either in a single step or through a series of steps with well defined intermediate compounds formed after each step. Until now, with proper selection of conditions, Tl based superconductive powders of high phase purity can be synthesized in short times without resorting to complicated wet processes [87].

2.2 Sample Preparation:

The superconductor samples of $(Cu_{0.5}Tl_{0.5})Ba_2Ca_2(Cu_{3-x}Sn_x)O_{10-\delta}$ (x = 0, 0.25, 0.5, 0.75, 1.0, 1.25, 1.5) superconductors were prepared by solid state reaction method. The precursor material of $(Cu_{0.5}Tl_{0.5})Ba_2Ca_2(Cu_{3-x}Sn_x)O_{10-\delta}$ (x=0, 0.25, 0.5, 0.75, 1.0, 1.25, 1.5) superconductors was prepared using Cu(CN), $Ba(NO_3)_2$, $Ca(NO_3)_2$, SnO_2 as starting compounds. These compounds were mixed according to above mentioned formula unit for one hour and 30 minutes in a quartz mortar and pestle. Thoroughly mixed material was put in a quartz boat and loaded into a preheated box furnace at 850°C. The mixed material was fired for 24 hours, following intermediate grindings. The precursor material after firing was mixed with a standard calculated amount of Tl_2O_3 to give$(Cu_{0.5}Tl_{0.5})Ba_2Ca_2(Cu_{3-x}Sn_x)O_{10-\delta}$ as final reactants composition. The pellets of thallium mixed material were prepared under 5.5 tons/cm^2 pressure. The pellets were enclosed in a gold capsule and sintered at 850°C for 10 minutes. After the heat treatment, pellets were quenched to room temperature and characterized by different techniques.

2.3 Post annealing of Samples:

In oxide superconductors, oxygen concentration in the unit cell plays a vital role; as it can modify the distribution of the carriers in various bands of compound. The electronic distribution ultimately controls the mechanism of superconductivity. Oxygen Annealing is performed in superconductor in a temperature window between 400-500°C. Therefore, we have carried out post-annealing of CuTl-1223 compound at 500°C for such

oxygen intercalation. This is done by loading the samples into a preheated tubular furnace at 500 °C for 5 hours followed by furnace cooling of the samples to room temperature.

2.4 Characterization and Measurement Techniques:

The characterization techniques used for the superconductors are:

1. X-Ray Diffraction.
2. Four Probe Resistivity Method.
3. AC & IN-Field (DC) Magnetic Susceptibility.

2.4.1 X- ray diffraction:

XRD (X-ray diffraction) analysis gives us the information about the crystal structure of the material. This technique is used to know whether the intended sample has the crystalline structure or not and also to know the cell parameters like of the lattice. The most important aspect in materials science is the study of crystal structure of material. The crystal structure determination is an important parameter. In the beginning of the field of materials science, it was assumed that the solids are made of atoms, which are periodically arranged, but there were no experimental evidences of this thought. The discovery of x-rays made it possible to probe the material for their structure determination. The wavelength of x-rays (0.5Å-2.5Å) is comparable to the spacing between the atomic planes in solids. The x-rays, which originate from the K shell transitions, are used for the diffraction analysis because these are of shorter wavelengths as compare to the one coming from L or M shell transitions. The commonly used target materials in x-ray tubes are Cu and Mo. These two target materials produce x-rays with wavelengths 1.54Å and 0.8Å respectively [88-89].

An incident x-ray beam on a material penetrates into it and the intensity in the direction of the reflected beam is determined by the periodicity of the atomic planes in the crystalline solid. The consideration of such an x-ray beam of wavelength 'λ' incident to a crystalline material at an angle 'θ' and diffracted also at the same angle is shown in fig.2.1.

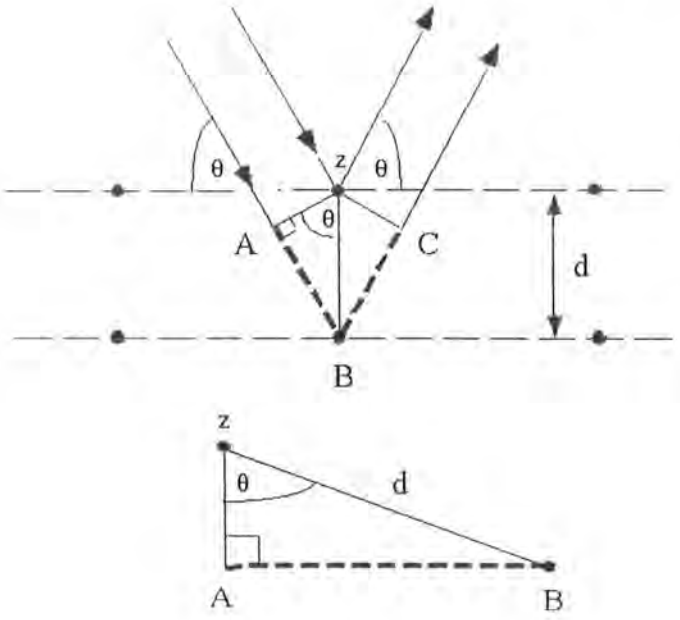

Fig. 2.1: Diffraction of X-rays from crystal planes.

The interplaner spacing of the material is equal to d. These rays will interfere constructively when the path difference between the rays is an integer multiple of the wavelength used. The path difference is

$$AB + BC = n\lambda$$

$$AB = d\sin\theta \text{ and } BC = d\sin\theta$$

$$2d\sin\theta = n\lambda,\ n = 0, 1..... \qquad (2.1)$$

Where n is the order of diffraction. The above diffraction rule was given by W. L. Bragg and is known as Bragg's law. Only the X-rays that satisfy this law will give the diffraction pattern.

The x-ray diffraction technique is also used to identify whether a material is a crystalline or amorphous. In crystalline solid many sharp crystalline peaks are observed due to periodic arrangement of atoms, but in the amorphous material there is no periodic structure and only one or two broad diffraction bands are observed. Through this technique we can also determine the size of the unit cell i.e. lattice parameters, atomic position and degree of crystallinity.

X-ray diffraction studies of the crystal structure with different orientation of the planes take place by adopting one of the following methods.

1. In the Laue's Technique a single crystal is held stationary and a beam of radiation is incident on it at a fixed angleθ, i.e., θ is fixed while wavelength λ is varied. These different wavelengths select the appropriate reflecting planes out of the numerous present in the crystal such that the Bragg's condition is satisfied.
2. In rotating crystal method a single crystal is held in the path of the monochromatic radiations and is rotated about an axis, λ is fixed while θ is varied. Different sets of parallel atomic planes are exposed to incident radiation for different values of θ and reflection takes place for those planes for which d and θ satisfied the Bragg's law.
3. In powder method a sample in the powdered form is placed in the path of monochromatic x-rays, i.e., λ is fixed while both θ and d vary. Thus a number of small crystallites with different orientations are exposed to x-rays. The reflections take place for those values of d, θ and λ which satisfied the Bragg's law. Superconducting sample is polycrystalline and the tiny crystals are randomly oriented so powder diffraction method is usually employed. A powder pattern is therefore, a reasonably complete display of the diffraction effects from a compound. The procedure to analyze the powder pattern of an unknown compound consists of measuring the diffraction angles, calculating the spacing of the reflecting planes and then deducing the dimensions of the unit cell [90]. The schematic diagram of an x-ray diffractometer is shown in fig. 2.2.The summary of methods are described below.

Method	**Wavelength (λ)**	**Angle of diffraction (θ)**
1) Lau Method	Variable	Fixed
2) Rotating Crystal Method	Fixed	Variable
3) Powder Method	Fixed	Variable

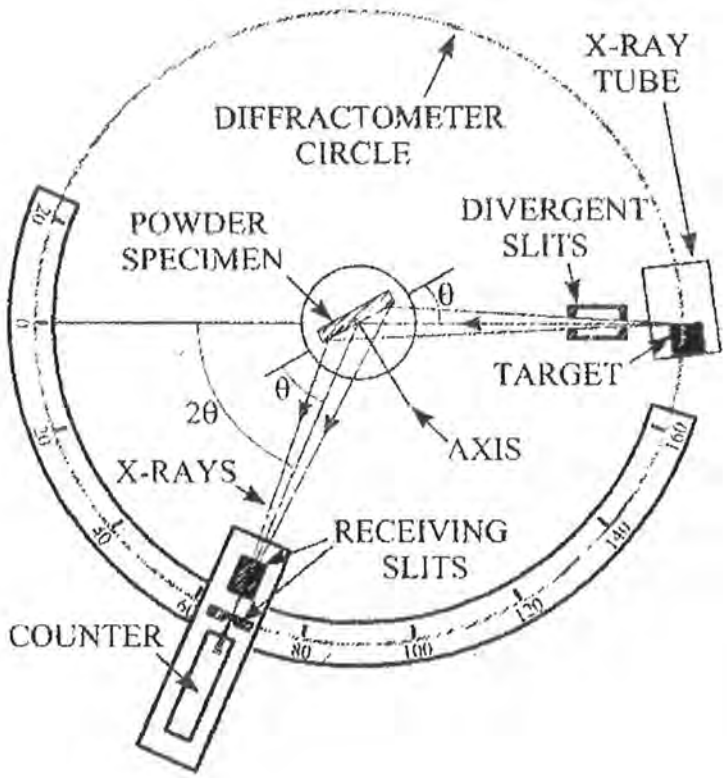

Fig.2.2: An x-ray diffractometer.

Once the scattered peaks data is obtain then the data is analyzed for the determination of the crystal structure. The process proceeds in stages. The first step is to compare the location of the peaks/rings with those produced by the various known crystal structures and effort is made to identify the crystal structure. Next step is refinement procedure; varying locations of atoms and intensities of the species best fitting data is obtained. In our work we used computer software "Check cell" which when provided with peak data, identified the crystal structure and also provide lattice parameters.

2.4.2 Four Probe Method for Resistivity:

We measured resistivity of the superconducting materials using the four-probe method. This method is widely used for measurements of resistivity in metals, semiconductors and superconductors. Fig. 2.3 shows the experimental arrangement for four-probe method. The contacts were made by silver paste on the surface of the Superconducting bulk material and copper wires. The distance between the middle contacts is 'L' and the cross sectional area 'A' (width × thickness) was measured and the voltage drop across the voltage contacts was also measured.

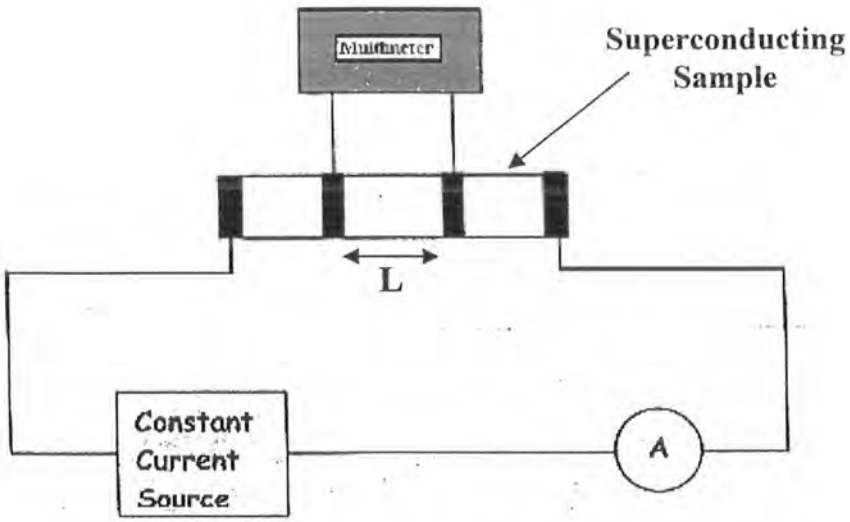

Fig. 2.3: Arrangement for resistivity measurements.

According to Ohm's Law

$$V = IR \tag{2.1}$$

$$\Rightarrow \quad R = \frac{V}{I} \tag{2.2}$$

Where V is the applied voltage and 'I' is the current flowing in the circuit and R is the resistance offered by the conductor to the moving electrons that constitute the current. Experiments have shown that the resistance of the conductor also depends upon the geometry of the conductor along with the temperature. It has been found that the resistance of the conductor is directly proportional to its length and inversely proportional to its area of cross section. If 'L' is the length of a certain superconductor and 'A' is the cross section area, then we can write,

$$R \; \alpha \; \frac{L}{A}$$

$$\Rightarrow \quad R = \rho \frac{L}{A} \tag{2.3}$$

where ρ is the proportionality constant and is called the resistivity of the conductor. The resistivity of a material depends upon the temperature as discussed earlier. So the resistivity in terms of temperature can be written as:

$$\rho\,(T) = \frac{A}{L} R$$

$$\rho(T) = \frac{A}{L}\frac{V}{I} \tag{2.4}$$

The unit of the resistivity used here is (Ω-cm). If length L, area of cross section A and the current I through the material are constant, then the resistivity variation is proportional to the voltage drop and are calculated by using eq. 2.4. The factors affecting the suitability of the methods and precision attainable include the contact resistance and form of a sample, usually in our case it was the bulk superconducting material. The samples in our case were superconductors of CuTl-1234 family. The simplest method of measuring resistivity is to measure voltage drop V across the sample, the current through the sample I and calculating the length L between voltage contacts and area of cross section A and using equation.

$$\rho(T) = \frac{VA}{IL}$$

The resistivity measurement employing four-probe method consists of following apparatus:

1. The constant current source was constructed by connecting a variable resistance in series with the MW2122A regulated DC power supply.
2. A micro-ammeter was connected in series, which can measure current up to 1000μA with an accuracy of 1.0μA.
3. The P-2000/E KEITHLEY multimeter was used to measure voltage drops across the samples corresponding to the variations in the temperature.
4. Temperature measurements were carried out by using a thermocouple.
5. The Cryostat, a simple cryostat consists of
    1. Liquid nitrogen Dewar.
    2. A brass pipe with sample holder at one end and connecting wires at the other end.

Resistivity measurements were carried out in a systematic way by using following steps.

1. The sample was washed with acetone and fixed with blue stick to the sample holder; at the other end of the blue stick is the hot junction of the thermocouple.
2. Electrical leads were attached to the sample using silver paste, which make Ohmic contacts of the leads with the sample.

3. The electrical leads were connected to the voltmeter, ammeter and multimeter. The other end of the thermocouple was attached with copper wire to produce a colder junction. This junction point of the thermocouple was dipped in the liquid nitrogen and kept at 77K during measurement.
4. The sample holder was covered with a metallic cap. The lowering or raising of the sample holder in the liquid nitrogen container controls the temperature of the sample.
5. The changes in the voltage drop across the sample with the temperature were recorded.
6. The data was measured during heating process.
7. The dimensions of the sample were measured by using Vernier Caliper and Screw Gauge.

2.4.3 AC &DC Magnetic Susceptibility:

AC magnetic susceptibility has been one of the subjects of interest in the investigation of the new ceramic superconductivity. It was believed that the magnetic susceptibility of the ceramic superconductors is a measure of the characteristics of the coupling status of the materials. These characteristics refer to how the weak-links, Josephson junctions and grain boundaries affect the magnetic properties of the bulk materials.

When a high T_c ceramic superconductor is placed under an external field, a certain configuration of superconducting loops will be established inside the superconductor. Owing to the granular structure of the ceramic material, the situation of the configuration of the superconducting loops inside the granular structured superconductor is in general very complicated. The superconducting loops are formed as an assembly with a certain distribution in inductance, critical current and orientation $\cos\theta$, where θ is the angle between the normal to the loop and the direction of the applied field [91].

The main characteristics of AC magnetic susceptibility can be explained in a unified way as has been treated in the previous section. The occurrence of the granular structure of the ceramic superconductors, when they are placed under an AC external

magnetic field, will lead to the formation of superconducting loops with a certain distribution of inductance, orientation and critical current [92].

The measurement of AC susceptibility, χ is a useful method to identify power losses in superconductor samples [93-95]. The AC susceptibility of superconductors is a function of temperature (T), magnetic field (H), frequency (ω) and state. It can be written as: $\chi_{ac} = f(T, H, w, state) = \chi' + i\chi''$ where χ' is the real part of χ_{ac} and χ'' is the imaginary part. The imaginary part of χ, i.e., χ'', is associated with of χ_{ac} losses. In a single phase superconductor we expect the following loss peaks in $\chi''(T)$:

(a) The intrinsic peak: represents losses associated with London field penetration, i.e. losses due to the screening of magnetic fields by the superconducting surface currents. The dissipation occurs through AC excitation of normal electrons. The intrinsic loss peak is expected to vary slowly with temperature, magnetic field, and frequency [96].

(b) The intergranular peak: is due to losses associated with flux penetrating the grain boundaries. This peak can also be called the coupling peak and can be explained by considering the weak links or Josephson junction (JJ) coupling of adjacent superconducting grains. This peak is expected to be observed at low magnetic fields, because of the weak JJ coupling in polycrystalline superconductor. The behavior of this peak as a function of magnetic field is expected to be similar to the behavior of the J_c, (critical current density) in polycrystalline materials [97].

(c) The Intragranular peak: is due to losses associated with de-pinning Abrikosov vortices. This peak appears for magnetic fields exceeding H_c ($H > H_c$). It can be explained by the Bean or critical state models [98].

(d) Low magnetic field region (H < Hc): in this region we can observe only the intrinsic, and the intergranular JJ peaks, because no magnetic flux penetrates the grains. There is no intragranular loss peak. Note that because of single crystal anisotropy and randomly oriented c-axes in the polycrystalline materials, it is not precisely defined.

(e) Intermediate magnetic field region: we can identify three loss peaks for $\chi''(T)$. In this region as magnetic flux lines penetrate the grains, the intragranular loss peak becomes evident. The intergranular JJ loss peak shifts rapidly to lower temperatures as field is increased. The intrinsic peak is much more slowly varying with applied DC field than the intra- and inter-granular peaks.

(f) In the high magnetic field region: the magnetic field destroys the JJ coupling between the grains and the coupling peak is no longer observed. This is similar to the behavior that we see in ground superconducting powder where only the intrinsic and the pinning peaks are observed. The position of the pinning peak T_p, is also strongly field dependent consistent with the field dependence of the critical state penetration. For complex ac susceptibility, the real part reflects the magnetic screening properties of a sample and is related to an energy difference of a sample in normal and superconducting states; the imaginary part corresponds to the amount of heat produced by the ac magnetic field. In ac susceptibility measurements, shielding superconducting current is induced in surface of the sample by the nonzero time derivative of a applied magnetic field H_{appl} produced by a primary coil system. Weak links behavior can be well understood by applying different values of magnetic fields and see the diamagnetism and peak temperature shifting with increasing fields. We investigate different values of critical current (J_c) for different fields.

The measurement of the ac susceptibility relies on the change of the mutual inductance of a set of two coils or the self-inductance of a single coil if a magnetic sample is inserted. First of all an ac signal of 1volt emf and frequency of 270 Hz is given to the primary coil of the susceptometer and the signals from the secondary coil are given to preamplifier. The weak signal is amplified and sent to lock in amplifier. From here signal is displayed with reference. This display on the lock in amplifier gives the susceptibility measurement, which is read on the digital multi-meter. Experimentally, the ac susceptometer operates as a modified Harshorn bridge network shown in fig. 2.4. Primary coil produces a small ac field and the resulting emf, directly proportional to the derivative of the magnetization of the sample, induced in the secondary (pick-up) coil wound around the sample is analyzed. The in-phase and out-of-phase components (w.r.t. the driving current of the primary coil) of the out-of-balance voltage are proportional to the real χ' and imaginary χ'' components of the susceptibility. It should be noted that the harmonics of the signal could also be detected for looking at non-linear effects such as those induced by inter-grain couplings in high temperature superconductors.

Moreover In-Field susceptibility measurements are carried out by putting the holder of sample in an electromagnet in either high or low field configurations. We

change values of current and obtain different values of magnetic fields applied using Ampere's law i.e., $B = [(\mu_0 n I_) / (2\pi r)]$ where symbols represent usual meanings and r is the radius of the cylindrical type electromagnet. Different values of DC Magnetic field were employed to study Jc, peak temperature T_P, T_c (onset) and magnitude of diamagnetism. A simplified diagram of ac susceptibility apparatus is shown in fig. 2.4.

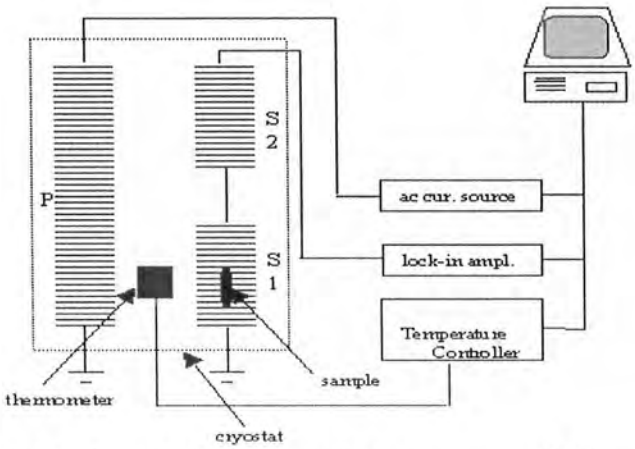

Fig 2.4: Harshorn bridge network for ac susceptibility measurements.

3.1 Introduction:

In oxide superconductors the mobile carriers in the conducting CuO_2 planes and their density in there plays an essential role in determining mechanism of high temperature superconductivity. For the understanding of mechanism of superconductivity the interactions of the carrier's with the atoms in the conducting planes play a very vital role to determine a critical temperature in the final compound. Therefore, the doping of atoms in the conducting CuO_2 planes at the copper site is essential for understanding the underlying mechanism of superconductivity. Also copper atoms, in almost all superconductor families, are in their $3d^9$ state which give them a remnant spin due to partially filled configuration of the outermost orbital constituting an anti-ferromagnetic aligned spin lattice there. Unlike copper, Sn^{+4} belong to fourth group in the periodic table after germanium, in which all the elements are semiconductors and their band gap decreases as one moves from top to the bottom. Being the last element in the periodic table, the band gap of Sn is very small and in most of the cases it is treated as metal. Therefore, Sn being at the borders of the metals and the semiconductors becomes an excellent choice for the studies of behaviour of the carriers and their role in determining the mechanism of high temperature superconductivity. It is expected that Sn would reduce the mobility of the carriers through its higher oxidation state Sn^{+4} which may develop some localization of carriers in their neighbourhood.

In the present studies tetravalent Sn^{+4} is doped in $(Cu_{0.5}Tl_{0.5})Ba_2Ca_2(Cu_{3-x}Sn_x)O_{10-\delta}$ (x=0, 0.25, 0.5, 0.75, 1.0, 1.25, 1.5) superconductors, to see any possible effect of decreased mobility of the carriers that possibility might be developed by the localization of the charge carriers in the neighbourhood of Sn^{+4} atoms. These studies have shown that the magnitude of diamagnetism is systematically decreased for increased Sn doping, which indicated that increased localization of the charge carriers at the Sn sites possibly suppress the density of mobile carriers thereby decreasing the overall mobility, the critical temperature and hence the magnitude of diamagnetism in the final compound. Due to the doping of Sn in $(Cu_{0.5}Tl_{0.5})Ba_2Ca_2(Cu_{3-x}Sn_x)O_{10-\delta}$, it is most likely that Sn would also be diffused at the inter-grain sites and may modify the their weak link behavior. We have, therefore, studied their weak link behaviour by carrying out in field magnetic measurements of $(Cu_{0.5}Tl_{0.5})Ba_2Ca_2(Cu_{3-x}Sn_x)O_{10-\delta}$ (x=0, 0.25, 0.5, 0.75, 1.0, 1.25, 1.5) samples.The infield magnetic measurements have shown sharp peaks observed in small external magnetic fields are converted to broader peaks, showing enhanced

decoupling of the grains under higher external magnetic fields. Critical current density as found by, Bean's critical model have been found to depress with increased external field and/or increased Sn-doping.

The polycrystalline HTSCs materials constitute an array of weak links through grain boundaries which usually limit their critical current density [J_c] to lower values due to their weak couplings [99].In the single crystal material there are no such grain boundaries and their population in the thin films materials is lower which results into higher critical current densities compare to bulk polycrystalline materials. It is, therefore, essential to synthesize a superconducting material with strong inter-grain coupling for physical characterization and practical applications. The strong inter-grain connectivity would be helpful in enhancing the transport J_c and higher thermodynamic critical field H_c. The random orientations of the grains, vacancies, oxygen deficiency, aggregates of secondary phases at the termination ends of crystals, and composition variation at the interface of the grains would enhance the weak link behavior of the final compound. The elimination of such sources would help in enhancing the inter-grain couplings and enhance J_c of the final compound.

The ac susceptibility measurements have extensively been employed for probing the nonlinear magnetic behavior [100] inter-granular couplings [100-107] for fining out the pinning potentials [34] and flux creep [39] in oxide superconductors. The real part of ac-susceptibility tell about the intra-grain magnitude of diamagnetism, whereas, the imaginary part of ac susceptibility gives the hysteresis losses due to inter-grain weak links [39,42,46,48,50,53,56,59,108-117].The intra-grain part of magnetic susceptibility χ' is in phase whereas the the imaginary part of susceptibility χ'' is 180 degrees out of phase to applied signal. The χ' gives information about superconducting volume fraction whereas χ'' about the hysteresis losses from the grain boundaries. A maximum in χ'' is observed when the superconducting volume is penetrated by applied magnetic field. At this point the shielding current is equal to the critical current density of material and flux dynamics at this point is controlled by pinning processes [118] When the applied field Ba penetrates to the centre of the sample, the J_c at that temperature (T_P) corresponds to peak value of χ'' and is according to Bean critical model given by equation [119]

$J_c = B_a/(ab)^{1/2}$

Where, 2a×2b is the cross-sectional area of the bar-shaped sample. Since the cross-sectional area of bar shaped sample is constant, therefore, J_c of the sample is proportional to applied external ac-field (B_a). The crystals in granular HTSC constitute an array of

Josephson's Junctions . The fitting of the J_c values at various fields versus $(1-T_p/T_c)^n$ and the value of exponent n can provide information about the nature of the weak links among the grain [120].For superconductor-insulator superconductor junction (S1S = junction),n=1 where as n = 2 for superconductor – normal metal – superconductor junction (SNS) [121] and the values in between 1 & 2 indicate the formation of superconductor insular – normal-metal - superconductor junction (SINS) [122]. The nature of the material at the inter-grain has been investigated from this data.

3.3 Results and Discussion:

3.3.1 As-prepared $(Cu_{0.5}Tl_{0.5})Ba_2Ca_2(Cu_{3-x}Sn_x)O_{10-\delta}$ Samples

x-ray diffraction scan of $(Cu_{0.5}Tl_{0.5})Ba_2Ca_2(Cu_{3-x}Sn_x)O_{10-\delta}$ (x=0, 0.25, 0.5, 1.0) superconductor samples are shown in Fig.3.1. All these samples have shown a tetragonal structure and most of the diffraction lines are fitted following P4/mmm symmetry. The resistivity measurements of these as-prepared samples are shown in Fig.3.2. All $(Cu_{0.5}Tl_{0.5})Ba_2Ca_2(Cu_{3-x}Sn_x)O_{10-\delta}$ (x=0, 0.25, 0.5, 0.75, 1.0, 1.25, 1.5) as-prepared samples have shown metallic variations of resitivity from room temperature down to onset of superconductivity. These samples have shown onset of superconductivity [T_c(onset)] around 121, 123, 121,118, 117.4, 117, 106K and zero resistivity critical temperature [T_c(R=0)] around 116, 112, 109, 105, 102, 97, 94K for x=0, 0.25, 0.5, 0.75, 1.0, 1.25, 1.5 in $(Cu_{0.5}Tl_{0.5})Ba_2Ca_2(Cu_{3-x}Sn_x)O_{10-\delta}$ superconductors. The normal state resistivity of these samples increases with increased Sn doping in the final compound. The onset of diamagnetism as observed in the in-phase component of magnetic susceptibility is around 116, 113, 109.3, 110.7, 108, 97.5, 94.7K with peak temperature (T_P) in the out-of-phase component at 109, 109, 105.5, 107.5,99.2 , 93.6, 91K for the $(Cu_{0.5}Tl_{0.5})Ba_2Ca_2(Cu_{3-x}Sn_x)O_{10-\delta}$ for the Sn doping of x=0, 0.25, 0.5, 0.75, 1.0, 1.25, 1.5, respectively. The in-field magnetic measurements of these samples are shown in Figures.3.3-3.9.

The infield ac-susceptibility measurements of samples without Sn doping i.e $(Cu_{0.5}Tl_{0.5})Ba_2Ca_2Cu_3O_{10-\delta}$ samples, are shown in Fig.3.3. These samples have shown onset of diamagnetism in the in-phase component of magnetic susceptibility around 116K and the peak temperature in the out-of-phase component of magnetic susceptibility at109K. The increased external magnetic field shifts both the onset and the peak temperatures to lower temperature values. In the applied magnetic fields of 19, 41, 67, 83, 99, 116, 141, 152, 162 175 A/M (or Oe) the onset of diamagnetism is shifted to 114.6, 113.6, 108.4, 107.4, 104.5, 100.7, 95.2, 93.1, 90.5, 90.5K in the in-phase component of magnetic susceptibility χ' and the peak temperature T_p in the out-of-phase component of magnetic susceptibility χ'' around 109, 107, 105, 102.5, 100.7, 95.1, 93.6, 91, 88.4, 84.5, 81.1K, respectively.

The infield magnetic measurements of Sn doped $(Cu_{0.5}Tl_{0.5})Ba_2Ca_2(Cu_{2.75}Sn_{0.25})O_{10-\delta}$ superconductors are shown in Fig.3.4. In the external magnetic fields of 13, 26, 71, 99, 116, 132, 141, 152 A/M, the onset of diamagnetism in χ' is observed around 112.5, 112,

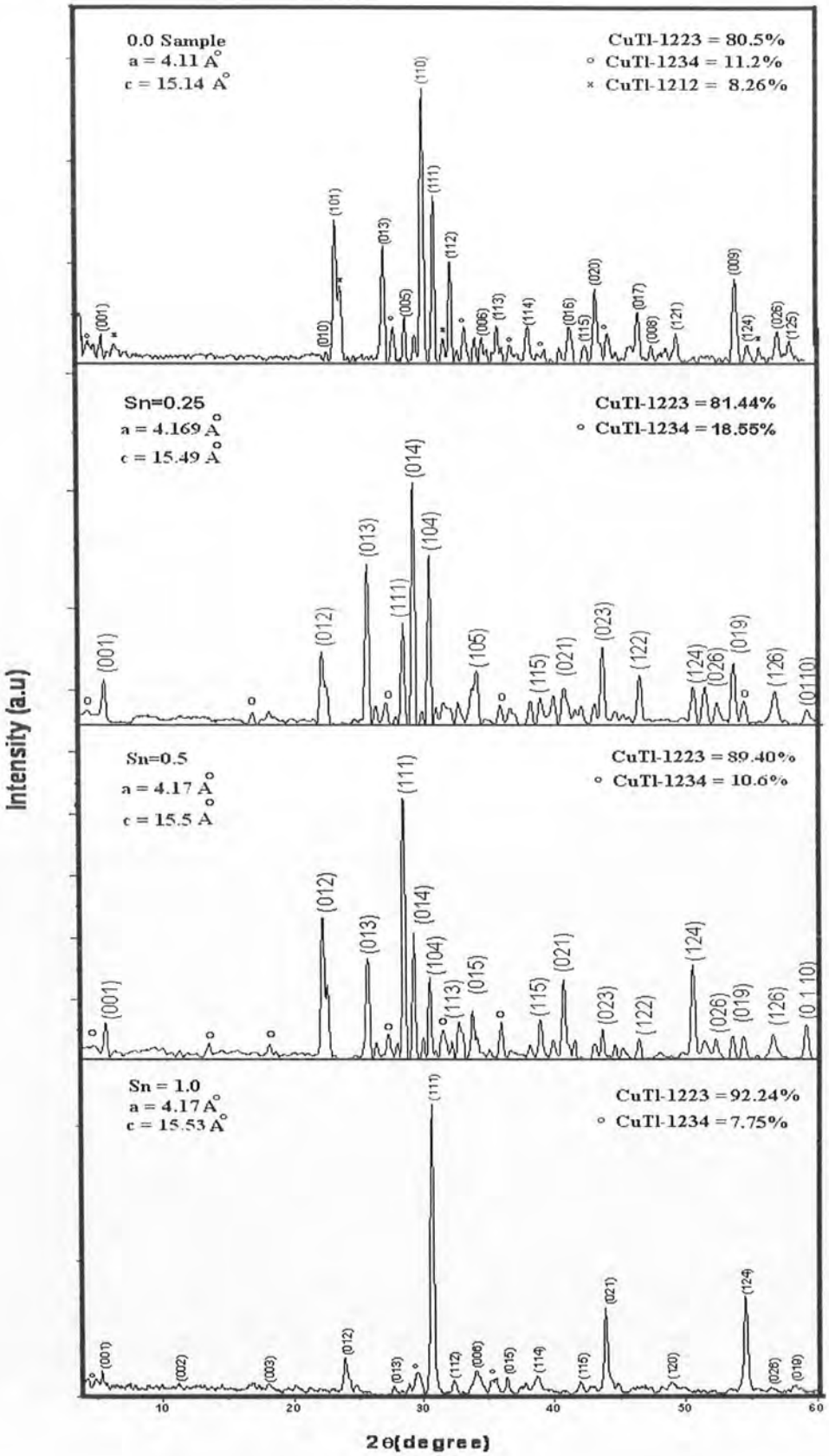

Fig.3.1 X-Ray Diffraction Pattern of (Cu0.5Tl0.5)Ba2Ca2(Cu3-xSnx)O10-δ where x = 0.0, 0.25, 0.5, 1.0

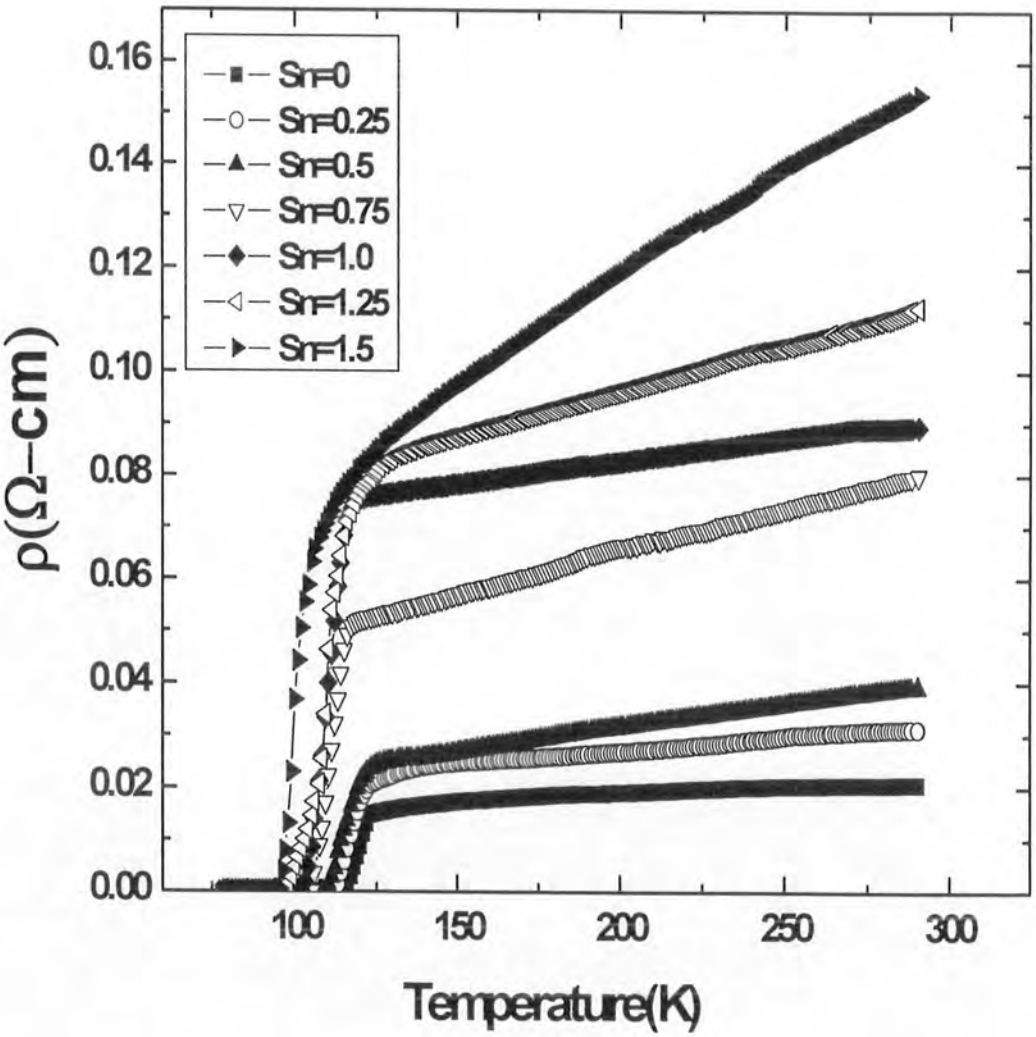

Fig.3.2 Resistivity curves of $(Cu_{0.5}Tl_{0.5})Ba_2Ca_2(Cu_{3-x}Sn_x)O_{10-\delta}$ (x=0, 0.25, 0.5, 0.75, 1,1.25,1.50) superconductor.

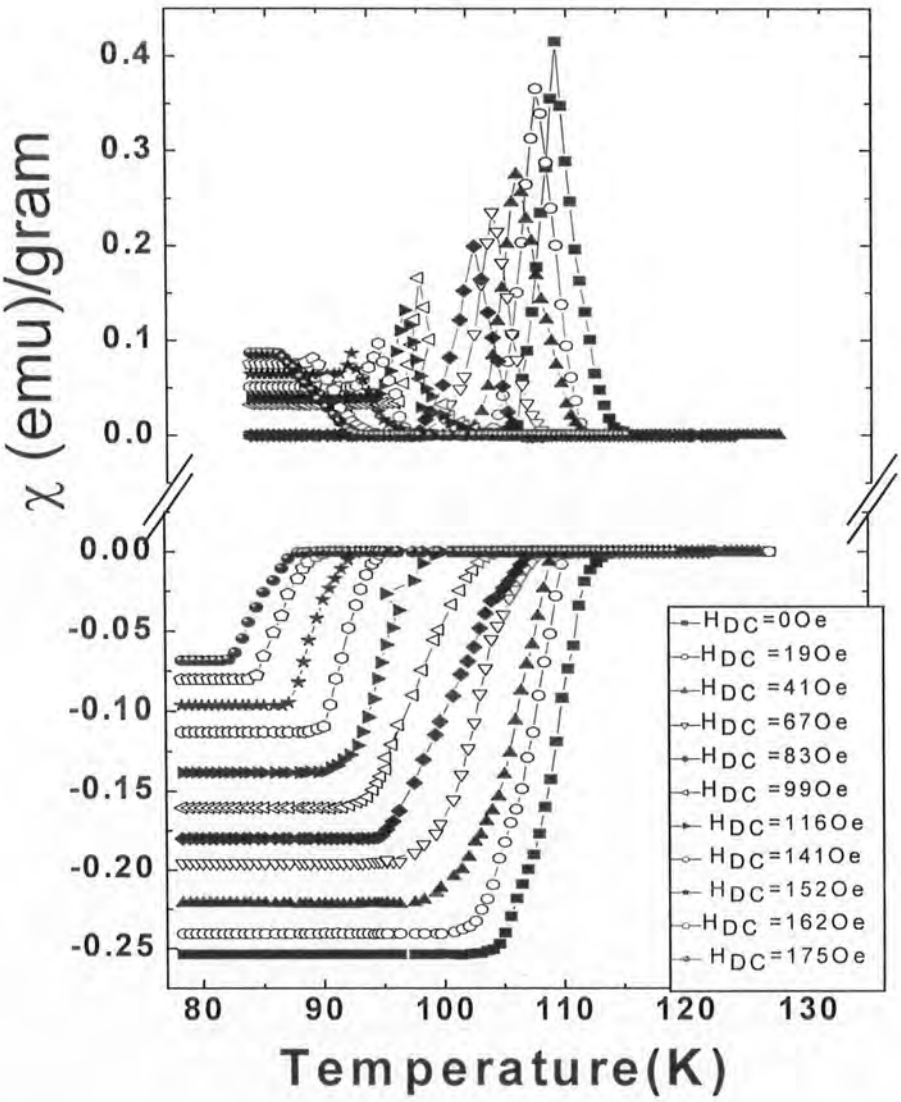

Fig. 3.3 In field AC-susceptibility measurements of$(Cu_{0.5}Tl_{0.5})Ba_2Ca_2(Cu_{3-x}Sn_x)O_{10-\delta}$(X=0) superconductor.

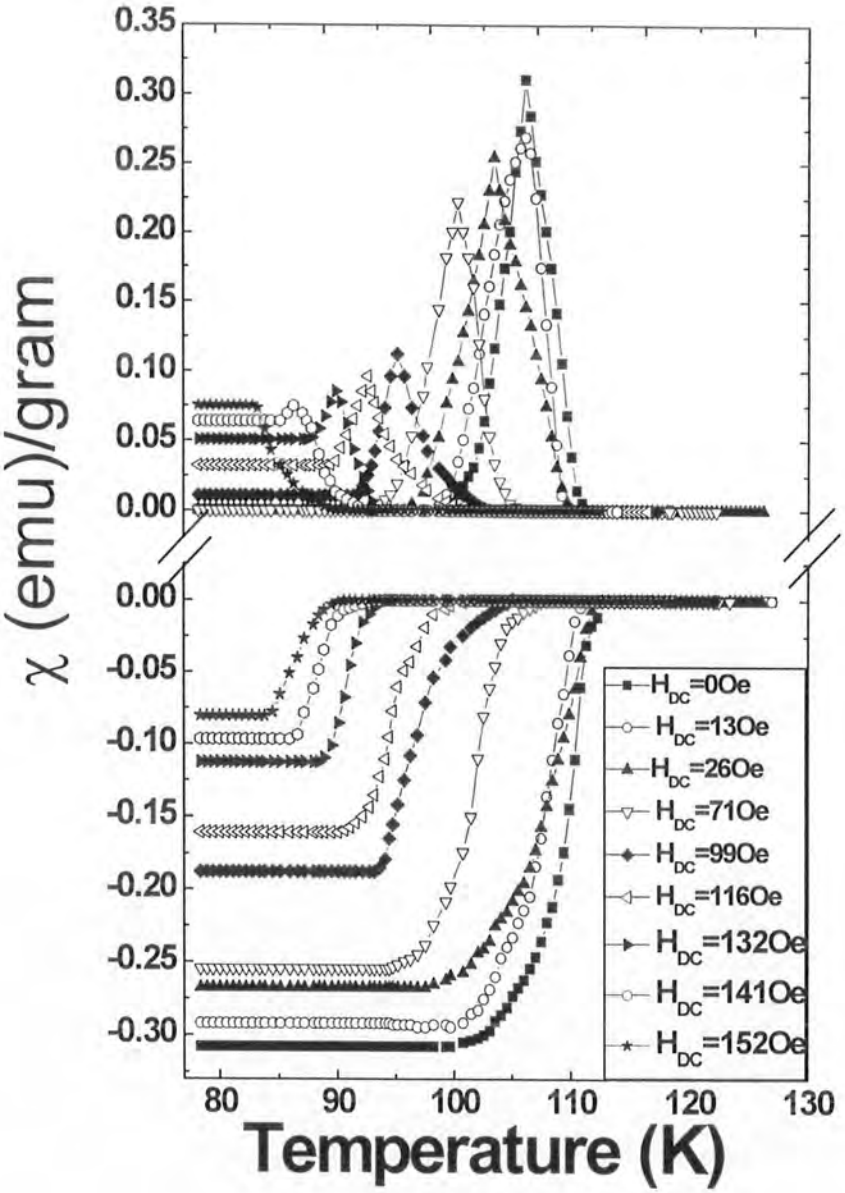

Fig. 3.4 In field AC-susceptibility measurements of $(Cu_{0.5}Tl_{0.5})Ba_2Ca_2(Cu_{3-x}Sn_x)O_{10-\delta}$ (X=0.25) superconductor.

107, 105.5, 101.1, 94.4, 93.1 and 90.5K. The peak temperatures T_p in the out-of-phase component of magnetic susceptibility χ'' under these external magnetic fields are observed around 109, 108.4, 106,102.5, 96.8, 94.1, 91.1, 87.1, 83.3K, respectively. In the zero applied external magnetic field these samples have shown onset of diamagnetism around 112.7K and peak temperature in the out-of-phase component of magnetic susceptibility around 109K.

In the infield ac-susceptibility measurements of $(Cu_{0.5}Tl_{0.5})Ba_2Ca_2(Cu_{2.5}Sn_{0.5})O_{10-\delta}$ samples with Sn doping of x=0.5 are shown in Fig.3.5. The onset of diamagnetism in the in-phase component of magnetic susceptibility in the zero applied field is observed around 109.3K and the peak temperature in the out-of-phase component of magnetic susceptibility around 105.5K. When the external magnetic field is increased, the onset of diamagnetism in in-phase component of magnetic susceptibility χ' and out-of-phase component susceptibility χ'' are shifted to lower temperature values. In the applied magnetic fields of 8, 13, 19, 26, 32, 67, 71 A/M (or Oe) the onset of diamagnetism in χ' is observed around 108.6, 108.5, 107.5, 101, 97.5, 97.5, 95.1K and the peak temperature T_p in χ'' around 99.7, 95.4, 95, 92.3 90.2, 87.6, 84K, respectively.

The infield magnetic measurements of $(Cu_{0.5}Tl_{0.5})Ba_2Ca_2(Cu_{2.25}Sn_{0.75})O_{10-\delta}$ samples are shown in Fig.3.6. In the applied external fields of 8, 13, 19, 26, 41, 54, 60 A/M, the onset of diamagnetism in χ' is observed around 109.2, 108.2, 105.5, 98, 95, 89.2, 86.5 and T_p in the out-of-phase component of magnetic susceptibility χ'' around 101.8, 99.7, 91.3, 89.7, 86.5, 83.8, 80K, respectively. In the zero applied external magnetic field these samples have shown onset of diamagnetism around 110.7K and peak temperature in the out-of-phase component of magnetic susceptibility around 107.5K.

In the infield ac-susceptibility measurements of $(Cu_{0.5}Tl_{0.5})Ba_2Ca_2(Cu_2Sn_1)O_{10-\delta}$ samples with Sn doping of x=1 are shown in Fig.3.7. The onset of diamagnetism in the in-phase component of magnetic susceptibility in the zero applied field is observed around 109.3K and the peak temperature in the out-of-phase component of magnetic susceptibility around 98K. When the external magnetic field is increased, the onset of diamagnetism in in-phase component of magnetic susceptibility χ' and out-of-phase component susceptibility χ'' are shifted to lower temperature values. In the applied magnetic fields of 8, 13, 19,

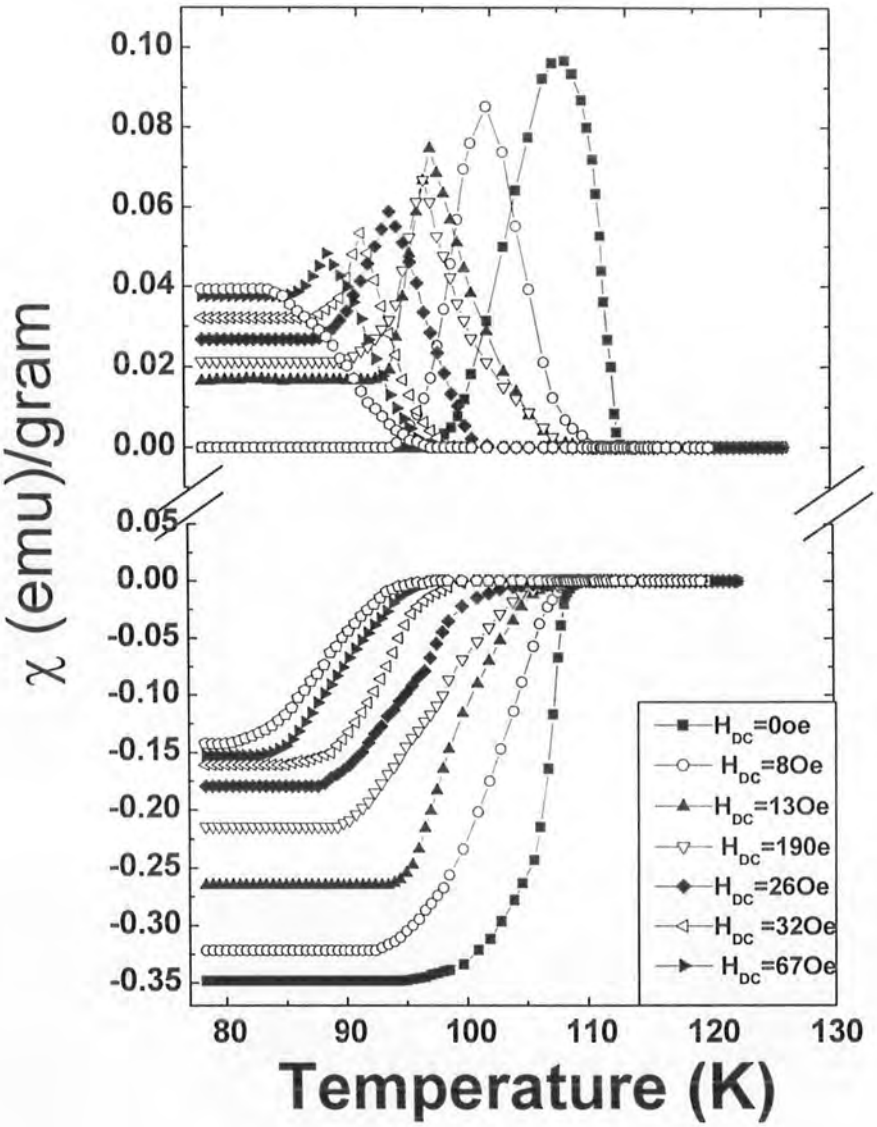

Fig. 3.5 In field AC-susceptibility measurements of $(Cu_{0.5}Tl_{0.5})Ba_2Ca_2(Cu_{3-x}Sn_x)O_{10-\delta}$ (X=0.5) superconductor.

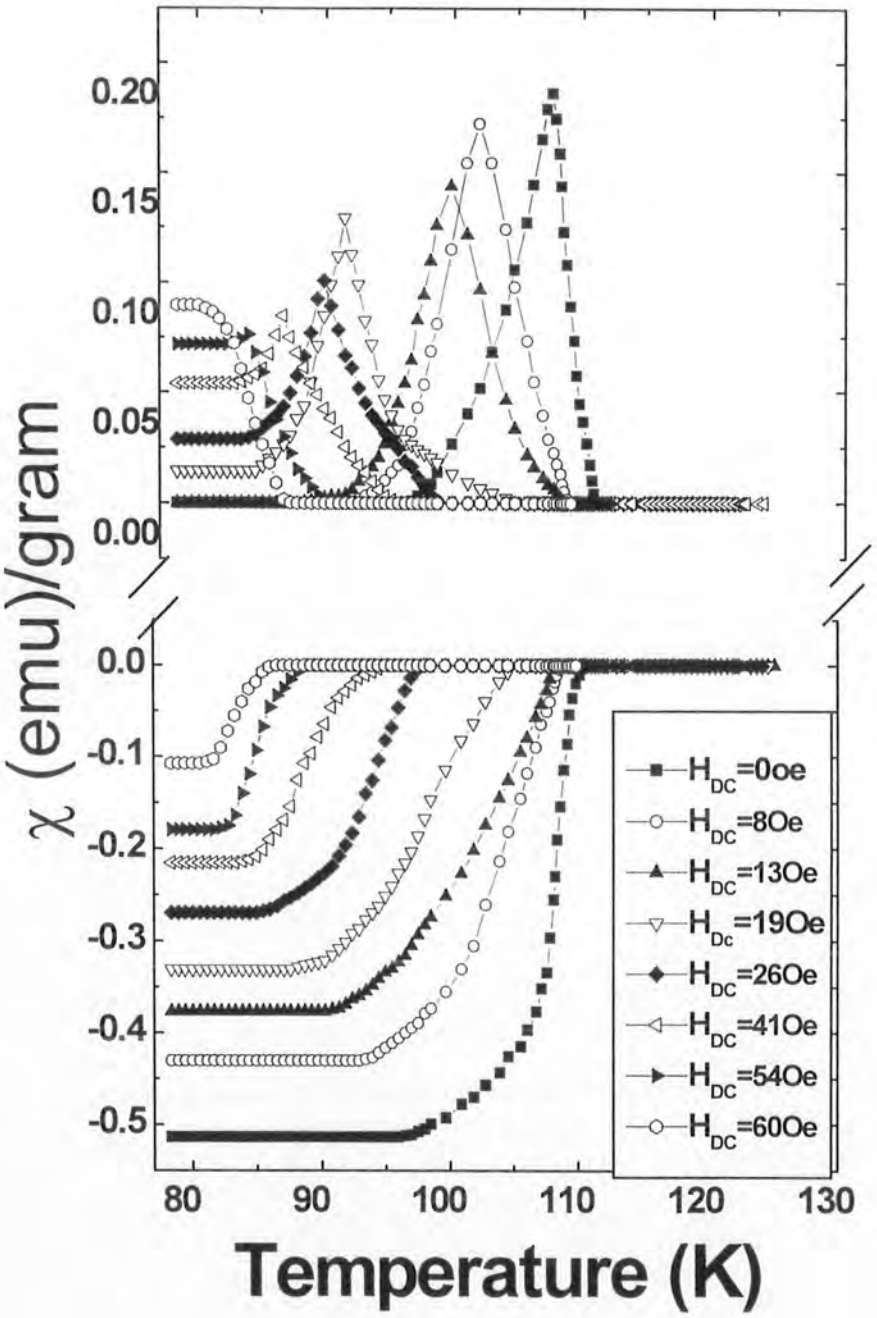

Fig. 3.6 In field AC-susceptibility measurements of $(Cu_{0.5}Tl_{0.5})Ba_2Ca_2(Cu_{3-x}Sn_x)O_{10-\delta}$ (X=0.75) superconductor.

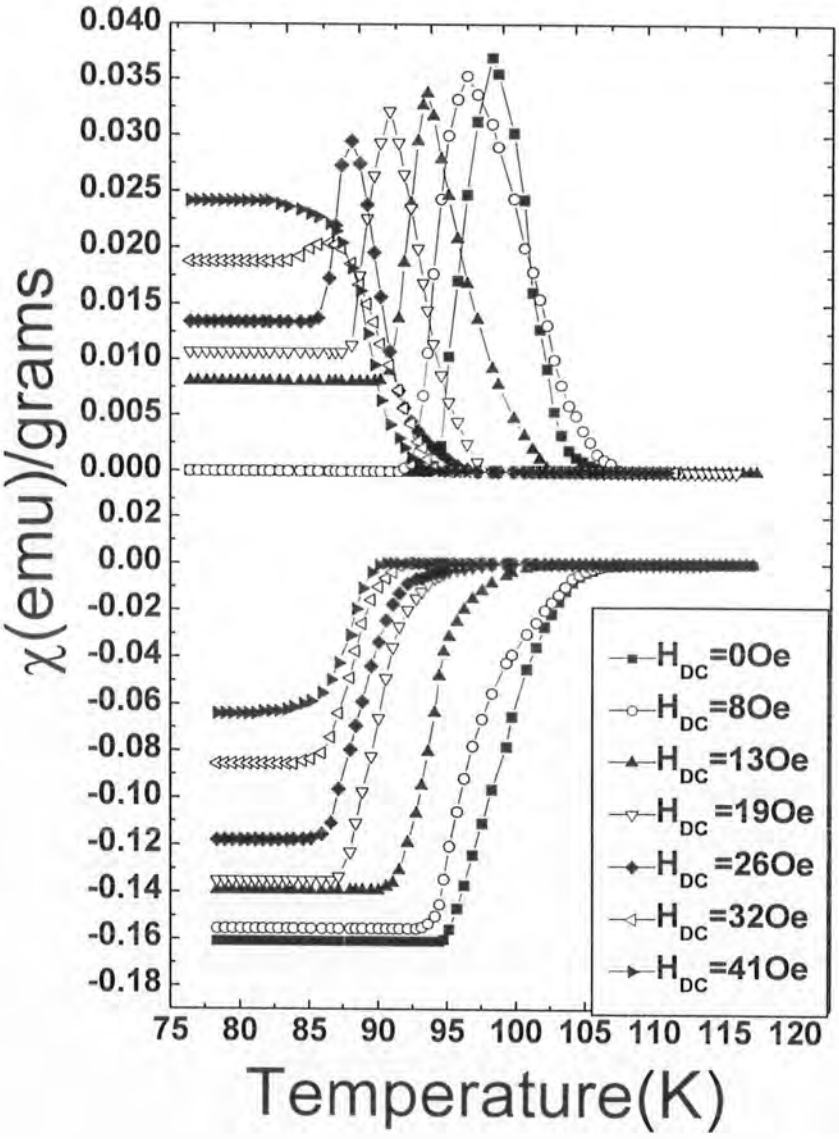

Fig .3.7In field AC-susceptibility measurements of $(Cu_{0.5}Tl_{0.5})Ba_2Ca_2(Cu_{3-x}Sn_x)O_{10-\delta}$ (X=1) superconductor.

26, 32, 41 A/M, the onset of diamagnetism in the in-phase component is observed around 108.6, 108.5, 107.5, 101, 97.5, 97.5K and the peak temperature T_p in χ'' around 99.7, 95.4, 95, 92.3 90.2, 87.6K, respectively.

In the infield ac-susceptibility measurements of $(Cu_{0.5}Tl_{0.5})Ba_2Ca_2(Cu_{1.75}Sn_{1.25})O_{10-\delta}$ samples shown in Fig.3.8. In the zero applied field, the onset of diamagnetism in the in-phase component of magnetic susceptibility is observed around 97.5K and the peak temperature in the out-of-phase component of magnetic susceptibility around 93.6K. The increased external magnetic field, shifted the onset of diamagnetism in in-phase component of magnetic susceptibility χ' and out-of-phase component susceptibility χ'' to lower temperature values. In the applied magnetic fields of 8, 13, 19, 26, 32 A/M, the onset of diamagnetism in χ' is observed around 97.5, 92.7, 91, 91, 91K and the peak temperature T_p in χ'' around 92.7, 91, 89.5, 88.4, 81.6K, respectively.

The infield ac-susceptibility measurements of $(Cu_{0.5}Tl_{0.5})Ba_2Ca_2(Cu_{1.5}Sn_{1.5})O_{10-\delta}$ samples with Sn doping of x=1.5 are shown in Fig.3.9. The onset of diamagnetism in the in-phase component of magnetic susceptibility in the zero applied field is observed around 94.7K and the peak temperature in the out-of-phase component of magnetic susceptibility around 91K. When the external magnetic field is increased, the onset of diamagnetism in χ' is shifted to 94.7, 93.6 and out-of-phase component susceptibility χ'' around 90, 805K in the applied magnetic fields of 8, 13A/M.

These infield magnetic measurements have shown that these samples posses better inter-grain connectivity because the peak in the out-of-phase component of magnetic susceptibility survives under much higher external magnetic field. The better inter-grain connectivity is most likely arising from the presence of higher concentration of oxygen in the final compound. The higher oxygen density in the final compound is most likely originating from higher affinity of oxygen towards Sn as compare to Cu atoms in CuO_2/SnO_2 planes. The enhanced concentration of oxygen in the final compound most likely promotes the formation of oxides at the inter-grain sites resulting into enhanced areas of shielding currents flow promoting higher critical current densities.

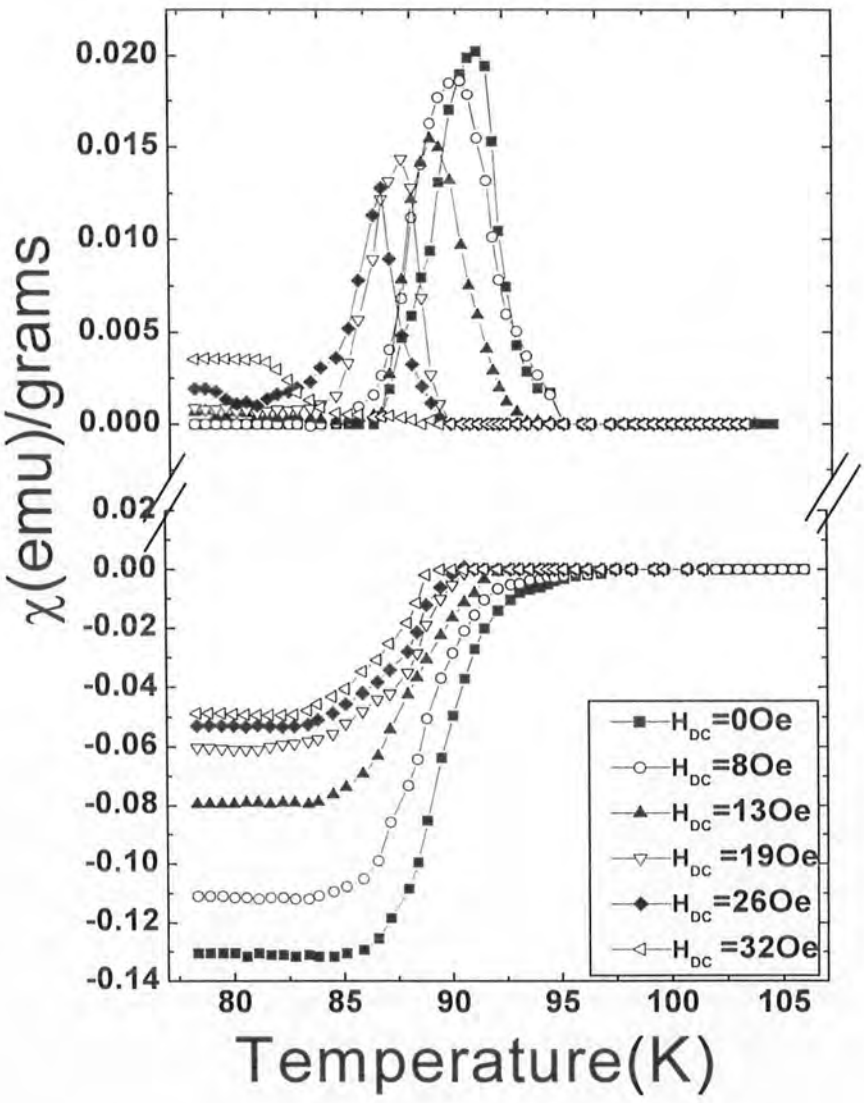

Fig .3.8I n field AC-susceptibility measurements of $(Cu_{0.5}Tl_{0.5})Ba_2Ca_2(Cu_{3-x}Sn_x)O_{10-\delta}$ (X=1.25) superconductor.

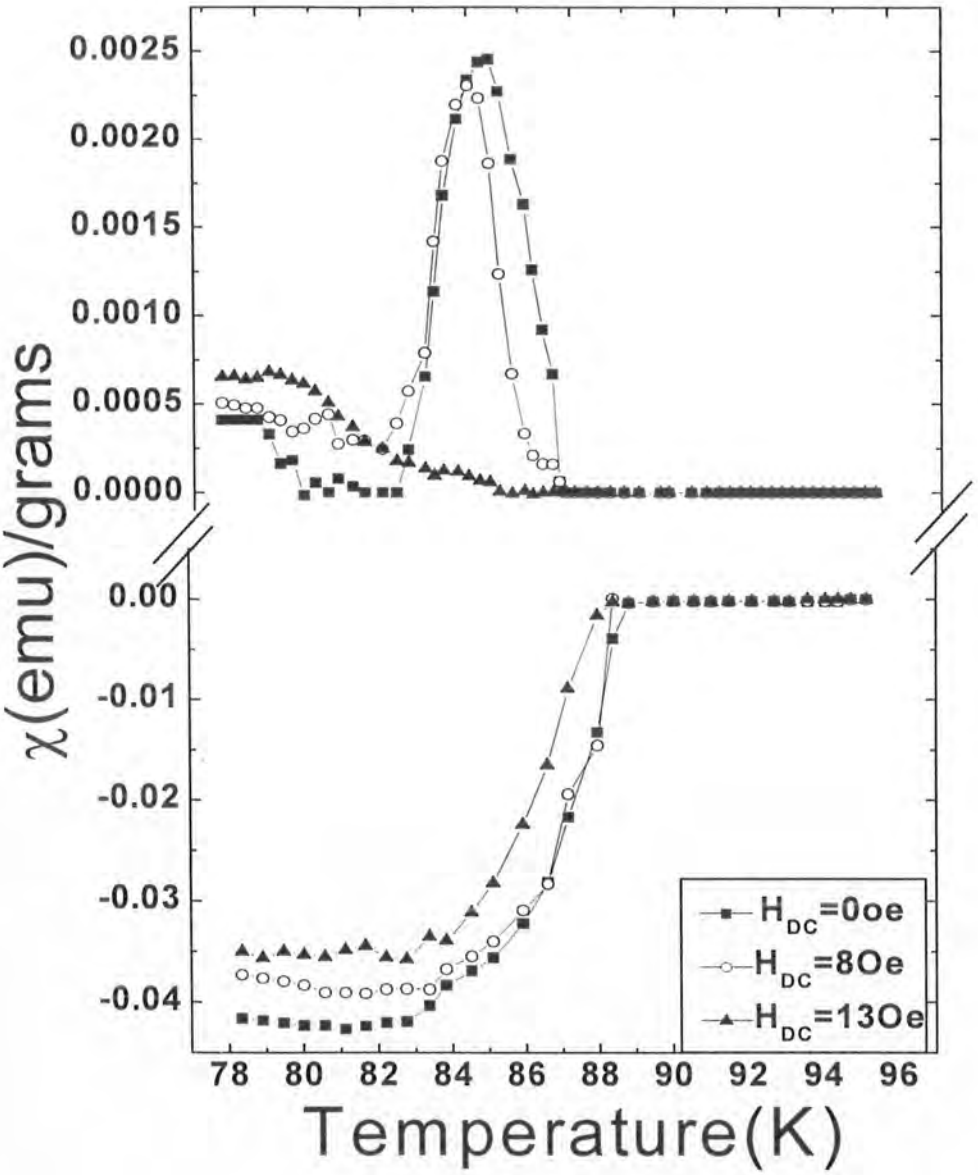

Fig .3.9In field AC-susceptibility measurements of $(Cu_{0.5}Tl_{0.5})Ba_2Ca_2(Cu_{3-x}Sn_x)O_{10-\delta}$ (X=1.5) superconductor.

3.3.2 Oxygen Post-annealed $(Cu_{0.5}Tl_{0.5})Ba_2Ca_2(Cu_{3-x}Sn_x)O_{10-\delta}$ Samples

The resistivity measurements of oxygen post-annealed samples are shown in Fig.3.10. All these $(Cu_{0.5}Tl_{0.5})Ba_2Ca_2(Cu_{3-x}Sn_x)O_{10-\delta}$ (x=0, 0.25, 0.5, 0.75, 1.0, 1.25, 1.5) samples have shown metallic variations of resistivity from room temperature down to onset of superconductivity, however, the slope of the metallic nature is significantly decreased after post-annealing in oxygen. In most of the samples doped with Sn the magnitude of diamagnetism is decreased after post-annealing in oxygen atmosphere. The decreased magnitude of diamagnetism is most likely arising from the increased diffusion of oxygen into the sample after post-annealing in oxygen atmosphere.

These samples have shown onset of superconductivity [T_c(onset)] around 129, 127, 145, 161, 144, 119, 106.5K and zero resistivity critical temperature [T_c(R=0)] around 121, 116, 110, 108, 107, 99, 96K for the Sn doping of x=0, 0.25, 0.5, 0.75, 1.0, 1.25, 1.5 in $(Cu_{0.5}Tl_{0.5})Ba_2Ca_2(Cu_{3-x}Sn_x)O_{10-\delta}$ superconductors. The normal state resistivity of these samples increases with increased Sn doping in the final compound. The decreased slope in the normal state resistivity, may possibility be associated with the decreased carrier's density originating from the increased oxygen diffusion in the final compound. In the in-phase component of magnetic susceptibility, the onset of diamagnetism is observed around 121, 116, 110.3, 109.3, 107.4, 99.6K with peak temperature (T_P) in the out-of-phase component at 107.9, 109.4, 104.5, 105.5, 95.2, 91K for the $(Cu_{0.5}Tl_{0.5})Ba_2Ca_2(Cu_{3-x}Sn_x)O_{10-\delta}$ for the Sn doping of x=0,0.25, 0.5, 0.75, 1.0, 1.25, respectively. The in-field magnetic measurements of these samples are shown in Figures. 3.11-3.16.

The infield ac-susceptibility measurements of oxygen post-annealed $(Cu_{0.5}Tl_{0.5})Ba_2Ca_2Cu_3O_{10-\delta}$ samples, are shown in Fig.3.11. These samples have shown onset of diamagnetism in the in-phase component of magnetic susceptibility around 121K and the peak temperature in the out-of-phase component of magnetic susceptibility at 107.9K. The increased external magnetic field shifts both the onset and the peak temperatures to lower temperature values. In the applied magnetic fields of 41, 67, 87, 99, 111, 132, 152, 162 A/M (or Oe) the onset of diamagnetism in the in-phase component of magnetic susceptibility χ' is shifted to 113, 109.4, 104.8, 104.5,99.28,93.1, 90.6, 90.4K and the peak temperature T_p in the out-of-phase

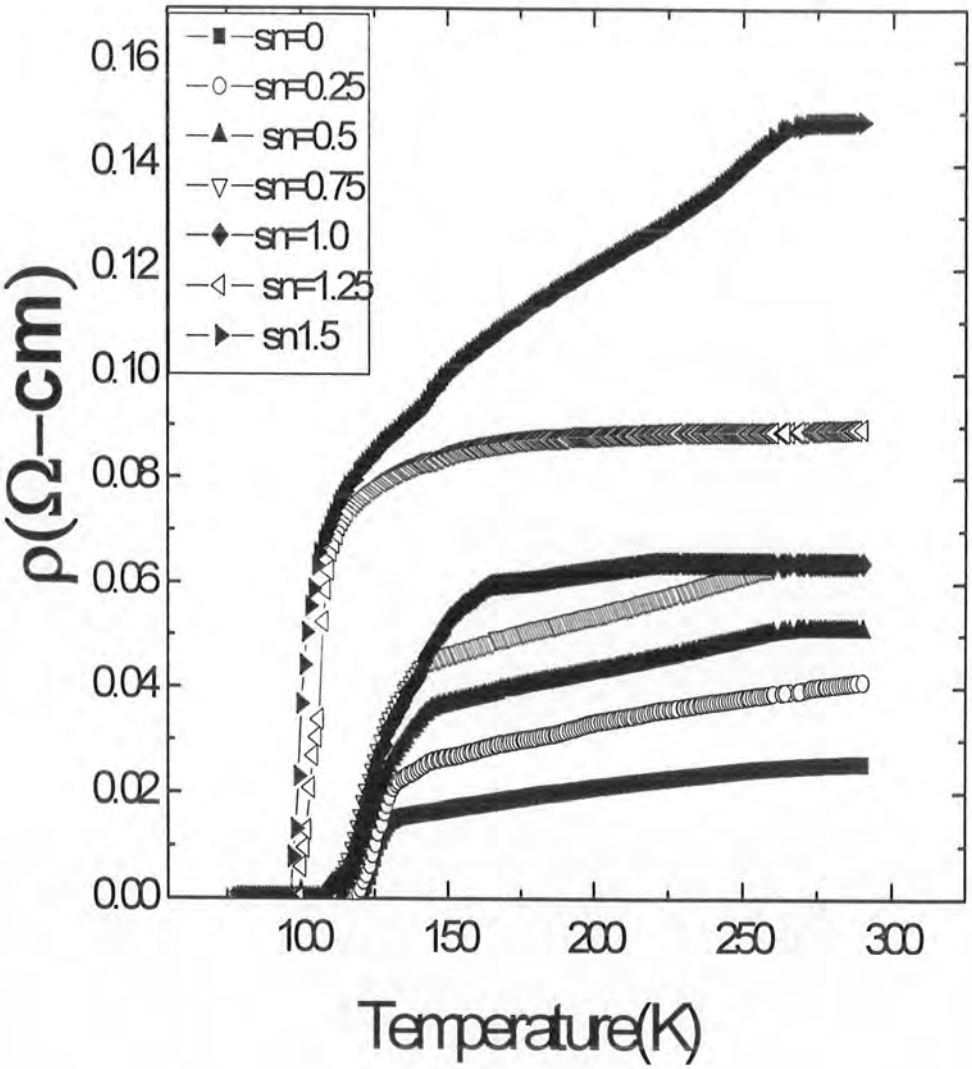

Fig. 3.10 Resistivity curves of oxygen annealed $(Cu_{0.5}Tl_{0.5})Ba_2Ca_2(Cu_{3-x}Sn_x)O_{10-\delta}$ (x=0, 0.25, 0.5, 0.75, 1,1.25,1.50) superconductor.

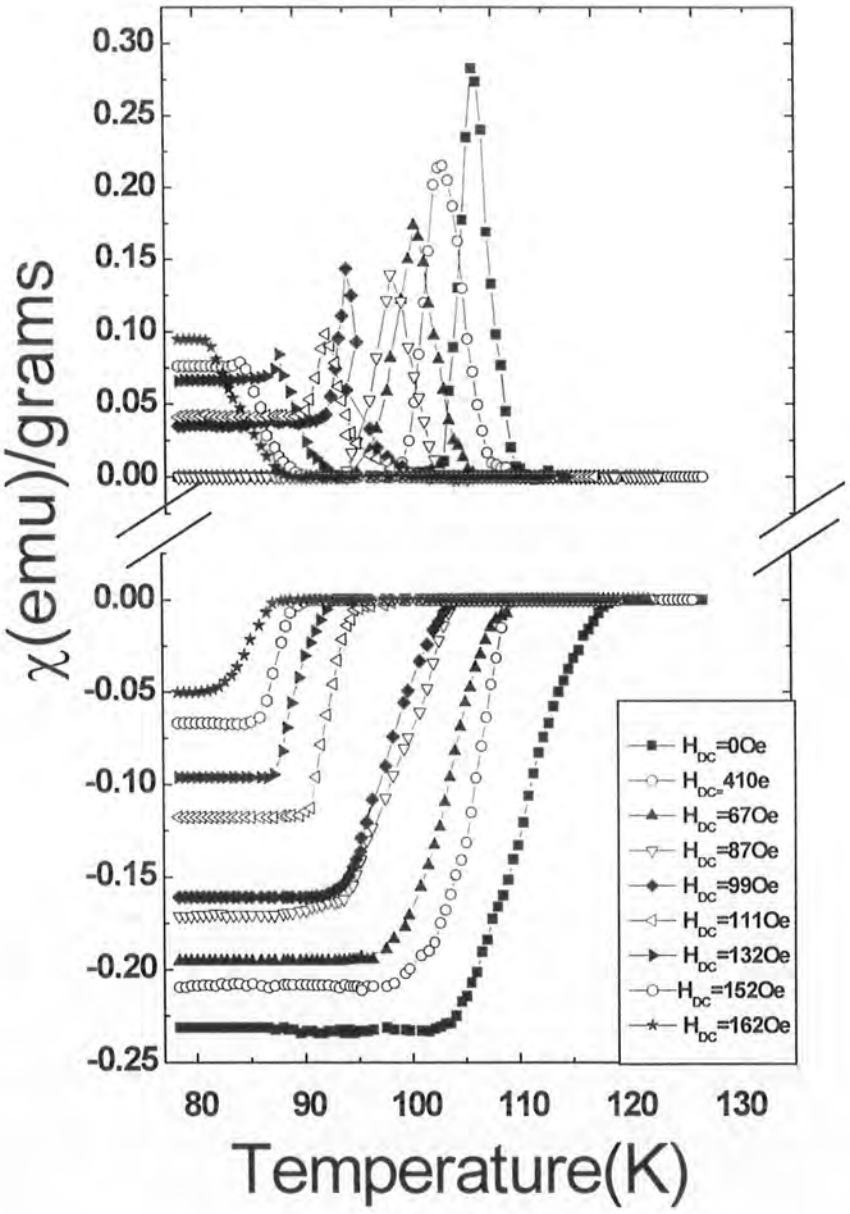

Fig3.11InfieldAC-susceptibility measurements of O_2annealed$(Cu_{0.5}Tl_{0.5})Ba_2Ca_2(Cu_{3-})O_{10-\delta}$ superconductor.

component of magnetic susceptibility χ'' to 104.5, 102.5, 99.6, 95.1, 78.3, 88.4, 84.5, 81.1K, respectively.

The infield magnetic measurements of oxygen post-annealed Sn doped $(Cu_{0.5}Tl_{0.5})Ba_2Ca_2(Cu_{2.75}Sn_{0.25})O_{10-\delta}$ superconductors are shown in Fig.3.12. In the external magnetic fields of 8, 19, 41, 54, 71, 99, 116, 132, 141, 152, 162 A/M, the onset of diamagnetism in χ' is observed around 113.6, 112.2, 108.4, 105.5, 103, 100.6, 96.8, 96.2, 94, 93.6, and 90.5K. The peak temperatures T_p in the out-of-phase component of magnetic susceptibility χ'' under these external magnetic fields are observed around 108.4, 105.5, 103.4, 101.4, 98.2, 96.2, 95, 94, 91, 87, 87.7K, respectively. In the zero applied external magnetic field these samples have shown onset of diamagnetism around 116K and peak temperature in the out-of-phase component of magnetic susceptibility around 109.4K.

Ac-susceptibility measurements in the applied external field of $(Cu_{0.5}Tl_{0.5})Ba_2Ca_2(Cu_{2.5}Sn_{0.5})\ O_{10-\delta}$ samples are shown in Fig.3.13. The onset of diamagnetism in χ' magnetic susceptibility in the zero applied fields is observed around 110.5K and the peak temperature in the out-of-phase component of magnetic susceptibility around 104.5K. When the external magnetic field is increased, the onset of diamagnetism in in-phase component of magnetic susceptibility χ' and out-of-phase component of susceptibility χ'' are shifted to lower temperature values. In the applied magnetic fields of 8, 13, 41, 48, 54, 60, 67, 71A/M (or Oe) the onset of diamagnetism in χ' is observed around 108.3, 105.5, 98, 95.8, 94.9, 91.3, 88.6, 88.6K and the peak temperature T_p in χ'' around 102.8, 97, 90.7, 89.7, 86, 83.8, 83.3, 80K, respectively.

The infield magnetic measurements of $(Cu_{0.5}Tl_{0.5})Ba_2Ca_2(Cu_{2.25}Sn_{0.75})O_{10-\delta}$ samples are shown in Fig.3.14. In the applied external fields of 8, 13, 19, 26, 41, 60 71, 78A/M, the onset of diamagnetism in χ' is observed around 108.2, 108.2, 105.5, 105.5, 98.5, 96.5, 95.3, 91.3K and T_p in the out-of-phase component of magnetic susceptibility χ'' around 102.8, 101, 97.5, 95, 91.8, 89.7, 88.1, 83.3K, respectively. In the zero magnetic field these samples have shown onset of diamagnetism around 109.1K and peak temperature in the out-of-phase component of magnetic susceptibility around 105.5K.

Ac-susceptibility measurements of $(Cu_{0.5}Tl_{0.5})Ba_2Ca_2(Cu_2Sn_1)O_{10-\delta}$ samples post-annealed in oxygen are shown under various applied field in Fig.3.15. In the zero applied fields, the in-phase component of magnetic susceptibility has shown onset of

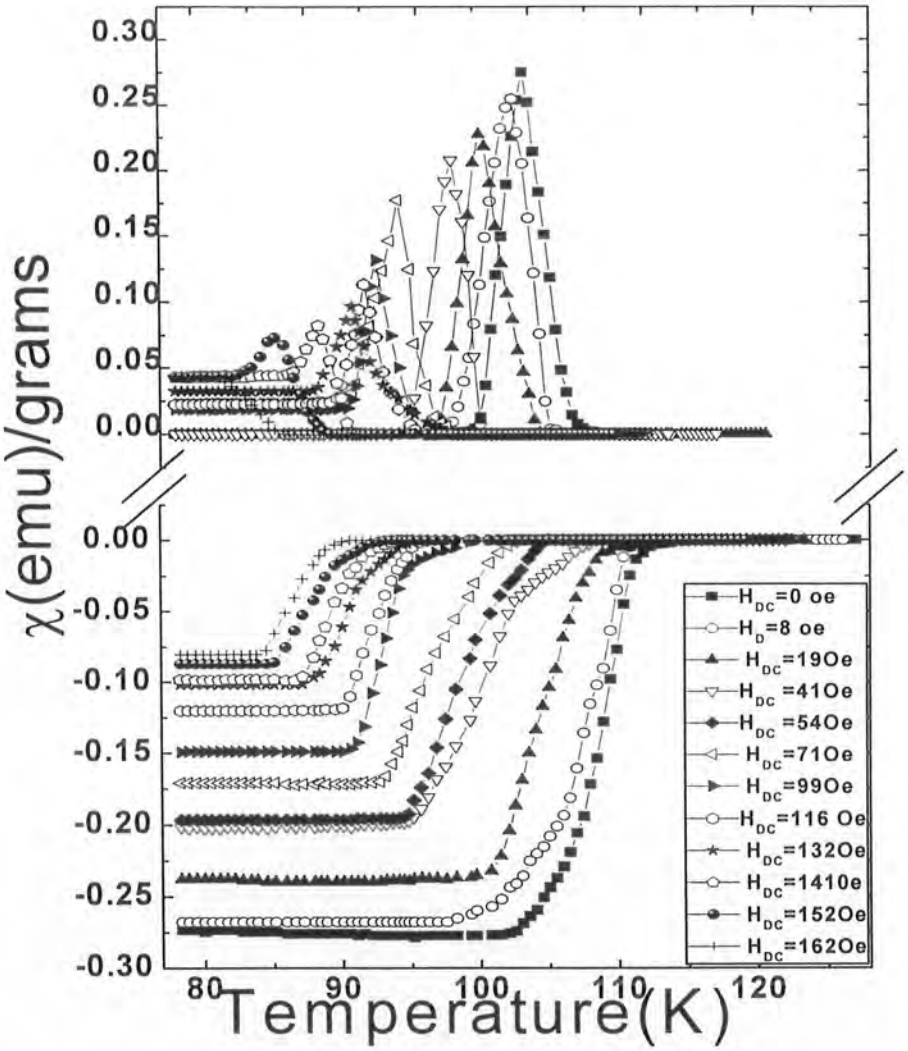

Fig.3.12 Infield AC-susceptibility measurements of O_2annealed $(Cu_{0.5}Tl_{0.5})Ba_2Ca_2(Cu_{3-x}Sn_x)O_{10-\delta}$ (X=0.25) superconductor.

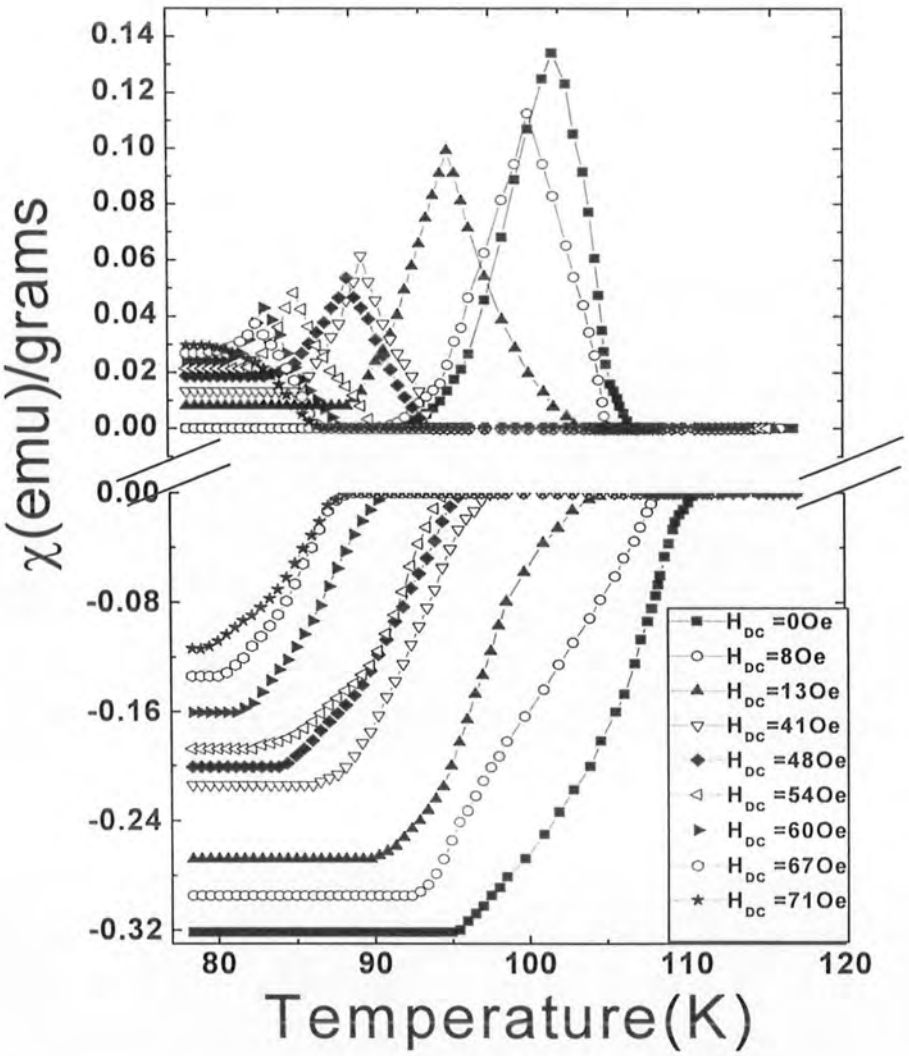

Fig 3.13 In field AC-susceptibility measurements of O_2 annealed $(Cu_{0.5}Tl_{0.5})Ba_2Ca_2(Cu_{3-x}Sn_x)O_{10-\delta}$ (X=0.5) superconductor

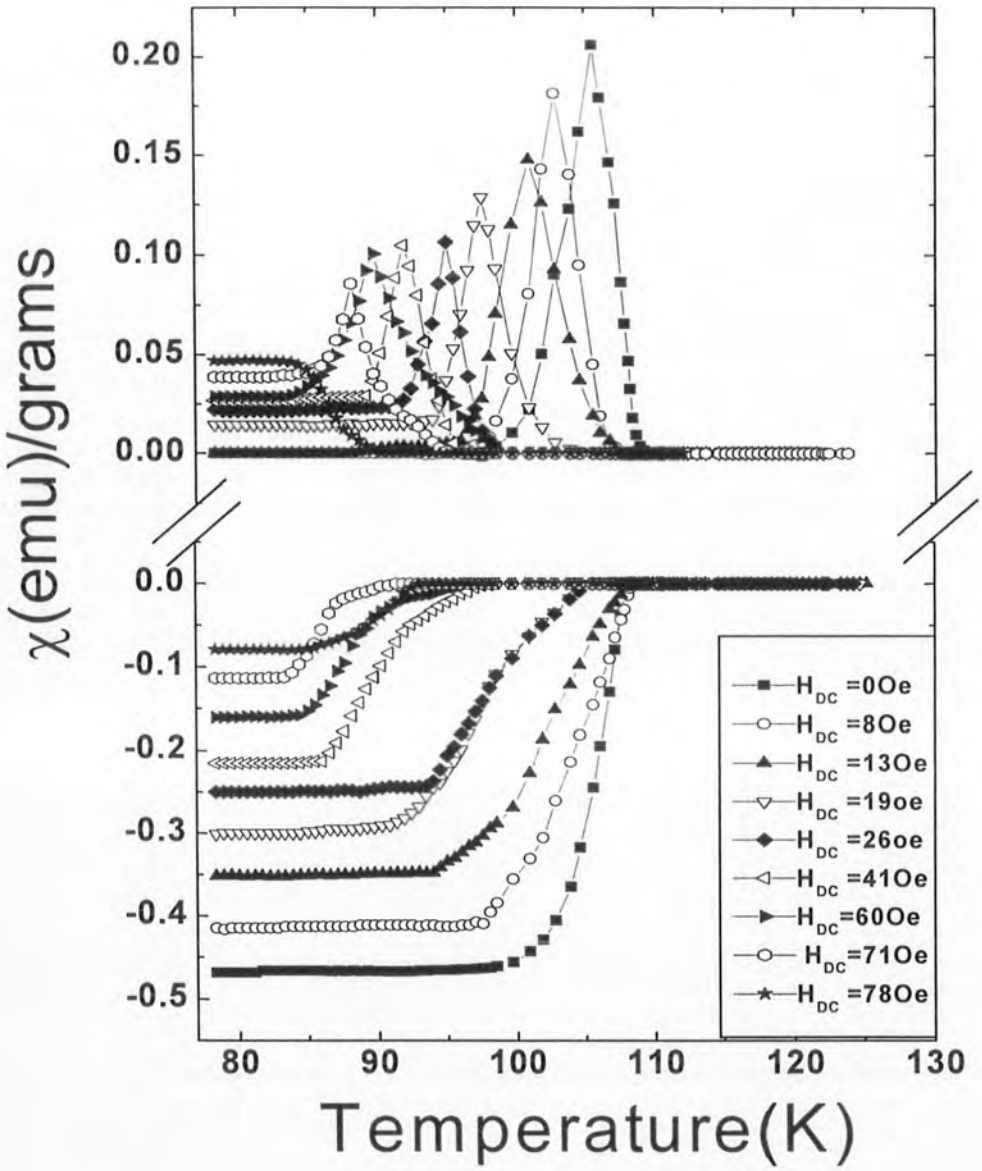

Fig 3.14 In field AC-susceptibility measurements of O_2 annealed $(Cu_{0.5}Tl_{0.5})Ba_2Ca_2(Cu_{3-x}Sn_x)O_{10-\delta}$ (X=0.75) superconductor

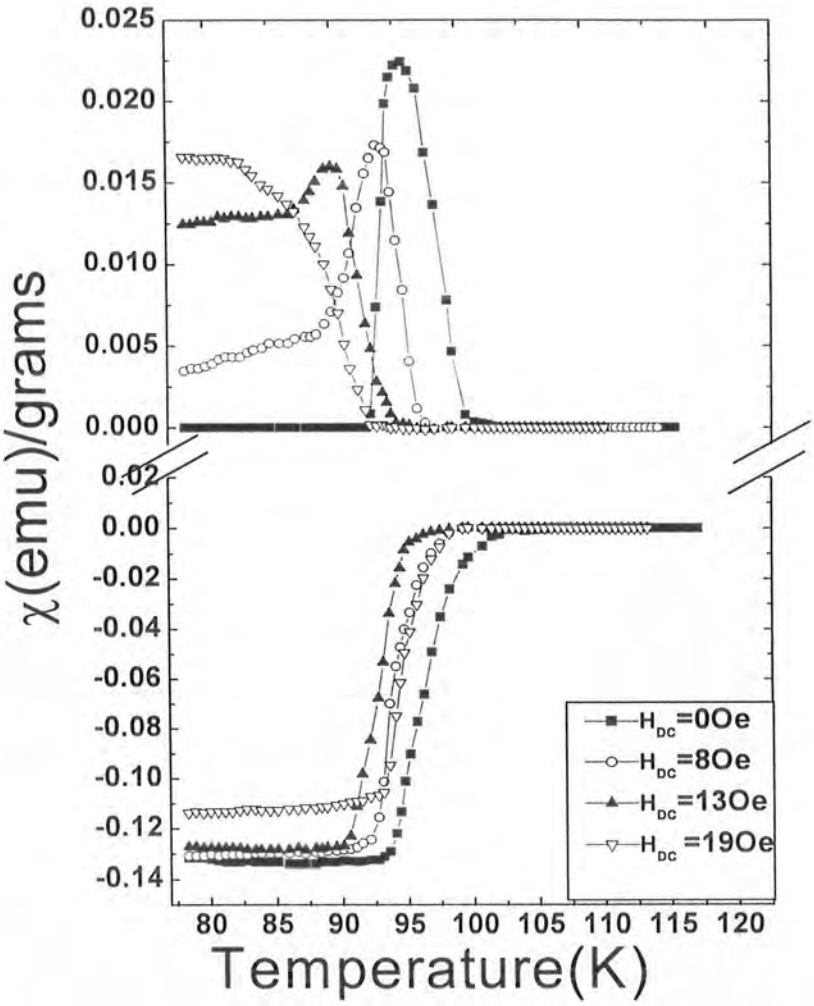

Fig 3.15 In field AC-susceptibility measurements of O_2 annealed $(Cu_{0.5}Tl_{0.5})Ba_2Ca_2(Cu_{3-x}Sn_x)O_{10-\delta}$ (X=1) superconductor

diamagnetism around 107.4K and the peak temperature in the out-of-phase component of magnetic susceptibility around 95.2K. When the external magnetic field is increased, the onset of diamagnetism in in-phase component of magnetic susceptibility χ' and out-of-phase component susceptibility χ'' are shifted to lower temperature values. In the applied magnetic fields of 8, 13, 19, A/M, the onset of diamagnetism in the in-phase component is observed around 100.8, 1008, 100.8K and the peak temperature T_p in χ'' around 93.6, 90, 82.7K, respectively.

The infield ac-susceptibility measurements of $(Cu_{0.5}Tl_{0.5})Ba_2Ca_2(Cu_{1.75}Sn_{1.25})\ O_{10-\delta}$ samples post-annealed in oxygen atmosphere are shown in Fig.3.16. In the zero applied field, the onset of diamagnetism in the in-phase component of magnetic susceptibility is observed around 99K and the peak temperature in the out-of-phase component of magnetic susceptibility around 91K. The increased external magnetic field, shifted the onset of diamagnetism in in-phase component of magnetic susceptibility χ' and out-of-phase component of susceptibility χ'' to lower temperature values. In the applied magnetic fields of 8, 13, A/M, the onset of diamagnetism in χ' is observed around 92, 91K and the peak temperature T_p in χ'' around 88.8, 81K, respectively. Beyond this field, the peak observed in the out-of-phase component of magnetic susceptibility disappears altogether, showing that a significant volume fraction of the sample has become normal beyond this field value.

It is our observation that magnitude of diamagnetism is decreased after post annealing in oxygen which is most likely arising from enhanced diffusion of oxygen in final compound.The increased oxygen diffusion in $(Cu_{0.5}Tl_{0.5})Ba_2O_{4-\delta}$ charge reservoir layer of $(Cu_{0.5}Tl_{0.5})Ba_2Ca_2(Cu_{3-x}Sn_x)O_{10-\delta}$ superconductors decreases the density of mobile carriers in the CuO_2/SnO_2 planes resulting into decreased superconductivity volume fraction. A small superconducting volume fraction associated with increased oxygen diffusion both at inter-grain and intra-grain sites makes the weak link behaviour of these compounds inferior. The peak value in the out-of-phase component of magnetic susceptibility survives under small values as compare to oxygen un-annealed samples.

Since the grain boundaries among the two grains act as Josephson junctions and the temperature dependence of H_c penetrating through these Josephson junctions can be written in the form of expression $H_c \sim (1-T_P/T_c)^n$. The value of exponent "n" determines the nature of the material at the junction site. The value of n is 2 for superconductor-normal metal-superconductor (SNS) junctions, 1 for superconductor-insulator-

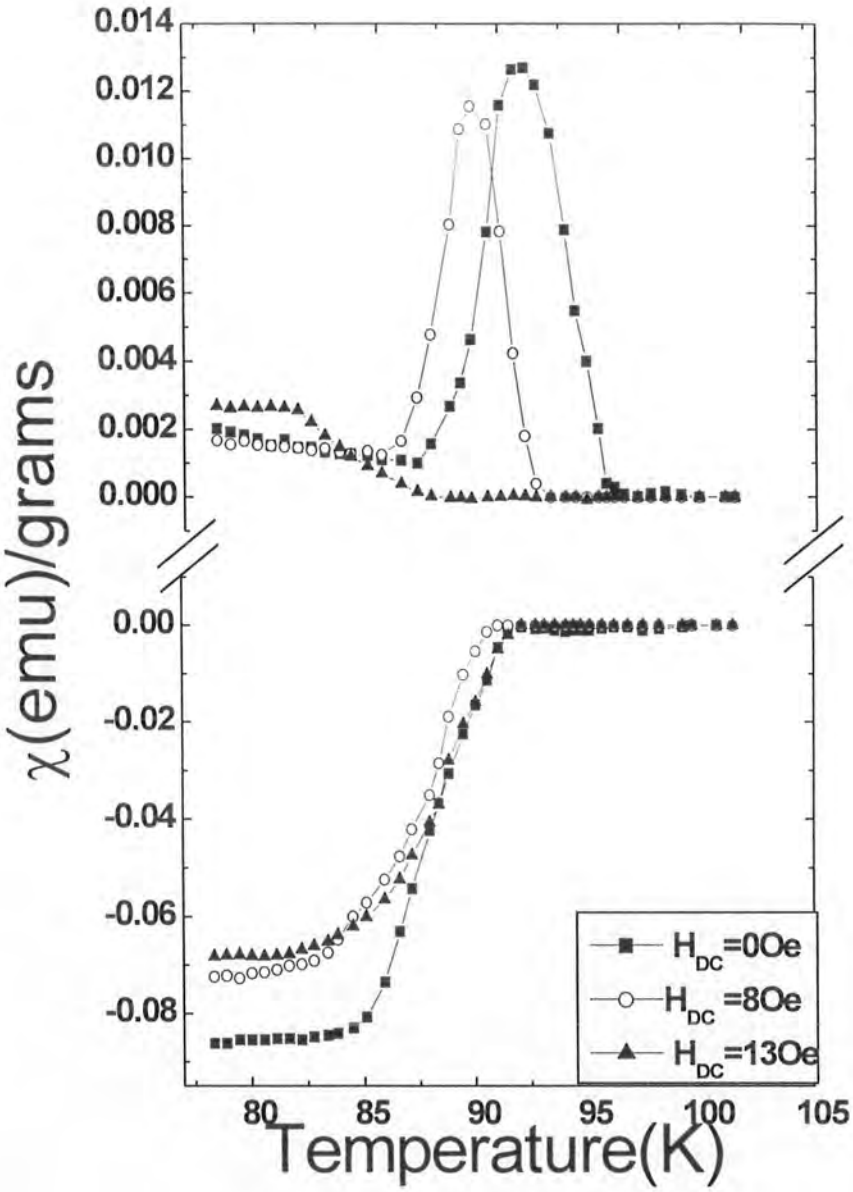

Fig 3.16 In field AC-susceptibility measurements of O_2 annealed $(Cu_{0.5}Tl_{0.5})Ba_2Ca_2(Cu_{3-x}Sn_x)O_{10-\delta}$ (X=1.25) superconductor

superconductor (SIS) junctions and the value of n between 1 and 2 indicates the formation of superconductor-insulator-normal metal-superconductor (SINS) junctions. The best fitting of our data for as prepared and oxygen annealed samples of $(Cu_{0.5}Tl_{0.5})Ba_2Ca_2(Cu_{3-x}Sn_x)O_{10-\delta}$ (x=0, 0.25, 0.5,0.75,1,1.25,1.50) and $Cu_{0.5}Tl_{0.5}Ba_2(Ca_{2-y}M_y)(Cu_2Sn_1)O_{10-\delta}$ (M=Be, Mg) is achieved for n = 1, which showed that the material at the inter-grain sites is insulating and forms a superconductor-insulator-superconductor (SIS) junctions, Fig .3.17& 3.18

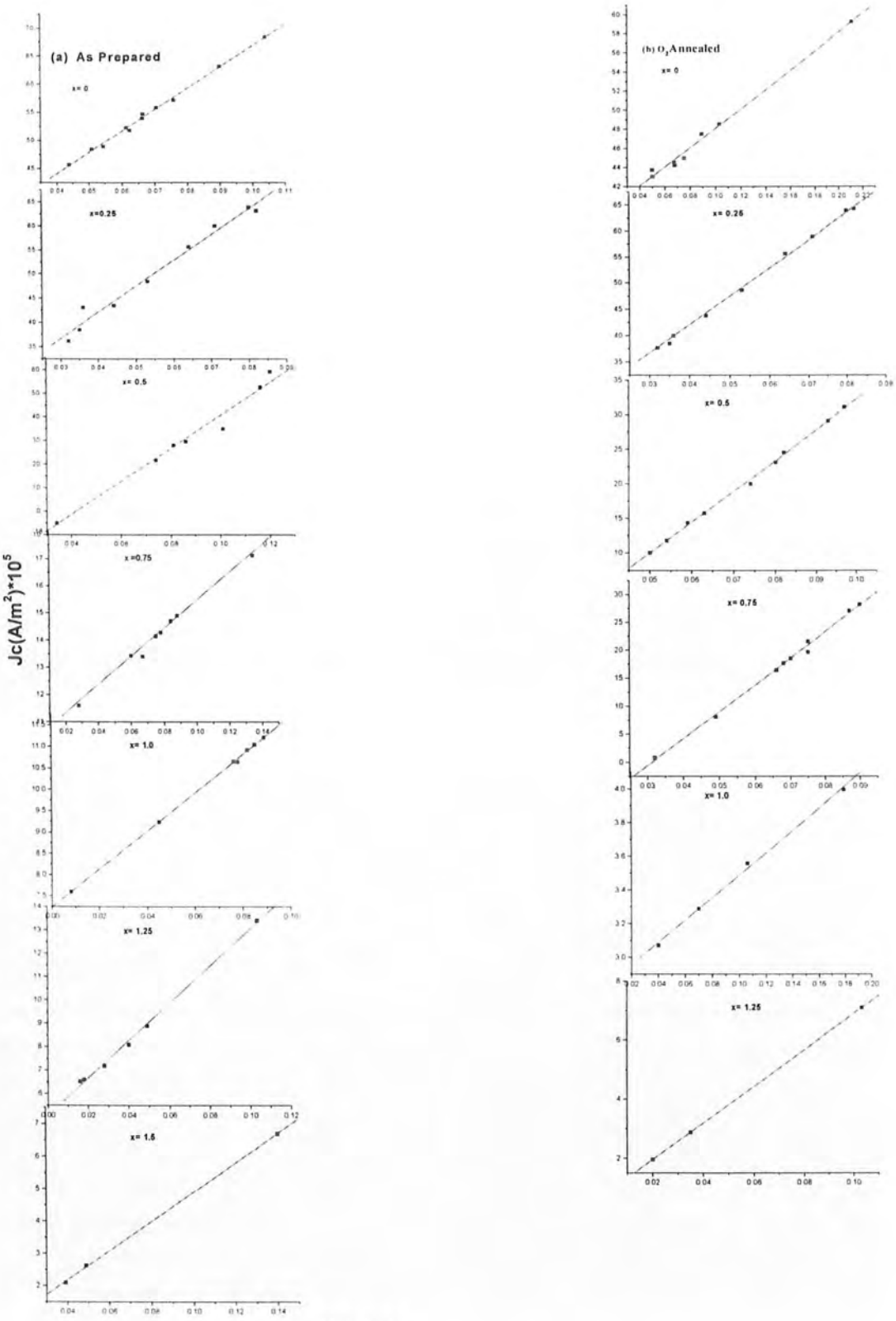

Fig.3.17. J_c vs $(1-T_p/T_c)$ for both As Prepared and O_2 Annealed Sample

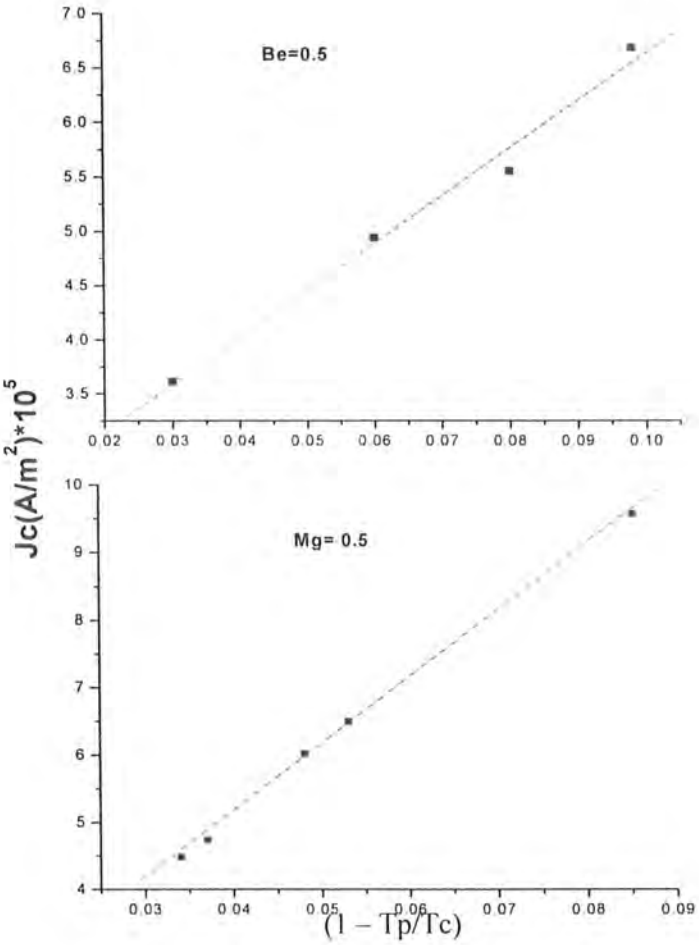

Fig.3.18. J_c vs $(1-T_p/T_c)$ for both As Prepared Samples

3.3.3 Be and Mg Doped $Cu_{0.5}Tl_{0.5}Ba_2(Ca_{2-y}M_y)(Cu_2Sn_1)O_{10-\delta}$ (M=Be, Mg) Superconductors

In our previous studies we have doped Mg and Be at the Ca sites to reduce the inter-plane distance which in turn enhances the interaction of the carriers in various planes. In the present studies it is interesting to see the effect of decreased distances among various planes and its effect on the magnitude of diamagnetism. We have chosen a moderate doping concentration of Mg and Be for such studies, i.e y=0.5. The resistivity measurements of Mg doped $Cu_{0.5}Tl_{0.5}Ba_2(Ca_{1.5}M_{0.5})(Cu_2Sn_1)O_{10-\delta}$ superconductors are shown in Fig. 3.19. These samples have shown metallic variations of resistivity from room temperature down to onset of superconductivity around 112K and T_c(R=0) at 101K. The magnitude of diamagnetism in these samples is decreased after Mg doping. The onset of diamagnetism is observed 102K and the peak temperature in the out-of-phase component of magnetic susceptibility at 97K. In the infield magnetic measurements the magnitude of diamagnetism systematically decreases with increased external field and the peak in the out-of-phase component of magnetic susceptibility disappears at much lower field as compare with Mg un-doped $(Cu_{0.5}Tl_{0.5})Ba_2Ca_2(Cu_2Sn_1)O_{10-\delta}$, Fig.3.20. The increased external magnetic field, shifted the onset of diamagnetism in in-phase component of magnetic susceptibility χ' and out-of-phase component susceptibility χ'' to lower temperature values. In the applied magnetic fields of 8, 13, 19, 26 A/M, the onset of diamagnetism in χ' is observed around 99.7, 96.5, 93.4, 89.2K and the peak temperature T_p in χ'' around 96.5 , 91.32, 85.4,84.9K, respectively.

The resistivity measurements of Be doped $Cu_{0.5}Tl_{0.5}Ba_2(Ca_{1.5}Be_{0.5})(Cu_2Sn_1)\ O_{10-\delta}$ samples are shown in Fig.3.21. These samples have shown metallic variations of resisitivity from room temperature down to onset of superconductivity with Tc(onset) around 108K and Tc(R=0) at 98K. In Be doped $Cu_{0.5}Tl_{0.5}Ba_2(Ca_{1.5}Be_{0.5})(Cu_2Sn_1)\ O_{10-\delta}$ samples the magnitude of diamagnetism is even more suppressed as compare with Mg un-doped $(Cu_{0.5}Tl_{0.5})Ba_2Ca_2(Cu_2Sn_1)O_{10-\delta}$ and Mg doped $Cu_{0.5}Tl_{0.5}Ba_2(Ca_{1.5}Mg_{0.5})(Cu_2Sn_1)O_{10-\delta}$ samples. The infield magnetic measurements of these samples are shown in Fig.3 22. In the applied magnetic fields of 8, 13, 19, A/M, the onset of diamagnetism in χ' is observed around 97, 89.2, 88.1K and the peak temperature T_p in χ'' around 89.2, 86.5, 79.4, respectively. These measurements have shown that decreased inter-plane distance

increases the inter-plane coupling which possibility results into increase interaction among Sn^{+4} atoms in the CuO_2/SnO_2 planes resulting into enhanced localization of the carriers at Sn^{+4} sites. The increased localization of the carriers most likely decreases the density of mobile carriers which results into decreased superconductivity parameters.

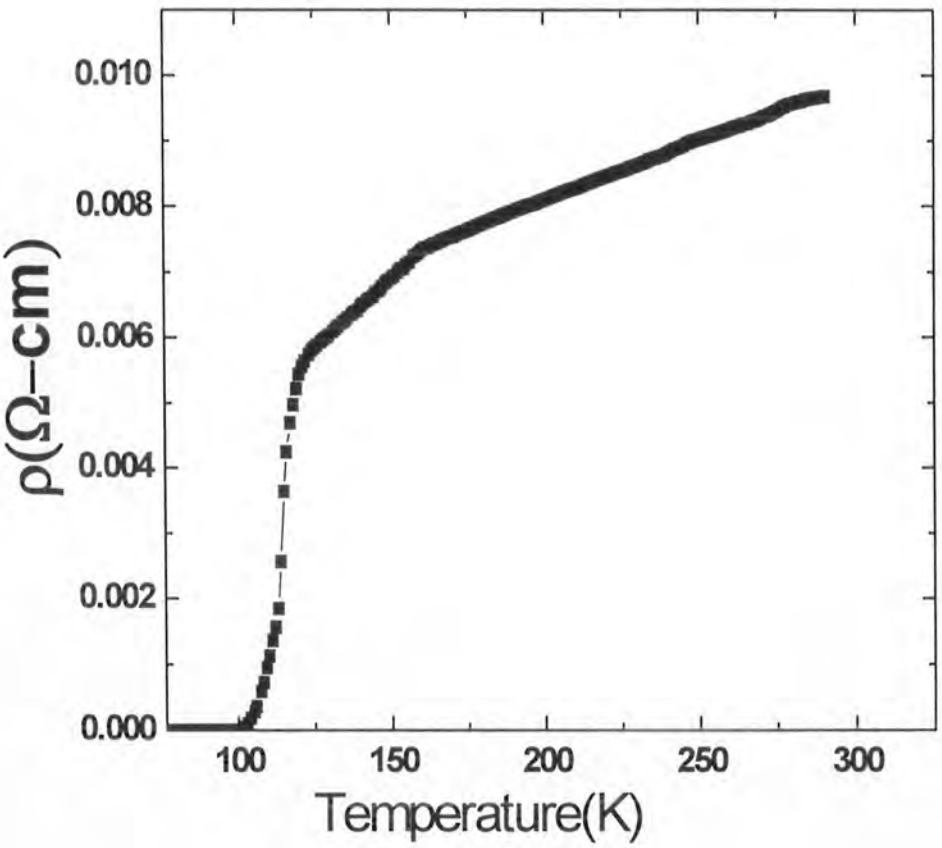

Fig3.19 Resistivity curves of $Cu_{0.5}Tl_{0.5}Ba_2(Ca_{2-y}M_y)(Cu_2Sn_1)O_{10-\delta}$ (M=Mg) Superconductors

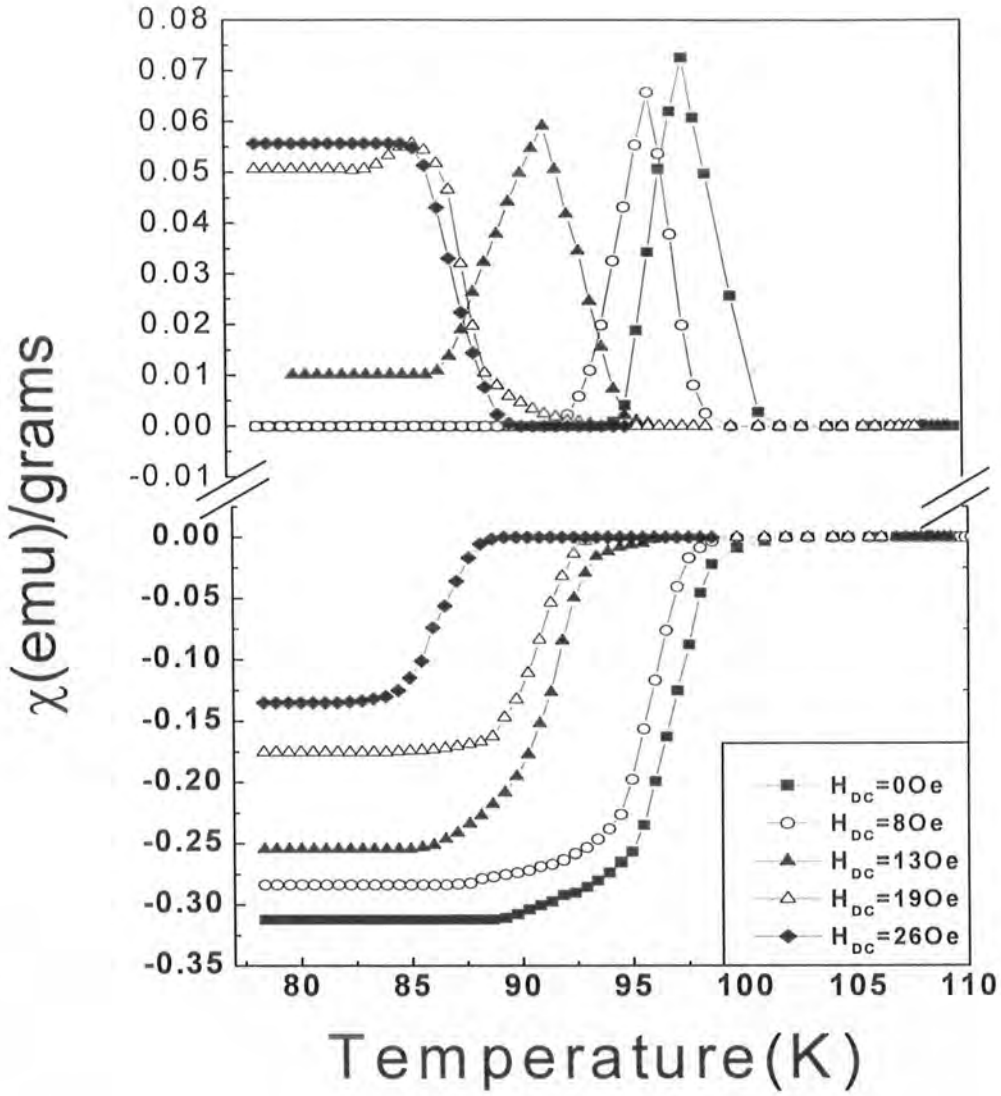

Fig 3.20 In field AC-susceptibility measurements of $Cu_{0.5}Tl_{0.5}Ba_2(Ca_{2-y}M_y)(Cu_2Sn_1)O_{10-\delta}$ (M=Mg)Superconductors

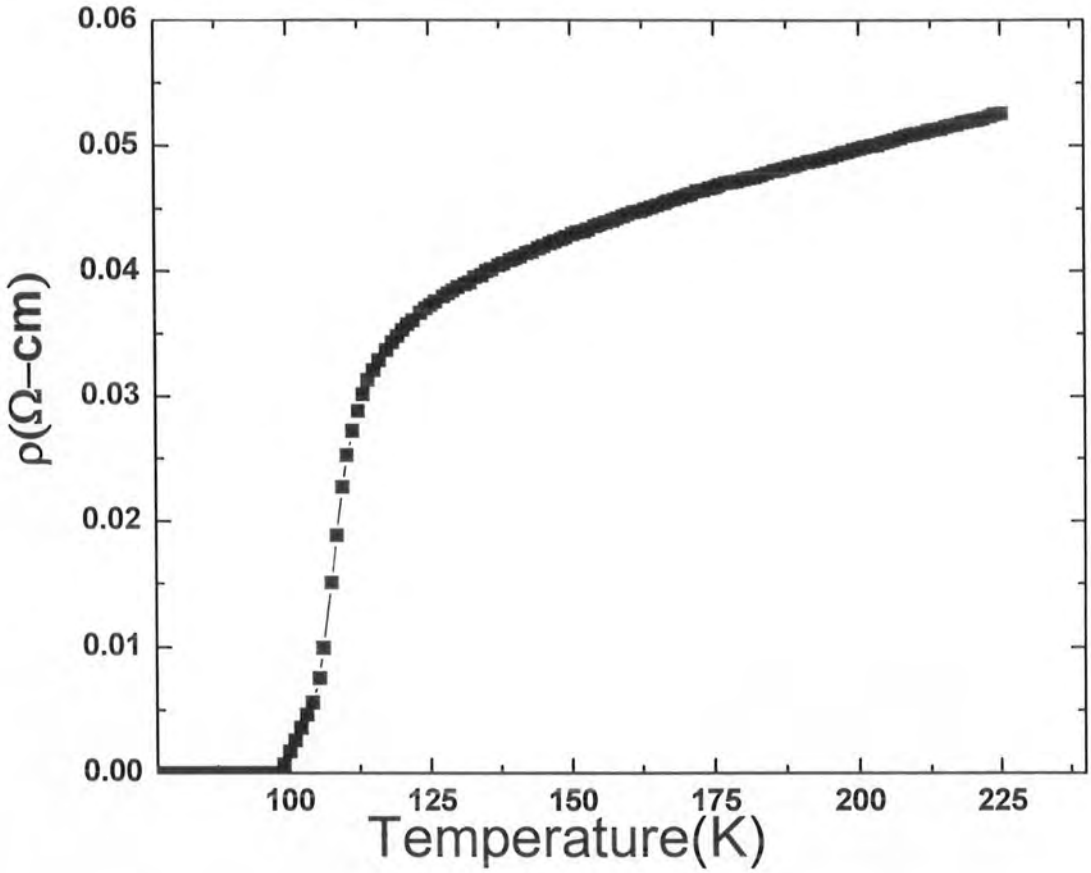

Fig3.21 Resistivity curves of $Cu_{0.5}Tl_{0.5}Ba_2(Ca_{2-y}M_y)(Cu_2Sn_1)O_{10-\delta}$ (M=Be) Superconductors

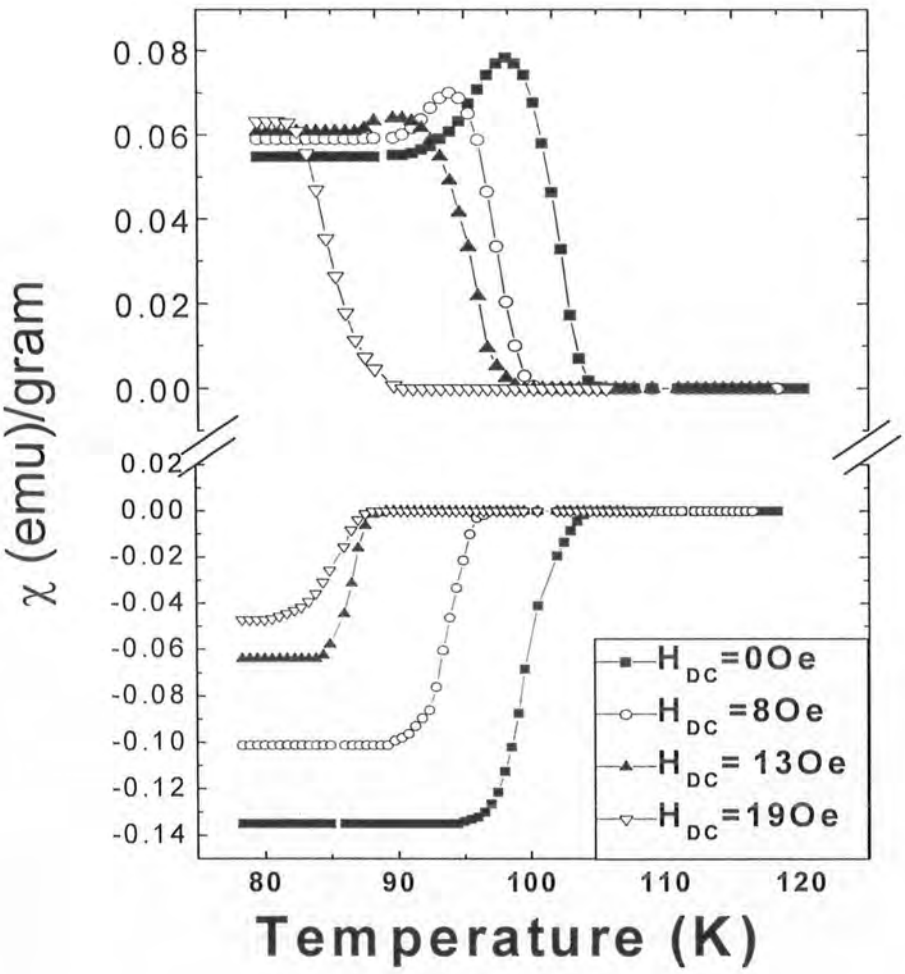

Fig 3.22 In field AC-susceptibility measurements of $Cu_{0.5}Tl_{0.5}Ba_2(Ca_{2-y}M_y)(Cu_2Sn_1)O_{10-\delta}$ (M=Be)Superconductors

4. Conclusions

1. We have successfully synthesized Sn-doped $(Cu_{0.5}Tl_{0.5})Ba_2Ca_2(Cu_{3-x}Sn_x)O_{10-\delta}$ (x=0, 0.25, 0.5, 0.75, 1.0, 1.25, 1.5) superconductors and studied their infield magnetic measurements.

2. These samples have shown metallic variations of resistivity from room temperature down to onset superconductivity with $T_c(R=0)$ around 116, 112, 109, 105, 102, 97, 94K x=0, 0.25, 0.5, 0.75, 1.0, 1.25, 1.5 in $(Cu_{0.5}Tl_{0.5})Ba_2Ca_2(Cu_{3-x}Sn_x)O_{10-\delta}$ superconductors. The onset of diamagnetism as observed in the in-phase component of magnetic susceptibility is around 116, 113, 109.3, 110.7, 108, 97.5, 94.7K with peak temperature (T_P) in the out-of-phase component at 109, 109, 105.5, 107.5, 106,93.6, 91K for the the Sn doping of x=0,0.25, 0.5, 0.75, 1.0, 1.25, 1.5.

3. The decreased magnitude of diamagnetism is most likely associated with the increased localization of the carriers at the Sn^{+4} sites, which in turn decreases the density of mobile carriers. Since the coherence length [ξ] of the carriers is associated with density of mobile carriers, therefore, decreased density of the carriers would promote decrease in ξ and hence reduce the superconductivity in the final compound.

4. The infield magnetic measurements have shown that Sn doped samples show a better inter-grain connectivity because the peak in the out-of-phase component of magnetic susceptibility survives under much higher oxygen external magnetic field. The better inter-grain connectivity is most likely arising from the presence of higher concentration in the final compound which promotes the formation of oxides at the inter-grain sites resulting in to a large surface areas of shielding currents flow giving higher critical current densities.

5. In order to optimize the carrier's concentration in the conducting CuO_2/SnO_2 planes, we have carried out post-annealing of $(Cu_{0.5}Tl_{0.5})Ba_2Ca_2(Cu_{3-x}Sn_x)O_{10-\delta}$ samples in oxygen atmosphere. These samples have shown [$T_c(R=0)$] around 121, 116, 110, 108, 107, 99, 96K for the Sn doping of x=0, 0.25, 0.5, 0.75, 1.0, 1.25, 1.5 and the onset of diamagnetism is observed around 116, 110.3, 109.3, 110.7, 108, 97.5, 94.7K.

6. The oxygen post-annealed samples have shown a decrease in the magnitude of diamagnetism and a relatively inferior coupling of the grains. The decreased magnitude of diamagnetism after post-annealing in the oxygen atmosphere is most likely associated with the enhanced diffusion of oxygen in final compound. The higher concentration of oxygen in the charge reservoir layer stops the flow of the electrons to the conducting

electrons to CuO_2/SnO_2 planes. As a result the density of the mobile carriers is decreased there, which result into a decreased superconductivity volume fraction. A small superconducting volume fraction associated with increased oxygen diffusion both at inter-grain and intra-grain sites makes the weak link behaviour of these compounds inferior.

7. We have also doped Be and Mg at the Ca sites to enhance the coupling of CuO_2/SnO_2 planes in $Cu_{0.5}Tl_{0.5}Ba_2(Ca_{1.5}M_{0.5})(Cu_2Sn_1)O_{10-\delta}$ superconductors. These measurements have shown that decreased inter-plane distance increases the inter-plane coupling which possibility results into increase interaction among Sn^{+4} atoms in the CuO_2/SnO_2 planes resulting into enhanced localization of the carriers at Sn^{+4} sites. The increased localization of the carriers most likely decreases the density of mobile carriers which results into decreased superconductivity parameters.

8. The fitting of J_c values to power law behaviour $(1-T/T_c)^n$, following Bean critical model, have shown a best fit when n=1, which showed the nature of weak links among the grains is superconductor – insulator -superconductor type.

4. References

[1] http://en.wikipedia.org/wiki/History of superconductors

[2] Kamerlingh Onnes, H. Comm. Phys. Lab. Univ. Leiden 122 and 124 (1911) 1226.

[3] Superconductivity,Superfluids and Condensates By James F. Annett Page (47).

[4] Kamerlingh Onnes, H., Comm. Physical Lab. Leiden 133d (1913) 51

[5] Kamerlingh Onnes, H. Comm. Physical Lab, Leiden 133b (1913) 29.

[6] Bednorz, G. and K.A. Müller, Phys. B, 64 (1986) 189-197.

[7] Wu M.K., et al., Phys. Rev. Lett. 58(9) (1987) 908-910.

[8] J. H. Schon et al., Nature 408 (2000) 549.

[9] Introduction to Solid State Physics, Charles Kittle, Seventh Edition, John Wiley & Sons New York.

[10] Meissner, W. and R. Ochsenfeld, Naturwissenschaften 21 (1933) 787-788

[11] Physics, Halliday, Resnick and Krane, Fifth edition, John Wiley & Sons New York, (2002).

[12] Solid state physics, S. O .Pillai, Revised Sixth edition, Newage International Publications (2000).

[13] F .London, and H. London, Proc. Roy. Soc. A149 (1935) 71-88.

[14] Bardeen, J et al., Phys. Rev. 108 (1957) 1175-1204.

[15] Cooper, L.N., Physical Review 104 (1956) 1189-1190.

[16] Gorkov, L.P., Soviet Physics JETP 10 (1960) 998-1004.

[17] Josephson, B.D., Phys. Lett. 1 (1962) 251-253 A. Damascelli et al., Rev. Mod.Phys. 75 (2003) 473.

[18] A. Damascelli et al., Rev. Mod. Phys. 75 (2003) 473.

[19] J. C. Campuzano et al., in Physics of Superconductors, Vol. II,(Ed. K. H. Bennemann & J. B. Ketterson), Springer Verlag, Berlin (2004), p. 167-273; cond-mat/0209476.

[20] Neutron Scattering in Layered Copper-Oxide Superconductors (Ed. A. Furrer), Kluwer Academic Publishers (1998), ISBN 0-7923-5226-2.

[21] B. W. Hoogenboom et al., Phys. Rev. B 62 (2000) 9179.

[22] K. McElroy et al., Nature 428 (2004) 542.

[23] A.Schilling, M. Cantoni, J.D. Guo, and H. R. Ott, Nature (London) 363(1993) 56.

[24] The physics of superconductors by P.Muller A.V.Ustinov, V.V.Schmidt An introduction to fundamentals and applications; Springer (1997)

[25] A. G. Lee, Chemistry of Thallium, Elsevier, New York. 1971.

[26] Journal of the American Ceramic Society, 78(1995), No.12

[27] Linhai Sun, Yening Wang, Huimin Shen, and Xiaohua Cheng, Phy.Rev.B 38 (1988) 5114-5117.

[28] Yasumoto Tanaka, Adrian Crisan, Dilip Dhondiram Shivagan, Akira Iyo, Kazuyasu Tokiwa, and Tsuneo Watanabe, Jpn J. App.Phy 46(2007)134-145.

[29] Ryoji Sugise, and Hideo Ihara, Jap. J. Appl. Phys. 27(1988)1709.

[30] S.S.P.Parkin, V.Y.Lee, A.I.Nazzal, R.Savoy, R.Beyers and J.La.Placa, Phys.Rev. Lett. 61 (1988) 750.

[31] G.B.S Narang, Material Science

[32] V. Rajendran, A. Marikani, Materials Science, Tata McGraw-Hill Publishing

[33] R. Hott, High Temperature Superconductivity 2 -Engineering Applications (Ed. A. V. Narlikar), Springer Verlag, Berlin (2004) p 35

[34] G. Zwicknag et al., Phys. Rev. B 63 (2002) 081103.

[35] G. Zwicknagl et al., Phys. Rev. B 68 (2003) 052508

[36] M. M. Abd-Elmeguid, Physica C 196 (1992) 315-322

[37] Candida C. Silva and M.E.McHenry, IEEE Trans. Appl.Supercond 7 (1997) 1596- 1599.

[38] Hung, K. C.; Lam, C. C.; Feng, J.; Jin, X.Physica C 282 (1997) 2171-2172.

[39] P. Kameli, H. Salamati, M. Eslami, Solid. State. comm,137 (2006) 30–35

[40] M. Tepe, I.Avci, H.Kocoglu, D.Abukay , Solid State Communications, 131 (2004) 319–323.

[41] Francesco Tafuri and John R Kirtley, Rep. Prog.Phy, 68 (2005) 2573-2663

[42] M.Yang, Y.H.Kao, Y.Xin and K.W.Wong, Phys. Rev.B, 50 (1994) 653- 658

[43] N Balchev, Supercond. Sci. Technol. 10 (1997) 65–70.

[44] Wu Ming Chen, Journal of Superconductivity, 11 (1998) 0896-1107.

[45] A F Dong, Supercond. Sci. Technol. 19 (2006) 206–211.

[46] J.Halbritter, Phys.Rev.B, 48 (1993) 9735-9746

[47] Yong Feng, J. Appl. Phys. 76 (1994) 2954.

[48] S.LO.Shinde, J.Morril, D.Goland, D.A.Chance and T.McGuire, Phys. Rev. B 41 (1990) 8838-8842

[49] J Feng, Supercond. Sci. Technol. 13 (2000) 215–224

[50] L. C. Pathak, S. K. Mishra S. K. Das, D. Bhattacharya and K. L. Chopra, Physica C 351 (2001) 295-300.

[51] J.Q. Li, PhysicaC 292 (1997) 295-304.

[52] A Hassen, Supercond. Sci. Technol. 19 (2006) 902–906.

[53] S.Celebi, A. I. Malik, F Inanir and S.A.Halim, Supcond.sci.technol, 17 (2004) 1121-1125.

[54] E. Kuzmann, Physica C 319 (1999) 12–20.

[55] E. Kuzmann, Physica C 312 (1999) 45–54.

[56] A. V. Herzog, P. Xiong, and R. C. Dynes, Phys.Rev.B, 58 (1998) 14199- 14202.

[57] Yang Li, Physica C 382 (2002) 243–250.

[58] J Q Li, Supercond. Sci. Technol. 11 (1998) 603–607.

[59] Anton V. Velichko and Adrian Porch,Phys.Rev. B 63 (2001) 094512 -094519

[60] Yang Li Physica C 312 (1999) 283–288.

[61] L.F. ti, Journal of Alloys and Compounds 242 (1996) 95-97.

[62] S. B. Mohamed, IEEE Transactions On Applied Superconductivity, 11 (2001) 2862.

[63] Takahito Saito, Physica C 171 (1990) 167-173.

[64] E.Govea-Alcaide, R.F.Jardim, P.Mune, Physica C 423(2005) 152-162

[65] D. Hettinger ,K. E. Gray ,D. J. Miller,D. H. Kim, D. G. Steel, B. R. Washburn, J. Sharping, C. Moreau ,M. Eddy,J. E. Tkaczyk, J. DeLuca, J. H. Kang,and J. Talvacchio, Physica C 273 (1997) 275-280.

[66] G. V. M. Williams, Phys. Rev. B 67 (2003) 104514.

[67] Y. Zhao, Physica C 252 (1995) 381-388.

[68] P.K. Nayak, S. Ravi , Solid State Communications 138 (2006) 377–381

[69] Y. L. Chen, Journal of Materials Science: Materials in Electronics 1 (1990) 197-200.

[70] F. J. OWENS, *J. Phys.* Chem Solids 58 (1991) 1481-1486.

[71] K. S. Aleksandrov, Amer. Instit. Of Phys. 756 (1989).

[72] Nawazish A Khan, P.Kameli, A.A.Khurram, Supercond. Sci. Technol. 19 (2006) 410–414.

[73] Thomas W. Krause Physica C 210 (1993) 333-342.

[74] F. Licci Physica C 196 (1992) 307-314.

[75] C.V. Tomy, State Communications, 74, (1990) p 493-496.

[76] Chen Angt , Phys. Cond. Matt. 4 (1992) 4981-4987.

[77] Z.H. He, Physica C 312 (1999) 261–268.

[78] Nawazish A. Khan, M.Mumtaz, J Low Temp Phys 151 (2008) 1221–1229

[79] D.K.Shukla ,S.Mollah and Ravi Kumar, J. Appl. Phys. **101** (2007) 013708.

[80] Kouichi Semba,Azusa Matsuda and Takao ishii, Phys. Rev. B **49** (1994)10043.

[81] M. K. Wu, J. R. Ashburn, C. J. Torng,P. H. Hor, R. L. Meng, L. Gao, Z. J Huang, Y. Q. Wang, and C. W. Chu, Phys. Rev. Lett. **58** (1987) 908.

[82] K. Heine, J. Tenbrink and M. Thoner, Appl. Phys. Lett. **55** (1989) 2441.

[83] Yuang. J. Y, Horng .J. h, Chen .S. P, Fu. C. M,Wu. K. H ,Uen .T. M and Gou. Y. S, Appl. Phys. Lett. **66** (1995) 885.

[84] S.H. Yun_and Wu. J. Z, Appl. Phys. Lett. **68** (1996) 862.

[85] Nawazish A. Khan· M. Mumtaz, K. Sabeeh, M. I. A. Khan and Mushtaq Ahmed, Physica C **407** (2004)103-114.

[86] Ihara H, Tokiwa K, Ozawa H, Hirabayashi M, Negishi A,. Matuhata M and Song Y S, J. Appl. Phys. **33** (1994) 503.

[87] Nawazish A Khan, and M.Mumtaz, Supercond. Sci. Technol. **19** (2006) 762–766.

[88] B. D. Cullity, Element of X-ray Diffraction, second edition, (Addision-Wesely Publishing company, Inc. London 1977.

[89] M. Ali Omer, Elementary Solid State Physics, First Edition, Edition Wesely Publishing Company (1974).

[90] http://www.sciencebuddies.org/mentoring/project_ideas/Elec_p025.shtml

[91] D. N. Zheng, A. M. Campbell, J. D. Johnson, J. R. Cooper, F. J. Blunt, A Porch, and P. A. Freeman, Phys. Rev. B **49** (1994) 1417.

[92] D. N. Zheng, A. M. Campbell, J. D. Johnson, J. R. Cooper, F. J. Blunt, A Porch, and P. A. Freeman, Phys. Rev. B **51** (1995) 1277.

[93] Ilya G. Kaplan, Jacques Soullard, Jorge Hernández-Cobos, Phys. Rev. B **65** (2002) 214509.

[94] V. N. Vieira, P. Pureur and J. Schaf , Phys. Rev. B **66** (2002) 224506.

[95] D. J. C. Walker, A. P. Mackenzie, and J. R. Cooper, Phys. Rev. B **51**(1995) 15653.

[96] H. B. Tang, Y. Ren, Y. L. Liu, Q. W. Yan, and Z. Zhang, Phy.Rev.B **39** (1989) 12290-12292

[97] H. Alloul, P.Mendals,H.Casalta,J.F.Marucco and J.Arabski, Phys. Rev. Lett. **67**(1991) 3140.

[98] Y. Shimakawa, Y.Kubo,T.Manako and H.Igarashi, Phys. Rev. B **40** (1989) 11400.

[99] J. Halbritter, Supercond. Sci. Technol. **16** (2003) R47–R69

[100] D. Koelle, R Kleiner, F. Ludwig, E.Dantsker, J.Clarke, Rev. Mod. Phys. **71** (1999)631; H. J.Barthelmess, F.Ludwig, M. Schilling, D. Drung, T.

[101] R. Hott, High Temperature Superconductivity 2 -Engineering Applications (Ed. A. V. Narlikar), Springer Verlag, Berlin (2004) 35.

[102] W. Buckel, R. Kleiner, Superconductivity - Fundamentals and Applications, WILEY-VCH Verlag, Weinheim (2004)

[103] K. Likharev, Dynamics of Josephson Junctions and Circuits, Gordon & Breach Science Publishers (1986) 30

[104] SQUID Handbook (Ed. J. Clarke, A. Braginski), WILEY-VCH Verlag, Berlin (2003).

[105] L. A. Knauss, A. B. Cawthorne, N. Lettsome, S. Kelly, S. Chatraphorn, E. F. Fleet, F. C. Wellstood, W. E. Vanderlinde, Microelectronics Reliability 41 (2001) 1211

[106] M.V.Kreutzbruck, High Temperature Superconductivity 2, Engineering Applications, (Ed. A. V. Narlikar), Springer Verlag, Berlin, (2004)299

[107] R. Hott, High Temperature Superconductivity, Vol. II Engineering Applications, (Ed. A. V. Narlikar), Springer Verlag, Berlin (2004)41; H. J.

M. ter Brake, G. F. M. Wiegerinck, Cryogenics 42 (2002) 705; M. R. Norman, C. Pepin, Rep. Prog.Phys. 66 (2003) 1547.

[108] Nawazish A. Khan , G. Husnain Physica C **436** (2006) 51–58.

[109] Hadi Salamati1, Ali A Babaei-Brojeny and Medhi Safa Supercond. Sci. Technol, **14** (2001) 816–819.

[110] L. González, E. V. L. de Mello, E. S. Yugue, M. T. D. Orlando, and E. Baggio- Saitovitch, Physica C **384** (2003) 102–110.

[111] J.R.Thompson, J.G.Ossandon, Yang .Ren .Sun, M.Paranthaman and J.Brynestad, Phys. Rev.B **48** (1993)14031-14034

[112] M.Prester, E.Babic, M.Stubicar and P.Nozar, Phys.Rev.B **49** (1994) 6967-6970

[113] S.A.L.Foulds, J.Smithyman, G.F.Cox, C.M.Muirhead, and R.G.Humphreys, Phys.Rev.B, **55** (1997) 9098-9106

[114] I. Isaac and J. Jung, Phys. Rev.B, **55** (1997) 8564-857.

[115] A Polyanskii, V Beilin, I Felner2, M I Tsindlekht, E Yashchin, EDul'kin, EGalstyan, M Roth, B Senkowicz and E Hellstrom,

[116] Nawazish A. Khan, Asim Javaid, A.A. Khurram, Naghma Haider, Physica C **425** (2005) 90–96.

[117] S.K.Agarwal and B.V.Kumaraswamy, Physics and Chemistry of solids, **66** (2005) 729-734.

[118] C.B.Bean, Rev.Mod.Phys **36** (1964) 31.

[119] I.V.Driessche, A.Buekenhoudt, K.Konstantinov, E.Brueneel, and S.Hoste, J.Am.Chem.Soc. **4**, (1996) 185.

[120] J.H.Lee, Y.C.Kim, B.J.Kim, and D.Y.Jeong, Physica C **350** (2001) 83:J.Supercond.**16**,(2006) 1.

[121] P.G.Degennes, Rev.Mod.Phys. **36** (1964) 225.

[122] V.Ambeggaokar and A.Baratoff, Phys.Rev.Lett. **10** (1963) 486.

[92] D. N. Zheng, A. M. Campbell, J. D. Johnson, J. R. Cooper, F. J. Blunt, A Porch, and P. A. Freeman, Phys. Rev. B **51** (1995) 1277.

[93] Ilya G. Kaplan, Jacques Soullard, Jorge Hernández-Cobos, Phys. Rev. B **65** (2002) 214509.

[94] V. N. Vieira, P. Pureur and J. Schaf , Phys. Rev. B **66** (2002) 224506.

[95] D. J. C. Walker, A. P. Mackenzie, and J. R. Cooper, Phys. Rev. B **51**(1995) 15653.

[96] H. B. Tang, Y. Ren, Y. L. Liu, Q. W. Yan, and Z. Zhang, Phy.Rev.B **39** (1989) 12290-12292

[97] H. Alloul, P.Mendals,H.Casalta,J.F.Marucco and J.Arabski, Phys. Rev. Lett. **67**(1991) 3140.

[98] Y. Shimakawa, Y.Kubo,T.Manako and H.Igarashi, Phys. Rev. B **40** (1989) 11400.

[99] J. Halbritter, Supercond. Sci. Technol. **16** (2003) R47–R69

[100] D. Koelle, R Kleiner, F. Ludwig, E.Dantsker, J.Clarke, Rev. Mod. Phys. **71** (1999)631; H. J.Barthelmess, F.Ludwig, M. Schilling, D. Drung, T.

[101] R. Hott, High Temperature Superconductivity 2 -Engineering Applications (Ed. A. V. Narlikar), Springer Verlag, Berlin (2004) 35.

[102] W. Buckel, R. Kleiner, Superconductivity - Fundamentals and Applications, WILEY-VCH Verlag, Weinheim (2004)

[103] K. Likharev, Dynamics of Josephson Junctions and Circuits, Gordon & Breach Science Publishers (1986) 30

[104] SQUID Handbook (Ed. J. Clarke, A. Braginski), WILEY-VCH Verlag, Berlin (2003).

[105] L. A. Knauss, A. B. Cawthorne, N. Lettsome, S. Kelly, S. Chatraphorn, E. F. Fleet, F. C. Wellstood, W. E. Vanderlinde, Microelectronics Reliability 41 (2001) 1211

[106] M.V.Kreutzbruck, High Temperature Superconductivity 2, Engineering Applications, (Ed. A. V. Narlikar), Springer Verlag, Berlin, (2004)299

[107] R. Hott, High Temperature Superconductivity, Vol. II Engineering Applications, (Ed. A. V. Narlikar), Springer Verlag, Berlin (2004)41; H. J.